SANDIA REPORT

SAND2017-4293
Unlimited Release
Printed April 2017

Nonlinear Feature Extraction and Energy Dissipation of Foam/Metal Interfaces

Laura D. Jacobs, John H. Hofer

Prepared by
Sandia National Laboratories
Albuquerque, New Mexico 87185 and Livermore, California 94550

Sandia National Laboratories is a multi-mission laboratory managed and operated by Sandia Corporation, a wholly owned subsidiary of Lockheed Martin Corporation, for the U.S. Department of Energy's National Nuclear Security Administration under contract DE-AC04-94AL85000.

Issued by Sandia National Laboratories, operated for the United States Department of Energy by Sandia Corporation.

Available to DOE and DOE contractors from
U.S. Department of Energy
Office of Scientific and Technical Information
P.O. Box 62
Oak Ridge, TN 37831

Telephone: (865) 576-8401
Facsimile: (865) 576-5728
E-Mail: reports@adonis.osti.gov
Online ordering: http://www.osti.gov/bridge

Available to the public from
U.S. Department of Commerce
National Technical Information Service
5285 Port Royal Rd.
Springfield, VA 22161

Telephone: (800) 553-6847
Facsimile: (703) 605-6900
E-Mail: orders@ntis.fedworld.gov
Online order: http://www.ntis.gov/help/ordermethods.asp?loc=7-4-0#online

SAND2017-4293
Unlimited Release
Printed April 2017

Nonlinear Feature Extraction and Energy Dissipation of Foam/Metal Interfaces

Laura D. Jacobs and John H. Hofer
Vibration/Acoustics Simulation
Sandia National Laboratories
P.O. Box 5800
Albuquerque, New Mexico 87185-MS0557

Abstract

The physical mechanisms of energy dissipation in foam to metal interfaces must be understood in order to develop predictive models of systems with foam packaging common to many aerospace and aeronautical applications. Experimental data was obtained from hardware termed "Ministack", which has large, unbonded interfaces held under compressive preload. This setup has a solid aluminum mass placed into two foam cups which are then inserted into an aluminum can and fastened with a known preload. Ministack was tested on a shaker using upward sine sweep base acceleration excitations to estimate the linearized natural frequency and energy dissipation of the first axial mode. The experimental system was disassembled and reassembled before each series of tests in order to observe the effects of the assembly to assembly variability on the dynamics. Additionally, Ministack was subjected to upward and downward sweeps to gain some understanding of the nonlinearities. Finally, Ministack was tested using a transient input, and the ring down was analyzed to find the effective stiffness and damping. There are some important findings in the measured data: there is significant assembly to assembly variability, the order in which the sine sweeps are performed influences the dynamic response, and the system exhibits nontrivial damping and stiffness nonlinearities that must be accounted for in modeling efforts.

ACKNOWLEDGMENTS

Martin Sanchez, Michael J. Starr, Sarah Leming, Robert Kuether, Gerald Thomason, Scott Smith, Antonio R. Garcia

CONTENTS

FIGURES

TABLES

NOMENCLATURE

FRF	frequency response function
PDMI	polymeric methylene diphenyl diisocyanate
SDOF	Single Degree of Freedom

1. INTRODUCTION

1.1. Motivation

Electronic and electromechanical components are packaged in foam to prevent excessive vibration amplitudes during transportation and operation. Solid foams are used to package defense components per MIL-STD 2073 [1]. This packaging leads to foam/metal interfaces, which have long been recognized as significant contributors to energy dissipation and nonlinearities in the system. The mechanisms for energy dissipation in these systems include friction, impacts, and the large inherent material damping common in most foams. Standards, such as MIL-STD 810G [2], require qualification of military components under vibration environments in their packaging. To be able to model and understand how systems containing foam to metal interfaces will respond to various vibration environments, it is important to understand the energy dissipation mechanisms and their effect on the dynamics. Currently, modeling capabilities to capture the dissipative behavior of metal parts in foam are being developed. Physical experiments are crucial to validate these models and gain an understanding of the physical phenomena required for future modeling.

1.2. Experimental Excitation Methods

In order to gain information about the dynamics of a physical system, vibration experiments can be run in a laboratory and then the collected data can be analyzed. There are three main types of excitations that can be used to excite the nonlinearities in a system: random, harmonic, and transient. They each provide varying levels of useful information and will be further discussed in the following paragraphs.

Random vibration provides a broadband excitation that inputs energy over a wide range of frequencies simultaneously. An advantage to this method is that it is possible to excite multiple modes of a system simultaneously, so system identification can happen quickly and efficiently. However, random vibration inherently linearizes the frequency response function (FRF) generated from its data. Therefore, it is not a good tool for extracting nonlinear information from a system, and will not be used in this study [16].

Harmonic excitation puts a single frequency at a time into a system. By stepping or sweeping through a series of frequencies, it is possible to determine a FRF for the system. The shape of the FRF can give some indication of the presence of stiffness nonlinearities by noting which direction distinct peaks lean. Additionally, if the harmonic excitation is run at different levels, a comparison can be made between the relative amplitudes and frequencies of the peaks at each level. This gives

information about the amplitude dependence of stiffness nonlinearities (shifts in the natural frequencies) and damping nonlinearities (changes in the amplitude of the FRF). Although harmonic excitation can provide a rich set of data to analyze, the necessity of running multiple frequencies at multiple amplitudes makes it a time consuming method [16]. To make testing more efficient it is possible to optimize the sweep rate based on the dynamics of the system and the acceptable error [17]. The time for the sweep, t_b, can be calculated as:

$$t_b \geq \frac{Q^2}{\eta * f_0} * \ln\left(\frac{f_2}{f_1}\right) \quad (1)$$

where Q is the maximum amplitude of the transfer function, □ is a factor relating to the error, f_0 is the natural frequency, f_1 is the lower frequency of the sweep, and f_2 is the upper frequency.

The final method is transient or shock excitation. Transient excitations can be used to extract nonlinear information of a system for a wide frequency bandwidth. By analyzing the ring down of the data, it is possible to extract backbone curves, which provide effective stiffness and damping characteristics based on amplitude. In addition to being useful for modeling purposes, the backbone curves can also be used to identify the type of nonlinearity in the system. The advantage of a shock excitation is that a single shock can be used to produce information about the system, making it an efficient testing method [16].

1.3. Nonlinear Feature Extraction

There are many types of nonlinearities that can be present in physical systems, and even multiple varieties of nonlinearities can be present in a given system. It is useful to be able to identify when nonlinearities are present in a system. When tasked with developing a model for a system, it is important to know whether or not the nonlinearities are significant and need to be included in order to predict accurate responses.

1.3.1. Visual Inspections of Frequency Response Functions of Harmonic Data

The first step in analyzing the data from a harmonic excitation is to compute the FRF, which is a ratio of the response to the input. The FRFs contain a lot of useful information.

One of the more critical pieces of information from this response data is the natural frequency–the frequency at which the highest peak in the response occurs.

A visual inspection of the FRFs can provide information about the types of nonlinearities present. If the peaks of the FRFs at the different excitation amplitudes shift, then there is a stiffness nonlinearity present. If the frequencies decrease with increasing amplitude, it is a softening system. If the frequencies increase with increasing amplitude, it is a stiffening system. If the amplitudes of the peaks of the FRFs change with amplitude, that would indicate the presence of nonlinear damping in the system.

In a linear system, the order or direction of the sine sweeps is irrelevant to the response of the system. However, if the response stiffness and/or damping for a given amplitude depend on the order of tests (i.e. starting at a low amplitude and increasing vs starting at a high amplitude and decreasing) it indicates that the loading history plays an important role in the equilibrium response of the system. This is a clear indication of nonlinearities in the system. Therefore, due to multiple equilibrium positions in a nonlinear system, the sweep direction will produce different FRFs.

1.3.2. Hilbert Transforms of Harmonic Data

A Hilbert transform is a linear operator that analyzes the real parts of a given set of data and will return the data as a complex data set. It has been found to be a useful tool to detect and identify nonlinearities in experimental response data. If the system is linear, then the FRF of the transformed data and the original data set will be equivalent. If the system is nonlinear, then the FRFs of the transformed data and the original data set will differ. The differences in the FRFs will indicate not only that there is a nonlinearity, but what type of nonlinearity is present. More information about this can be found in [18].

1.3.3. Backbone Curves from Resonance Decay Responses

Backbone curves can offer insight into the nonlinear behavior of systems. The approach used in this study is based on the work of Londono et al. [19]. The approach is based on estimations of the instantaneous frequency and an envelope of the decaying response after a transient excitation. The steps are further explained in the following paragraphs.

The first step in the technique is to determine the instantaneous frequencies as a function of time. The technique suggests using the zero crossings of the decay response. The instantaneous frequency at the crossing point, t_i^0 , can be computed such that

$$f_i^0 = (t_{i+1}^0 - t_{i-1}^0)^{-1} \tag{1}$$

The frequency is estimated from the inverse of the period along one complete cycle and is assigned to the crossing time in the center of the period.

The second step in the technique described in [19] is to estimate the instantaneous amplitude over the decay response in order to extract the response envelope. This can be accomplished by tracking the peaks of the signal within each zero-crossing time interval. Once the peaks have been determined, a polynomial interpolation can be used to determine the instantaneous amplitude at the same times that the instantaneous frequencies have been found.

The dissipative characteristics of the system can be determined by investigating the envelope of the decaying response. The effective damping of the system can be calculated as

$$\xi_{t_i^0} = \frac{1}{\omega_0(t_i^0) * t_i^0} (\ln(A_0) - \ln\left(A(t_i^0)\right) \quad (2)$$

where $\omega_0(t_i^0)$ is the instantaneous angular frequency in rad/s, A_0 is the initial amplitude, and $A(t_i^0)$ is the instantaneous amplitude of the response.

Once the instantaneous amplitudes, frequency, and damping have been calculated, the effective stiffness and damping can be estimated using properties of the system. The effective stiffness $k_{effective}$ can be estimated as

$$k_{effective_i} = {\omega_i}^2 * m \quad (3)$$

where m is the mass of the system. The effective damping $c_{effective}$ can be estimated as

$$c_{effective_i} = 2 * m * \xi_{t_i^0}(t_i^0) * \omega_i^0(t_i^0) \quad (4)$$

1.3.4. Estimating Energy Dissipation

The amount of energy dissipation in a system can be estimated from the frequency response function. The maximum amplitude of the transfer function gives Q, the amplification factor of the input at the natural frequency. The amplification factor, Q, can then be used to calculate the energy dissipation of Ministack using Eq. 5 derived in [15] as

$$\frac{\pi * Q * A_b^2}{f_n^2} \quad (5)$$

where f_n is the natural frequency of the first axial mode in Hz, A_b is the amplitude of the excitation in g's, and Q is the amplification factor of the response. Previous studies [3-12] have shown that when energy dissipation is plotted versus the input acceleration on a log-log plot, the data should be a straight line, indicating a power law relationship between energy loss per cycle and the input acceleration. When the system has contact friction, 2 is the theoretical value of the exponent for the equation fit to the data [3].

2. EXPERIMENTAL SETUP

To create a system with a dominant axial mode that exercises the large foam to metal interfaces, a solid aluminum mass was placed in foam cups and then inserted into an aluminum can, as illustrated in Figure 1. A preload was then applied to the steel disk on the top of the foam cups using a press, and then a threaded steel ring was tightened to secure the preload. The aluminum can has an inner diameter of 4 inches, an outer diameter of 5 inches and a depth of 6 inches. The can was welded to a square plate that has nine bolt holes (Figure 1) to allow the specimen to be attached to a shaker. The plate has a recess in the bottom (not shown) of it to accommodate a uniaxial accelerometer to control the input acceleration. A triaxial accelerometer was placed on top of the solid internal mass cylinder to measure the response of the system. The steel disk has a hole in the middle to allow for the accelerometer cable to exit the specimen.

Figure 1: Test Specimen

2.1. Foam Specimen Details

The foam specimens are made from 20 pound per cubic foot closed cell PMDI foam. The foam specimens are in two parts, a top half which has an access hole for attaching an accelerometer and a bottom half which has a solid bottom. The two halves are cup-like in nature with an outer diameter of 4 inches and an inner diameter of 3 inches. The bottoms and sides of the cups are all half an inch. The surface of the foam specimens are friable.

Two different cup depths were used in the experiment. One set of foam specimens has an interior depth of 2 inches. Nominally, the solid mass would fit exactly in the specimens yielding parallel load paths through the solid mass and through the foam. However, with machining tolerances, there are cases where the load path is either through the foam alone or through the mass alone in addition to the cases of parallel load paths. During the experiments, some interesting behavior was observed in terms of the natural frequency of the system under different preloads (Section 3.1.4). The responses were not as initially expected. The deviation from expected behavior was attributed to the load paths not being

parallel as assumed. Therefore, a second set of foam specimens was designed to ensure that the preload path goes through the solid mass to gain more insight into the behavior. The second set of foam specimens has an interior depth of 1.875 inches. Nominally, there would be a 1/4 inch gap between the two pieces of foam, thus ensuring a load path through the solid mass even with variations due to machining tolerances.

2.2. Solid Mass Details

Three solid masses of different diameters were used in the experiments to determine the effects of snugness of fit on the energy dissipation characteristics of the system. The nominal, or no gap, specimen has a diameter of 3 inches, so that it fits snugly in the foam specimens. The $1/16^{th}$ inch gap specimen has a diameter of 2.9375 inches so that there is a gap between the solid mass and the foam. The final specimen has a diameter of 2.875 inches. All three solid masses are 4 inches in length and made from 6061-T6 Aluminum. They have a recessed area at the top that can accommodate a triaxial accelerometer.

2.3. Specimen Assembly

The solid mass was placed in both halves of the foam cups, with markings on the cups being lined up to help limit the variability in alignment from assembly to assembly. Then, the cups were placed in the can, with markings on the cups and the can being aligned to help with the repeatability of assembly. The steel plate was placed on top of the foam and solid mass assembly in the can, after which a load cell was placed on top of the assembly. A preload was applied using a press until the reading on the load cell is approximately the nominal preload. The retaining ring was tightened to maintain the preload, the press was released, and Ministack was ready for testing.

In this study, three preloads were used: 400lb, 700lb, and 1000lb. Varying the preload enabled determination of what effect, if any, the preload had on the natural frequencies and energy dissipation of the specimen.

2.4. Equipment Details

Two main types of accelerometers were used in these experiments: uniaxial and triaxial. The uniaxial accelerometer used in this experiment is an Endevco 2220. It can measure responses in the frequency range from 1Hz to 10kHz and accelerations up to 1000g. Two different triaxial accelerometers were used, because a larger measurement range was needed for some of the specimens. The first was an Endevco 6510. It can measure responses in the frequency range from .04Hz to 10kHz and accelerations up to 500g. The second triaxial accelerometer used was the PCB 356A30. It can measure responses in a frequency range from 0.5Hz to 10kHz and accelerations up to 1000g.

The tests were performed on Unholtz-Dickie T1000 and T2000 shakers. The shakers are capable of providing excitations from 10Hz to 3000Hz in a sinusoidal mode. They have a 2 inch stroke and can input forces up to 25,000lbs.

2.5. Test Specifications and Data Collection

In order to determine the natural frequencies and energy dissipation constant for the specimen, a sine sweep was run from 500 to 3000Hz. Four different amplitudes, 1g, 2g, 5g and 10g were chosen to determine the effects of excitation amplitude on the response of the test article. On some of the specimens, the sine sweeps were run from both 500 to 3000Hz (an upward sine sweep) and 3000 to 500Hz (a downward sweep) at the four different amplitudes. The sweeps were performed at a rate of 3 octaves per minute (an octave represents a doubling of frequency). This sweep rate was chosen using equation

$$t_b \geq \frac{Q^2}{\eta * f_0} * \ln\left(\frac{f_2}{f_1}\right) \qquad (1.$$

A Q of 50, a natural frequency of 900, and an error of 1% were chosen. These values are conservative, so would lead to lowest value for the sweep rate. Based on the calculations, a sweep rate of 3.11 octaves per minute would yield natural frequency and damping values. For ease of representation and added conservatism, the sweep rate was rounded down to 3 octaves per minute for this study. Finally, some specimens were subjected to a transient excitation tailored to the natural frequency of Ministack, and the ring down response was measured and analyzed.

A triaxial accelerometer measured data in the three mutually perpendicular directions at the top of the solid mass. A uniaxial accelerometer attached to the baseplate was used to control the input to the structure. The data measured at the triaxial accelerometer at the top of the solid mass and the control accelerometer at the base were used to calculate transfer functions between the responses of the three different axes at the top of the solid mass and the input accelerations.

2.5. Test Matrix

A configuration is comprised of one set of the two lengths of foam cups, one of the three solid masses, and one of the three preloads. An upward sweep test series was run for all possible combinations. Between series of tests on each configuration, the setup was disassembled and then reassembled. This reassembly allows for determination of the assembly to assembly variation of the response of the test article. The test sequences are enumerated in Table 1. In all assemblies in Table 1, the sequence of tests was always repeated to determine if vibrating the specimen changed the dynamic characteristics. The final test assembly 3 was run to see if the order in which the amplitudes were applied affected the dynamics.

Table 1 Test Sequence for Upward Sweep Test Series

Assembly Number	**Sweep Series Amplitudes**
1	1g, 2g, 5g, 10g, 1g, 2g, 5g, 10g
2	1g, 2g, 5g, 10g, 1g, 2g, 5g, 10g
3	10g, 2g, 5g, 1g, 10g, 5g, 2g, 1g

Additional tests were run on the configuration of cups that consisted of the full length cups, the nominal solid mass, and 700lb preload. The first was a series of upward and downward sweeps at the four amplitudes used for the upward sweep test series. The tests are enumerated in Table 2.

Table 2 Upward and Downward Test Sequence

Excitation Amplitude (g)	**No. Upward Sweeps**	**No. Downward Sweeps**
1	3	3
2	1	1
5	1	1
10	1	1

The second series of tests were shock pulses applied in the following order: 8.5g, 12g, 17g, 24.5g, 35g. That sequence was then repeated, followed by a sequence in reverse order twice.

3. TEST RESULTS

3.1. Axial Tests: Sinusoidal Excitation

For the axial testing, the test article was oriented so that the plate on the bottom of specimen is placed flat on the shaker, as shown in Figure 2. This orientation means that the specimen was being excited in the direction of the load path for the preload. The energy dissipation is expected to come from the foam rubbing against the metal interface as well as the interface between the two sets of foam for the cases when there is contact. In this set of tests, the sine sweeps were upward (i.e. starting at a low frequency and going to a high frequency) only.

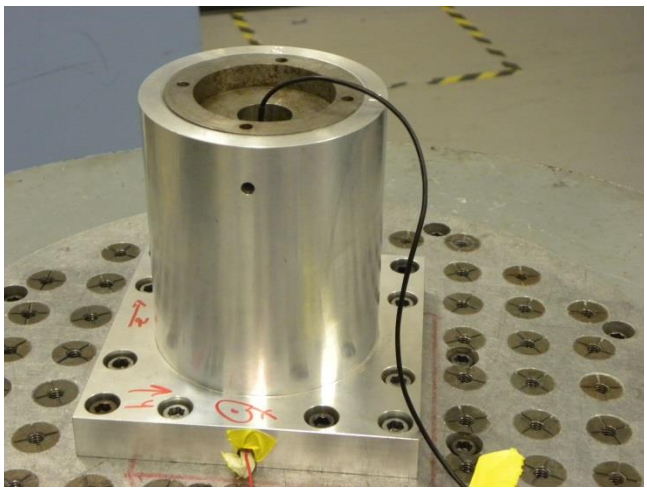

Figure 2: Test Article on Shaker in Axial Testing Orientation

3.1.1. Effects of Amplitude

This subsection shows the resulting transfer functions for the three test sequences in Table 1 on the configuration with the foam cup depth of 2 inches and the solid mass diameter of 3 inches (i.e. no gap). In this configuration, the load path goes through both the foam and the solid mass and the solid mass fits snugly into the foam cups. The results for the test sequences shown in Figure 3 and Figure 4 show that the natural frequency decreases and the amount of energy dissipation increases as the excitation amplitude increases. The frequency shifts suggest that the foam to metal interface loses stiffness at high excitation levels, likely due to micro- or possibly macro-slip. The impacts and the friction between the contact interfaces introduce nonlinear energy dissipation observed at higher excitation levels.

When starting the test series at 1g and increasing the amplitude to 10g, the natural frequency from the second run is lower than the first; and the amount of energy dissipation is lower. These phenomena are seen in the data in Figure 3 and Figure 4. When starting the test series at 10g and decreasing the amplitude down to 1g, there is no appreciable difference in the natural frequency and energy dissipation as seen in Figure 5. One hypothesis for this behavior could be attributed to the higher amplitude sine sweeps

causing wear or loss of preload in Ministack. Going from the 1g to 10 g sweeps and repeating, the settling position of the solid mass after the 10g run may be different than the initial 1g run. This could explain why the stiffness and the damping in the transfer functions during the second runs shifted a noticeable amount. It should also be noted that the magnitude of the response of the system changes a nearly imperceptible amount from assembly to assembly, which indicates a consistency in the assembly process.

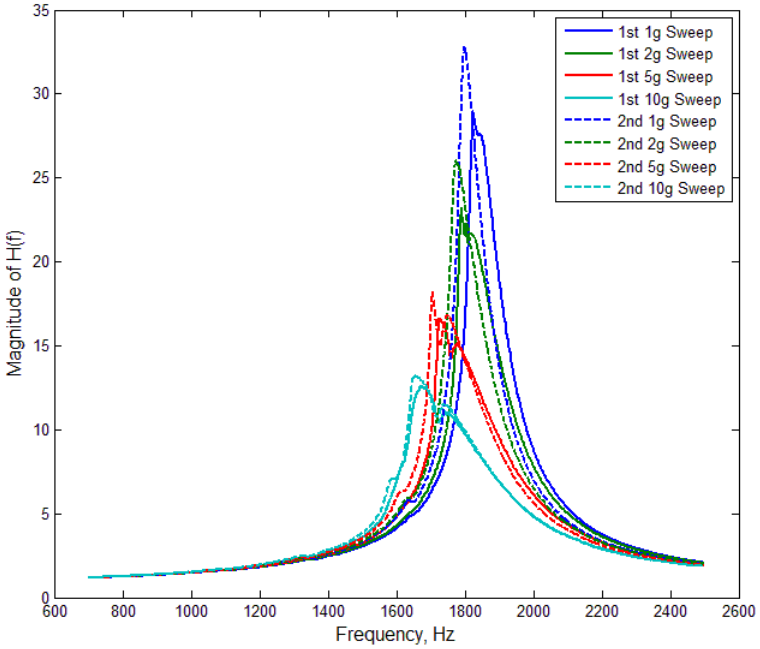

Figure 3: Transfer Functions for a Specimen Preloaded to 700lbs Through Foam and Solid Mass, Assembly 1.

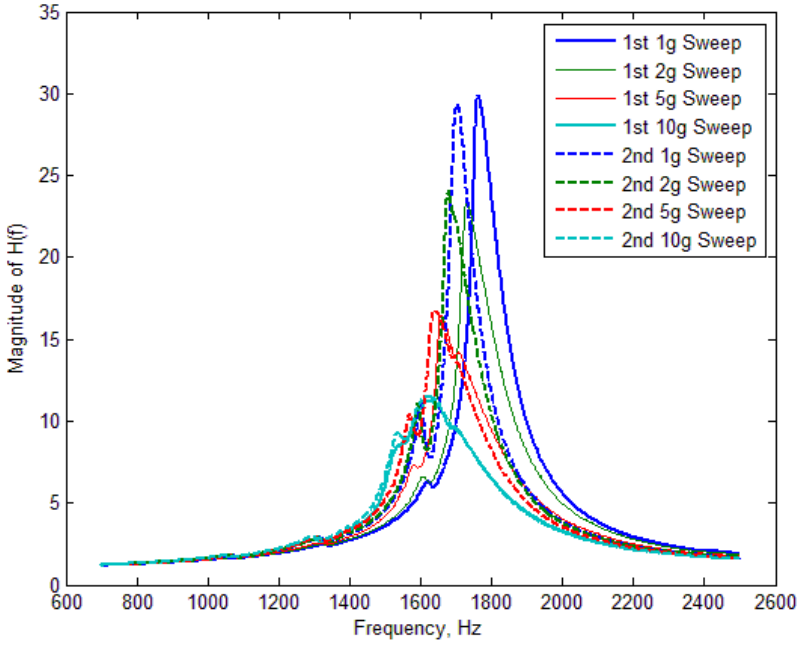

Figure 4: Transfer Functions for a Specimen Preloaded to 700lbs Through Foam and Solid Mass, Assembly 2.

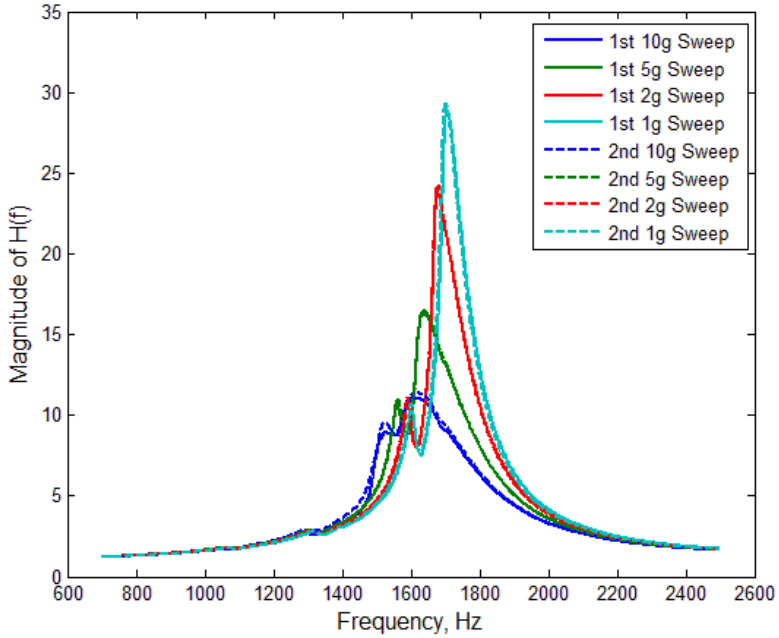

Figure 5: Transfer Functions for a Specimen Preloaded to 700lbs Through Foam and Solid Mass, Assembly 3.

3.1.2. Effects of Sweep Direction

The configuration for this series of tests is a set of foam cups that are 2 inches in depth, the solid mass that is 3 inches in diameter (i.e. the "no gap" specimen), and a preload of 700lbs. The specimens are then subjected to a series of upward and downward sweeps, which are enumerated in Table 2. Nonlinear systems can have multiple equilibrium points for a given frequency of response based on the original state of the system. For this reason, the sine sweeps were executed in both upward and downward in frequency to observe if there is a difference between the frequency response functions (FRF), which would be an indication of the nonlinearity of the system. Two different specimens were tested, and each of them were disassembled and reassembled one time to assess the assembly to assembly variation.

It is observed that there is a distinct difference in the FRFs between sweeping up in frequency and sweeping down in frequency as shown in Figure 6. This difference in the observed behavior is likely due to the nonlinear system having multiple equilibrium conditions for each frequency based on the previous state of the system. The data show that as the excitation amplitude increased, the FRF is skewed to the left to an increasing degree, indicating a nonlinear softening stiffness. Additionally, the damping increases with the excitation level, indicating nonlinear damping properties present in the foam to metal interfaces as well.

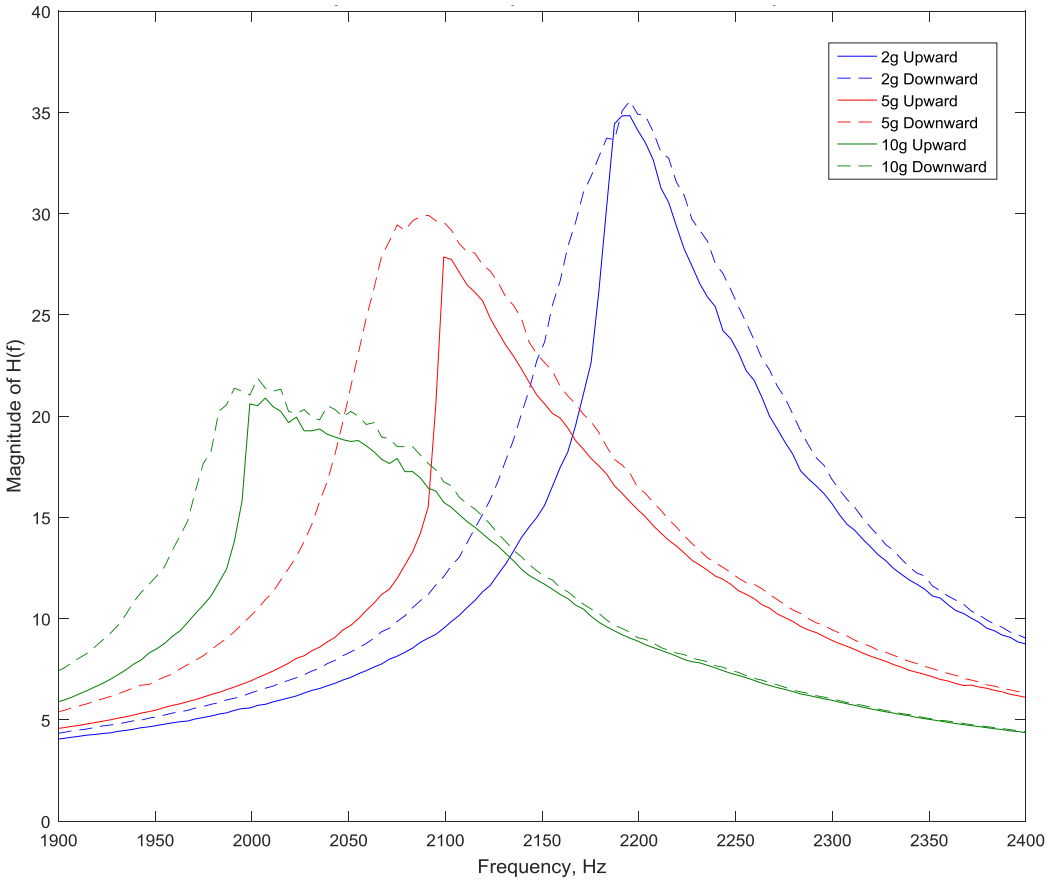

Figure 6: Transfer Functions for a Specimen Preloaded to 700lbs Through Foam and Solid Mass, Upward and Downward Sweeps.

3.1.3. Hilbert Transform

The Hilbert transform can be a powerful tool for determining both the existence and type of nonlinearity in a system by comparing the FRF of a signal before and after a Hilbert transform. If the FRF is the same before and after a Hilbert Transform, then the system is linear. If the two FRFs are different, then nonlinearity exists in the system. Additionally, the nature of these differences can be an indicator of the type of nonlinearity present in the system.

For this study, a Hilbert transform was performed on the data from the upward sine sweeps on the specimen with no gap, a 700lb preload, and the load path through the foam and the solid mass. The data shown in Figure 7 shows that there is nonlinearity present in the system. Additionally, because the transform yields a larger amplitude than the untransformed data shown in Figure 7, it indicates that the nonlinearity present is due to nonlinear damping. The data also show evidence of softening stiffness due to the increasing resonant frequency when looking at the transformed vs. untransformed response.

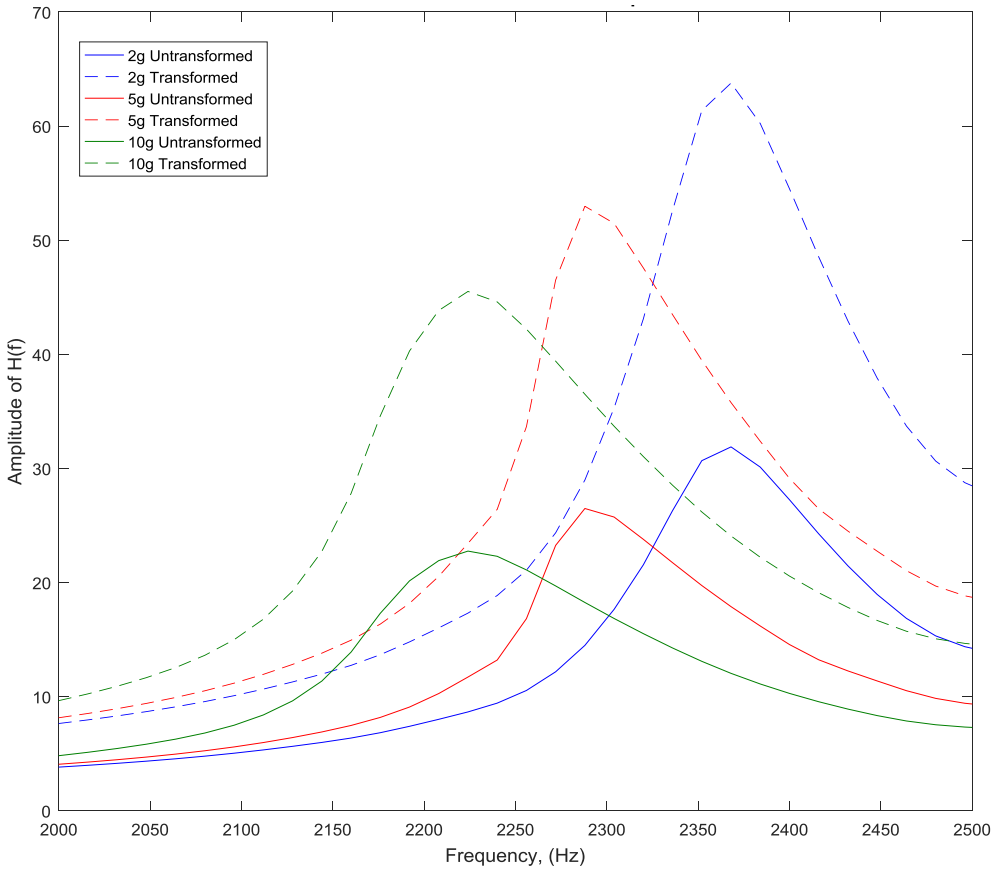

Figure 7: Hilbert Transforms of Sine Sweep Data on No Gap, 700lb Preload, Load Path Through Both Foam and Solid Mass.

3.1.4. Effects of Preload

In assessing the effects of preload on the dynamics of the system, two parameters are studied: the natural frequency and the normalized energy dissipation.

3.1.4.1. Effects of Preload on Natural Frequency

The first parameter studied is the natural frequency. Figure 8 through Figure 10 show the distribution of the natural frequency of the specimen as a function of input acceleration and preload for specimens with the preload path through the foam and solid mass. Each marker in the figure corresponds to one sine sweep on an assembly. It should be noted that in Figure 8, the data from the 400lb preload yields natural frequencies that are in an identical range to the 700lb preload, and thus the data from the 400lb preload may be difficult to see on the graph.

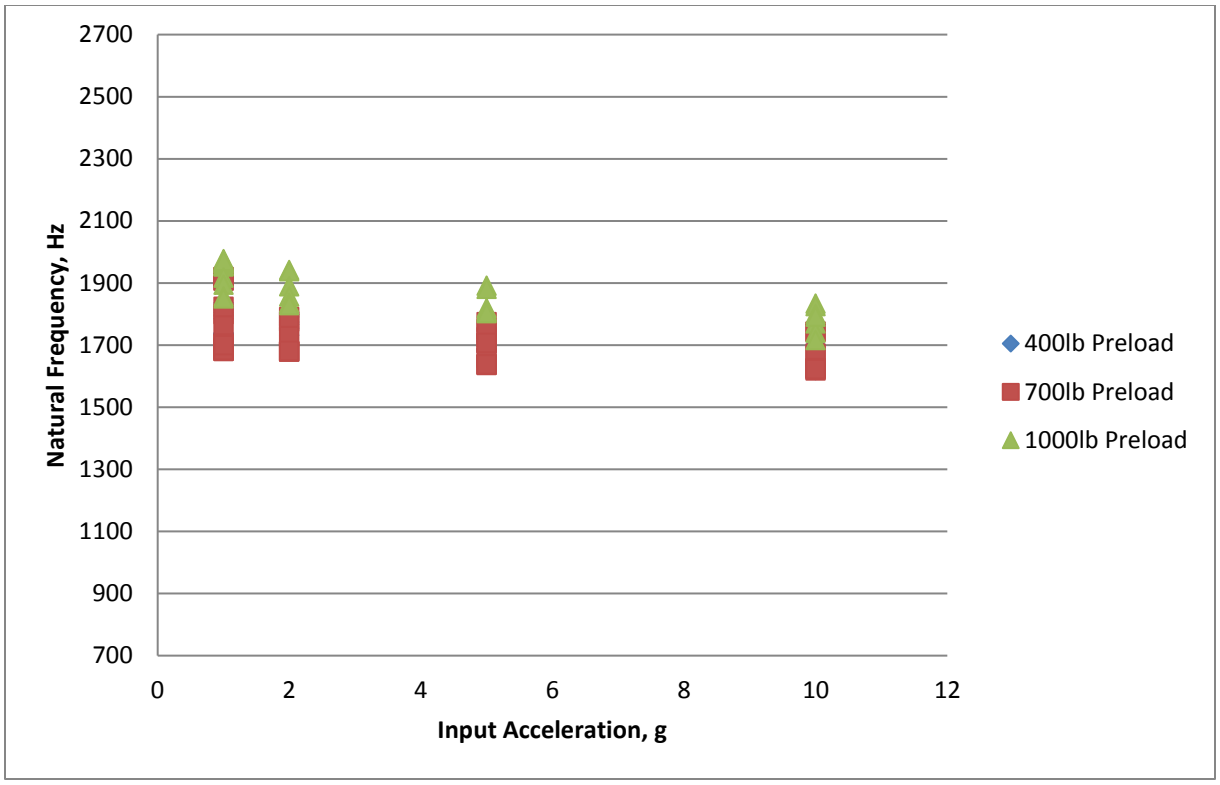

Figure 8: Distribution of Natural Frequency per Preload with No Radial Gap and Preload through the Foam and Solid Mass.

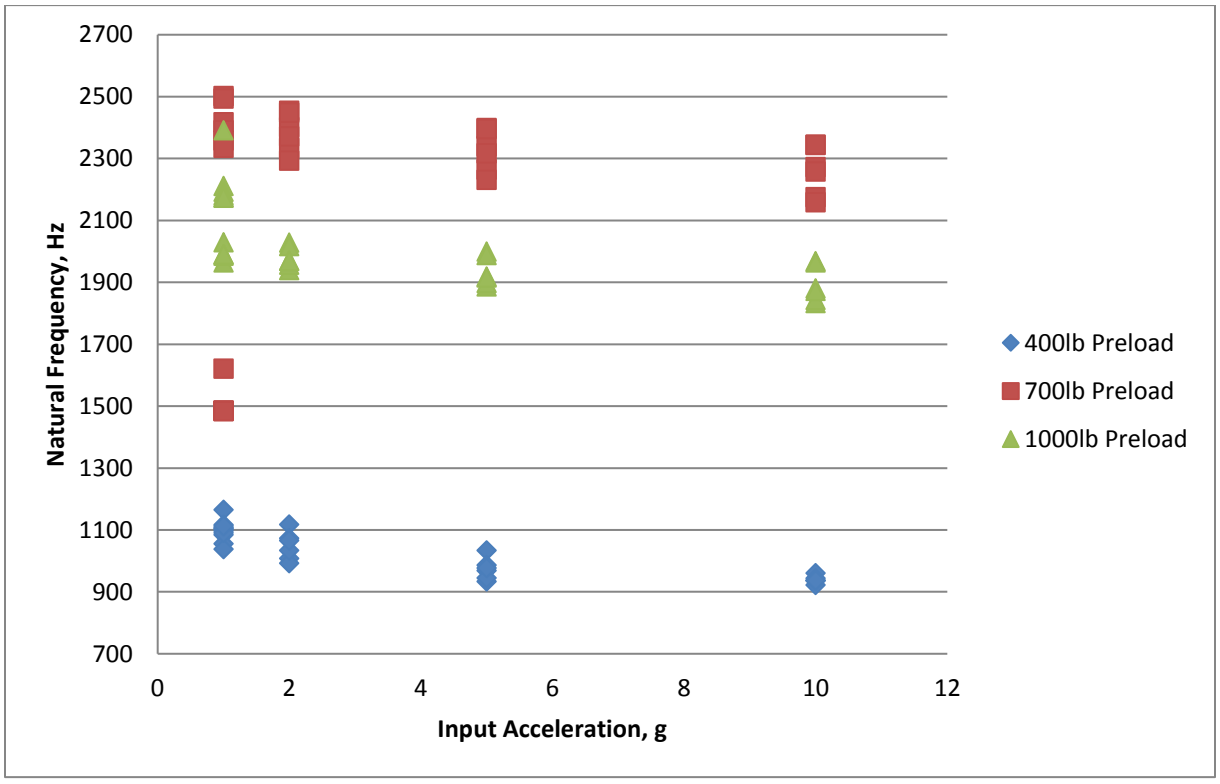

Figure 9: Distribution of Natural Frequency per Preload with a 1/16" Radial Gap and Preload through the Foam and Solid Mass.

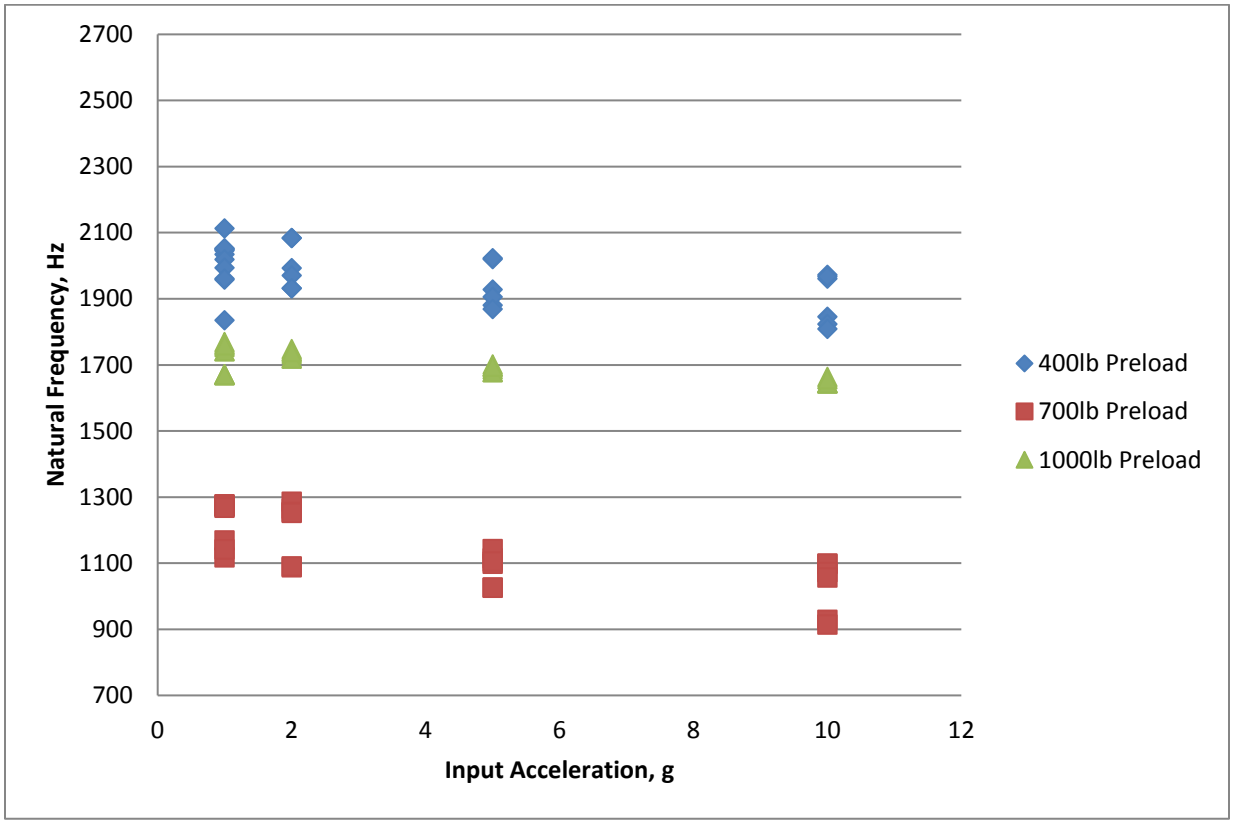

Figure 10: Distribution of Natural Frequency per Preload with a 1/8" Radial Gap and Preload through the Foam and Solid Mass.

When the preload goes through the foam and solid mass, the spread of the natural frequency is consistent regardless of preload. The value of the natural frequency varies with the preload, but it is not consistent across the various gap sizes. Contrary to expectations, the preload has no predictable effect on the natural frequency. The deviation from expected behavior was attributed to the load paths not being parallel as assumed. Due to tolerance stack ups, there are cases where the load path goes through the foam alone and cases where the load path goes through the solid mass alone.

Figure 11 through Figure 13 show the distribution of the natural frequency of the specimen as a function of input acceleration and preload for specimens with the preload path through the solid mass only.

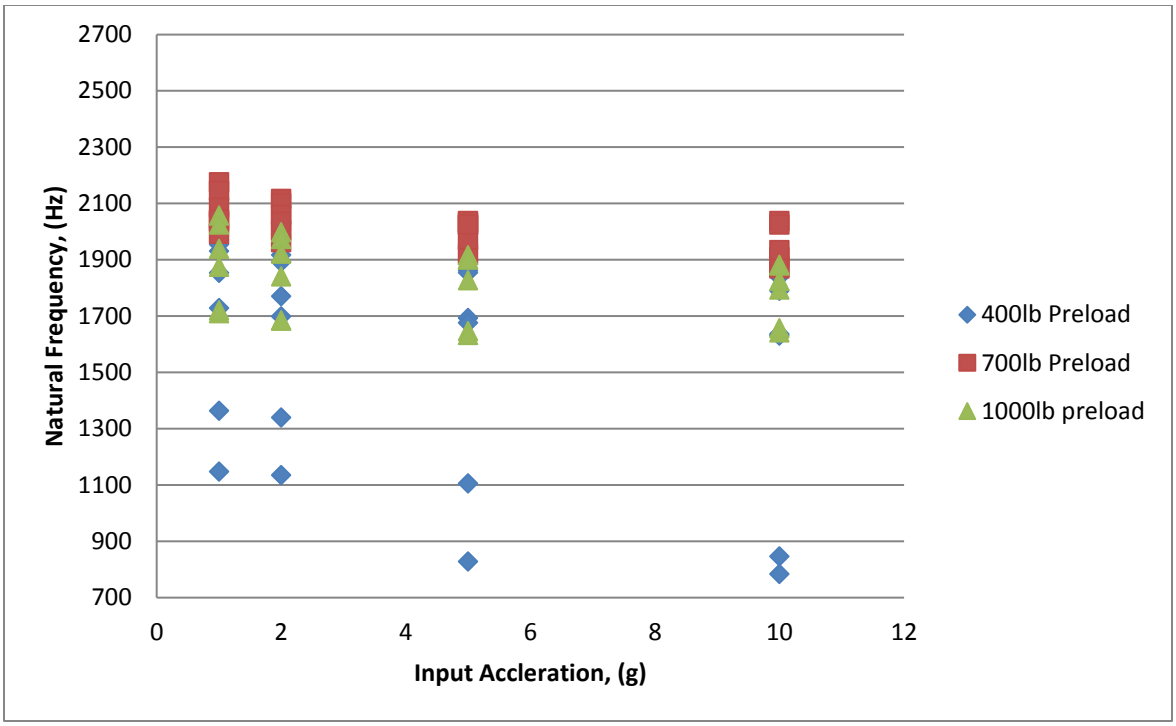

Figure 11: Distribution of Natural Frequency per Preload with No Radial Gap and Preload through the Solid Mass Only.

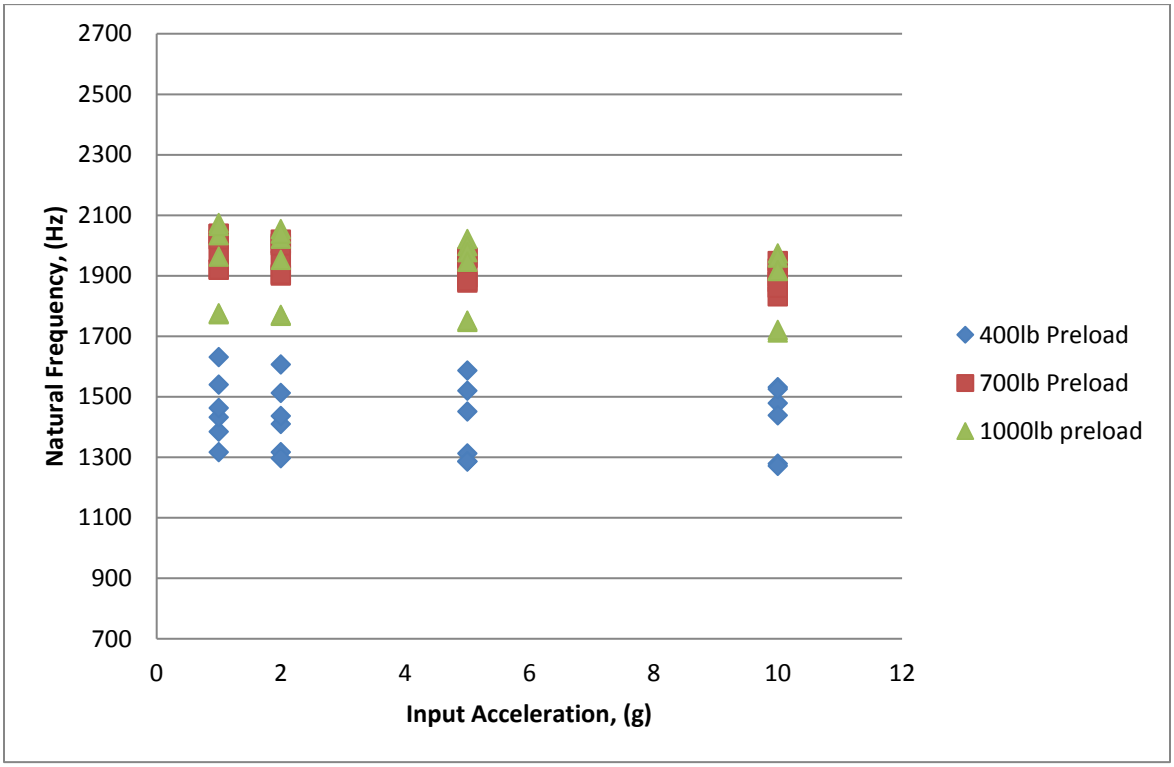

Figure 12: Distribution of Natural Frequency per Preload with a 1/16" Radial Gap and Preload through the Solid Mass Only.

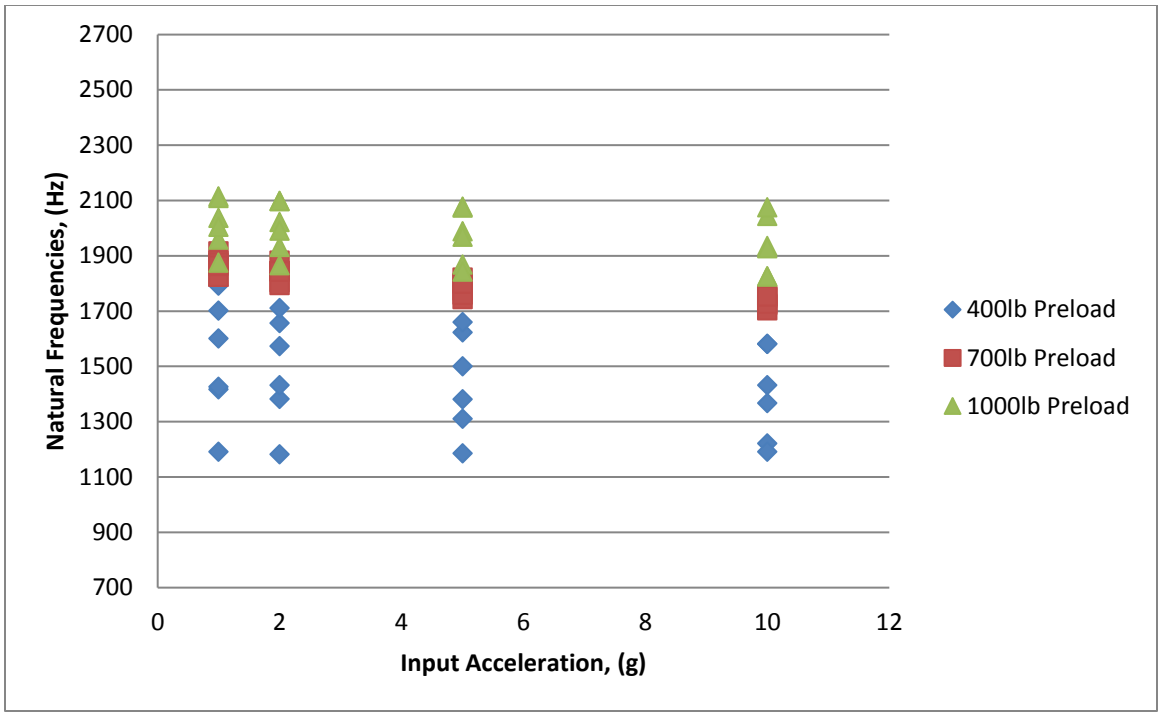

Figure 13: Distribution of Natural Frequency per Preload with a 1/8" Radial Gap and Preload through the Solid Mass Only.

When the preload goes through the solid mass only, the specimens with a 400lb preload have the largest spread in the values of natural frequency and the 700lb preload has the smallest, regardless of gap size. The natural frequencies for the specimens with a 400lb preload were lower than those of other preloads, but there is no consistency in the value of the natural frequencies for the other preloads. It is possible that once a threshold preload value is achieved, increasing the preload has no appreciable effect on the natural frequency. As when the preloads went through the solid mass and foam, the preload cannot be used to predict the natural frequency of the specimen. The 1/8" gap data yields results that are closest to the expected results, due to little or no effect of friction on the outer walls of the cylinder. With the large gap size, the system is approximately a simple oscillator along its axis between two rigid supports. In the other, smaller gap, cases the sidewall effects may be non-trivial.

When the preload goes through the foam and mass, the preload has no statistically significant effect on the variance of the natural frequency, indicating gap size does not affect the repeatability of the assembly process. When the load path goes through both the mass and the foam, the snugness of fit has an impact on the natural frequency. The smaller gap case has higher natural frequencies than the no gap case and the larger gap case has lower natural frequencies than the no gap case. When the load path goes through the mass alone, the natural frequency is higher in the case where there is no gap than in the cases where there are gaps. These results suggest that the snugness of fit has a larger effect on the stiffness of the system when the load path goes through the mass and the foam than when the load path goes through the mass only. Additionally, the uncertainty of the natural frequency is larger in the case of the preload going through the mass and the foam, likely due to the variation in the foam.

3.1.4.2. Effects of Preload on Energy Dissipation

The second parameter studied is the energy dissipation. Figure 14 through Figure 16 show the distribution of the energy dissipation of the specimen as a function of input acceleration and preload for specimens with a load path through the foam and solid mass. A power line is fit to the data to determine the coefficient of the energy dissipation equation.

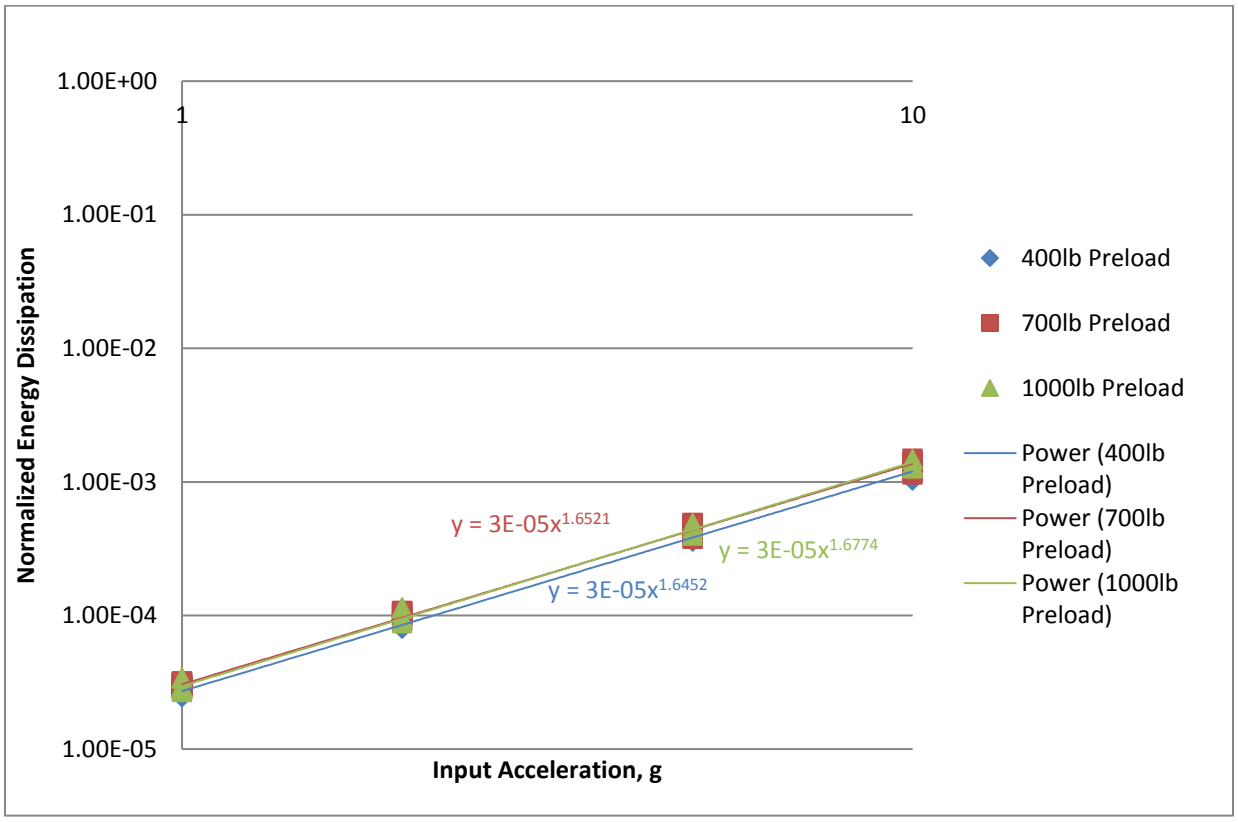

Figure 14: Distribution of Normalized Energy Dissipation per Preload with No Radial Gap and Preload through the Foam and Solid Mass.

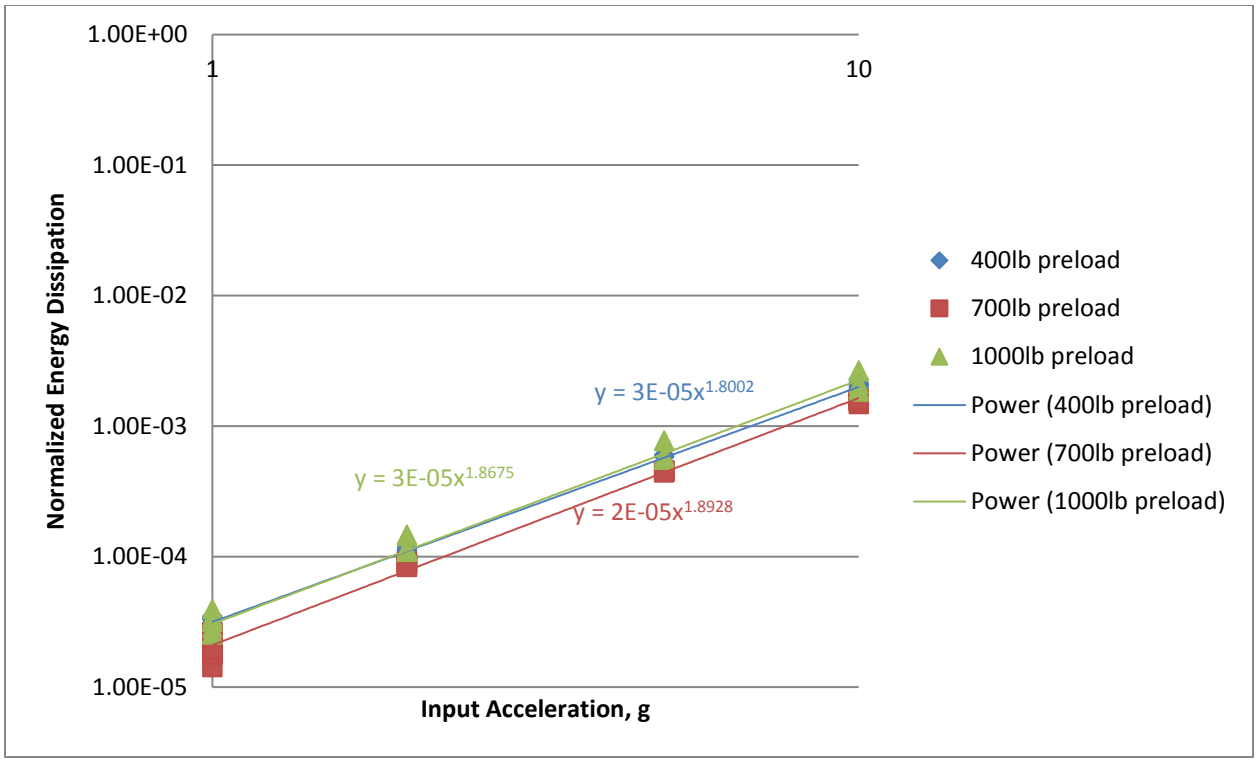

Figure 15: Distribution of Normalized Energy Dissipation per Preload with a 1/16" Radial Gap and Preload through the Foam and Solid Mass.

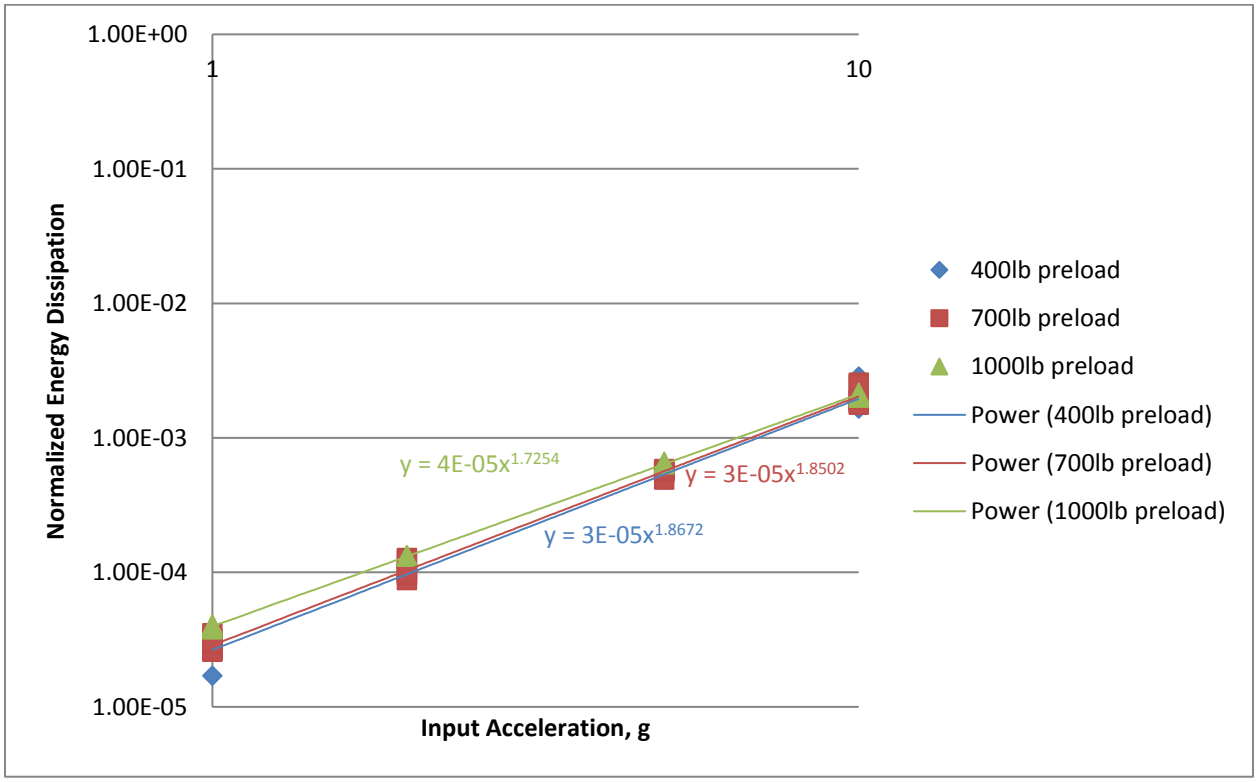

Figure 16: Distribution of Normalized Energy Dissipation per Preload with a 1/8" Radial Gap and Preload through the Foam and Solid Mass.

The amount of energy dissipation when the specimens that are preloaded through the foam and solid mass are fairly consistent. As done in previous studies [3-12], the normalized energy dissipation is plotted vs the input acceleration on a log-log plot. The data show the anticipated straight line, indicating a power law relationship between energy loss per cycle and the input acceleration. In the fitted results, the slope ranges from 1.65 to 1.89, where 2 is the theoretical value which would be obtained for a linear system with contact friction [3].

Figure 17 through Figure 19 show the distribution of the energy dissipation of the specimen as a function of input acceleration and preload for specimens with a load path through the solid mass only. Again, a power line is fit to the data to determine the coefficient of the energy dissipation equation.

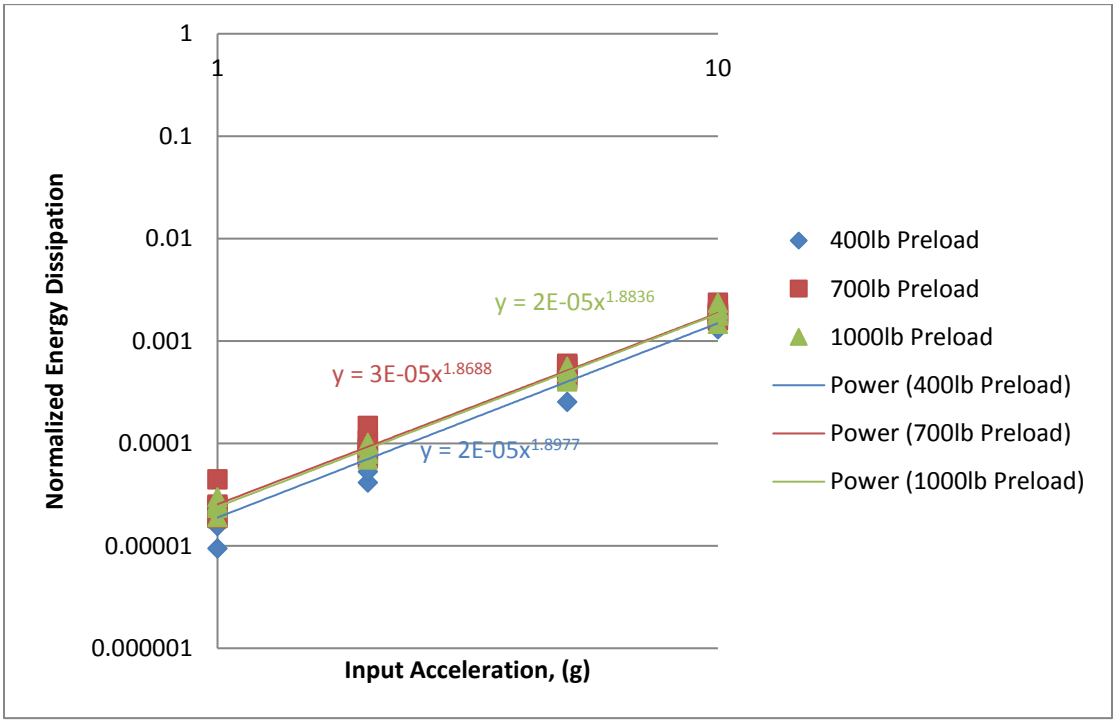

Figure 17: Distribution of Normalized Energy Dissipation per Preload with No Radial Gap and Preload through the Solid Mass Only.

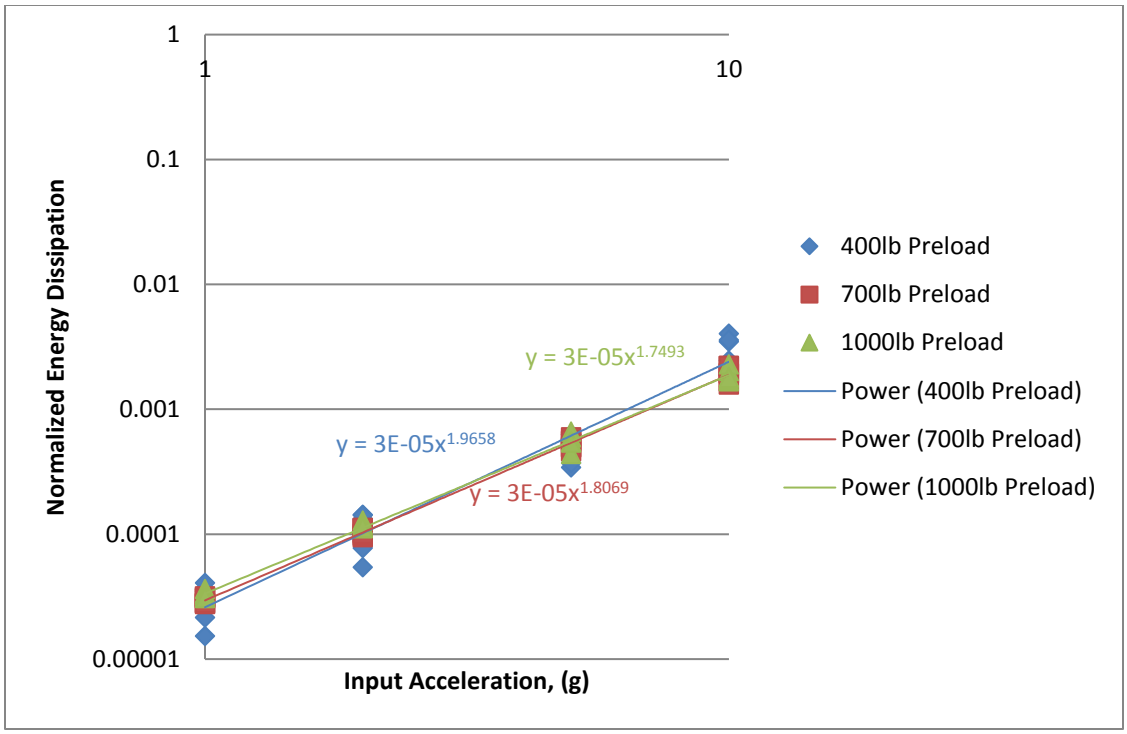

Figure 18: Distribution of Normalized Energy Dissipation per Preload with a 1/16" Radial Gap and Preload through the Solid Mass Only.

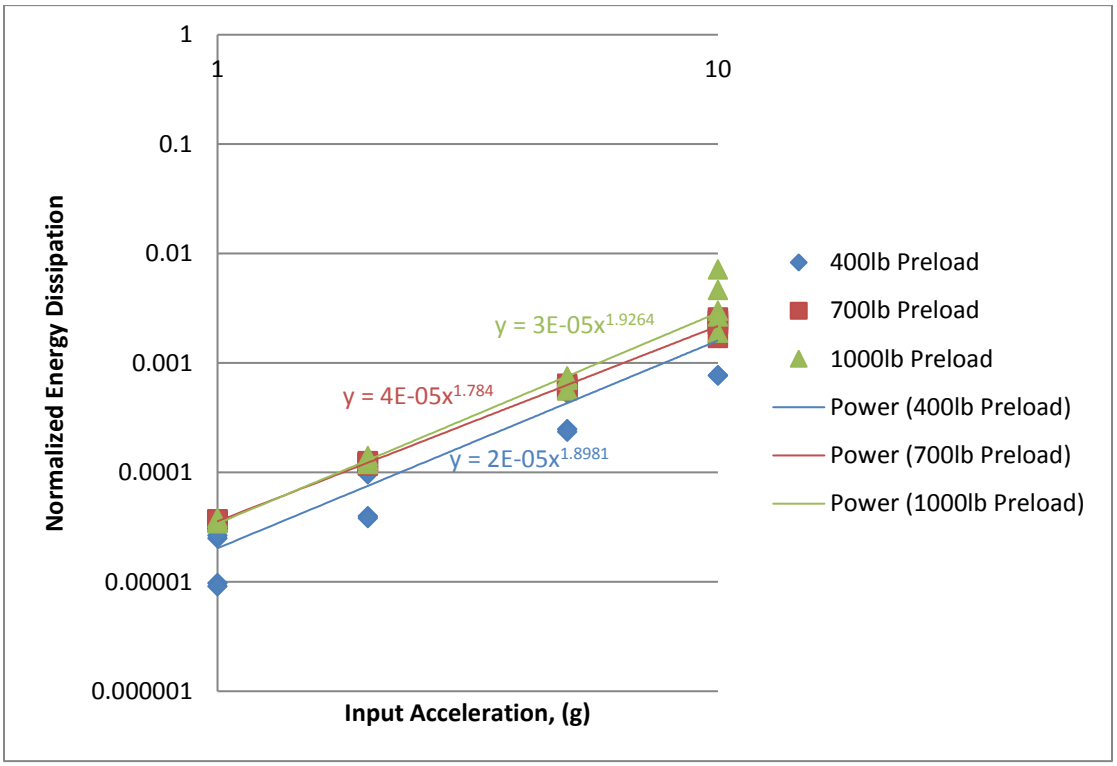

Figure 19: Distribution of Normalized Energy Dissipation per Preload with a 1/8" Radial Gap and Preload through the Solid Mass Only.

The amount of energy dissipation observed when the specimens are preloaded through the solid mass only and to a level of 700lbs or 1000lbs are consistent. The amount of energy dissipation of the 400lb preloaded specimens is either greater in the case of the 1/16" radial gap, or lower in the case of the other two solid mass sizes. Similar to the case of preload through the foam and solid mass, the data for the preload through the solid mass only show the anticipated straight line, indicating a power law relationship between energy loss per cycle and the input acceleration. The slope ranges from 1.75 to 1.97 in the fitted results. In both types of load paths, with the exception of the specimens with the 1/16" gap, energy dissipation increases with increasing preload. This result suggests that the increasing preload makes the energy dissipation more efficient, likely due to higher levels of load even as the preload is lost.

3.1.5. Effects of Snugness of Fit

As with assessing the effects of preload, when assessing the effects of snugness of fit on the dynamics of the system, two parameters are studied: the natural frequency and the normalized energy dissipation.

3.1.5.1. Effect of Snugness of Fit on Natural Frequency

The first parameter studied is the natural frequency. Figure 20 through Figure 22 show the distribution of the natural frequency of the specimen as a function of input acceleration and gap size for specimens with the preload path through the foam and solid mass.

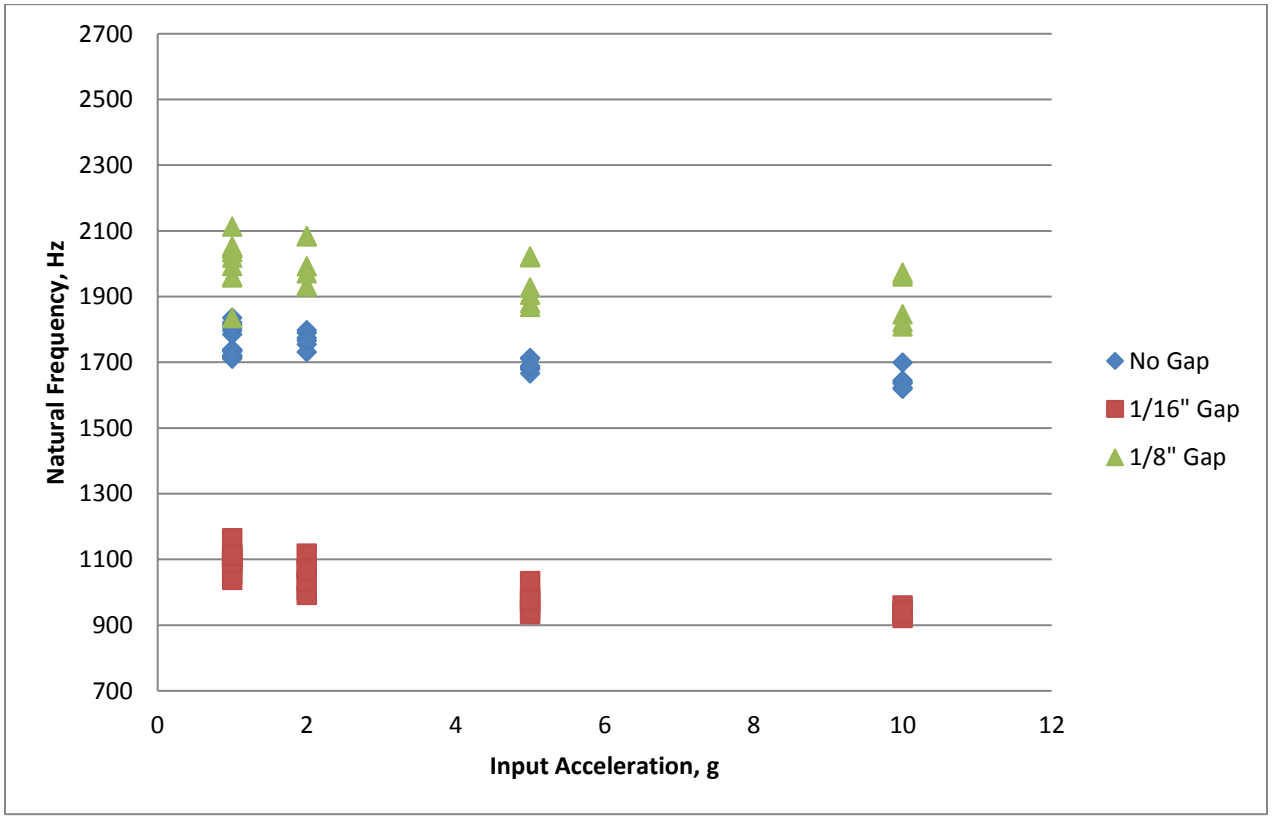

Figure 20: Distribution of Natural Frequency per Gap Size with a 400lb Preload through the Foam and Solid Mass.

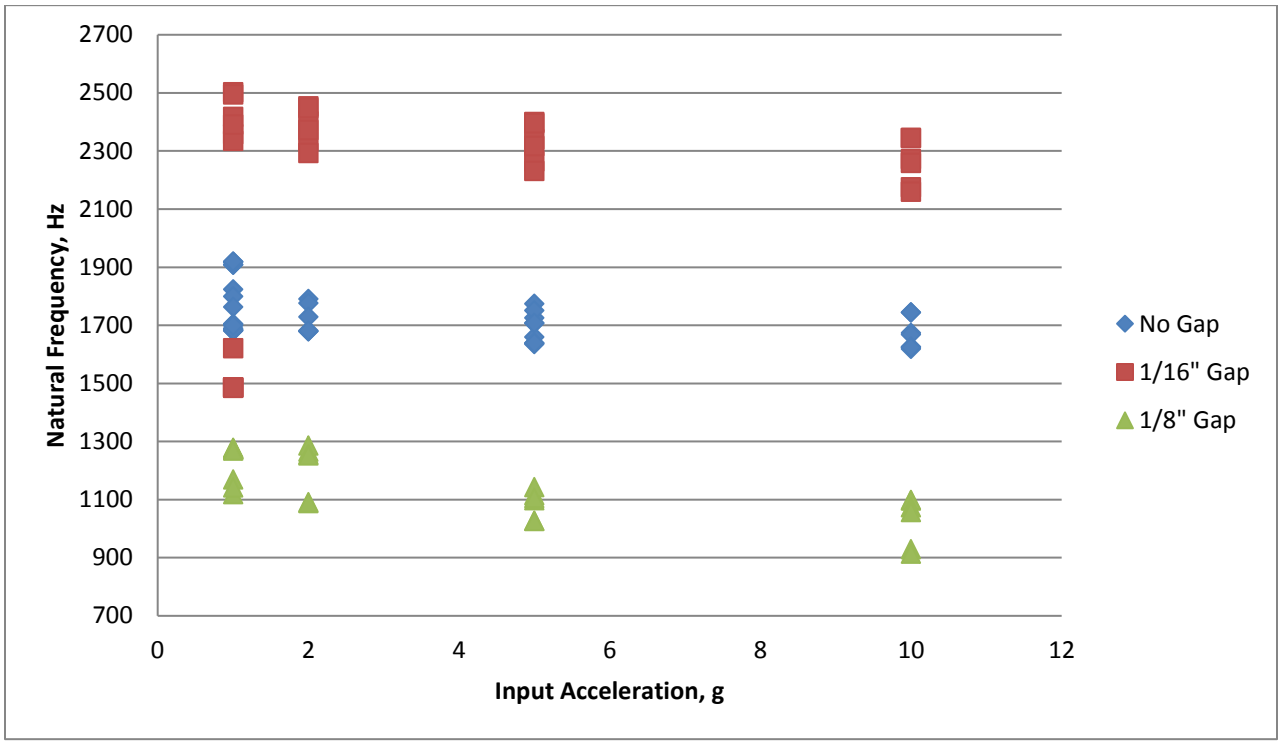

Figure 21: Distribution of Natural Frequency per Gap Size with a 700lb Preload through the Foam and Solid Mass.

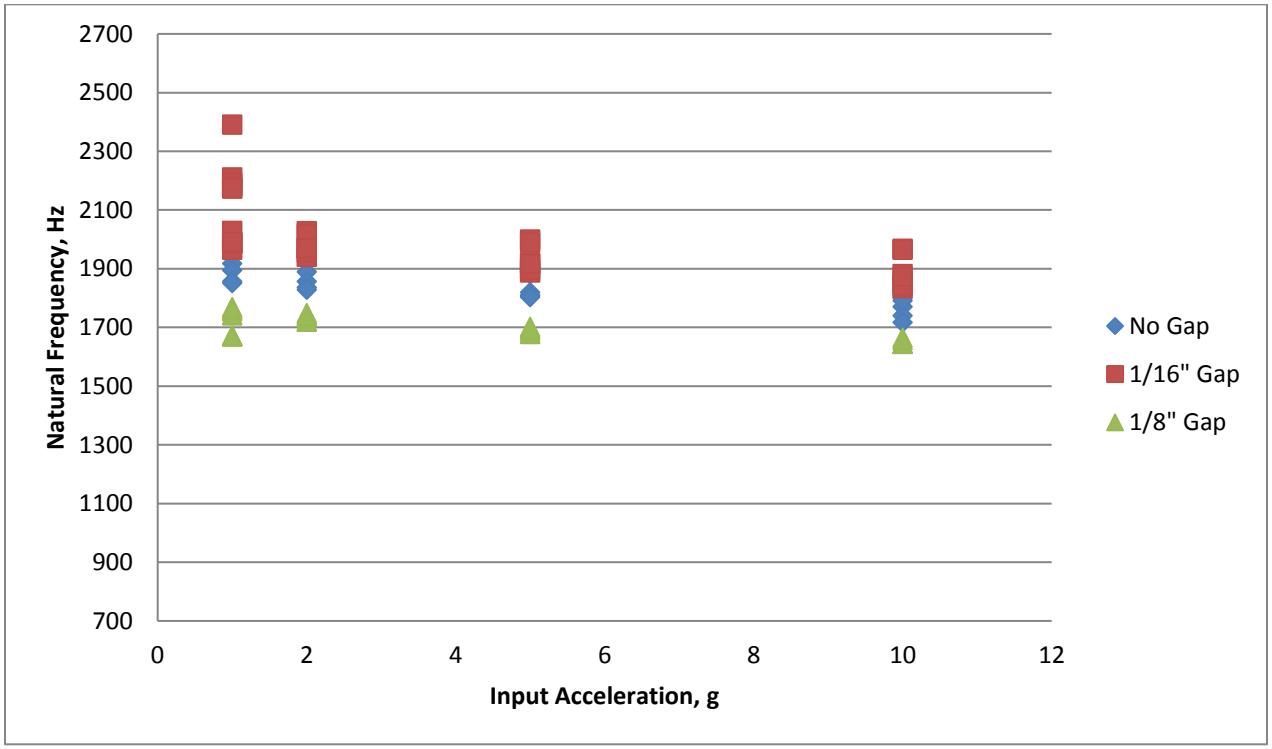

Figure 22: Distribution of Natural Frequency per Gap Size with a 1000lb Preload through the Foam and Solid Mass.

Regardless of the load path, the snugness of fit has no statistically significant effect on the variance of the natural frequency, indicating gap size does not affect the repeatability of the assembly process. When the load path goes through both the mass and the foam, the snugness of fit has an impact on the natural frequency. With the exception of the 400lb preload, when the gap size is 1/16 inches, the natural frequency is higher than when there is no gap. With the exception of the 400lb preload, the natural frequencies are lower when the gap size is 1/8th inches than either of the other two gap sizes.

Figure 23 through Figure 25 show the distribution of the natural frequency of the specimen as a function of input acceleration and gap size for specimens with the preload path through the solid mass only. When the preload goes through the solid mass only, the specimens show no appreciable difference in the distribution of natural frequencies and the values of the natural frequencies.

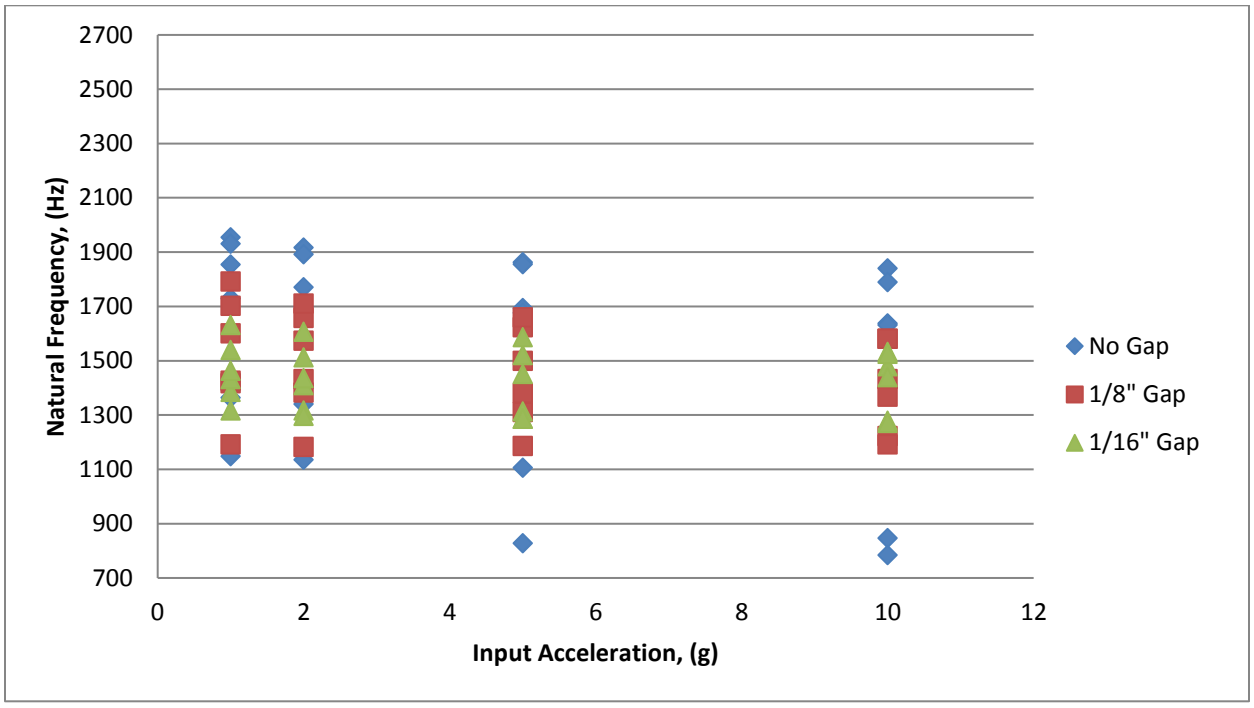

Figure 23: Distribution of Natural Frequency per Gap Size with a 400lb Preload through the Solid Mass Only.

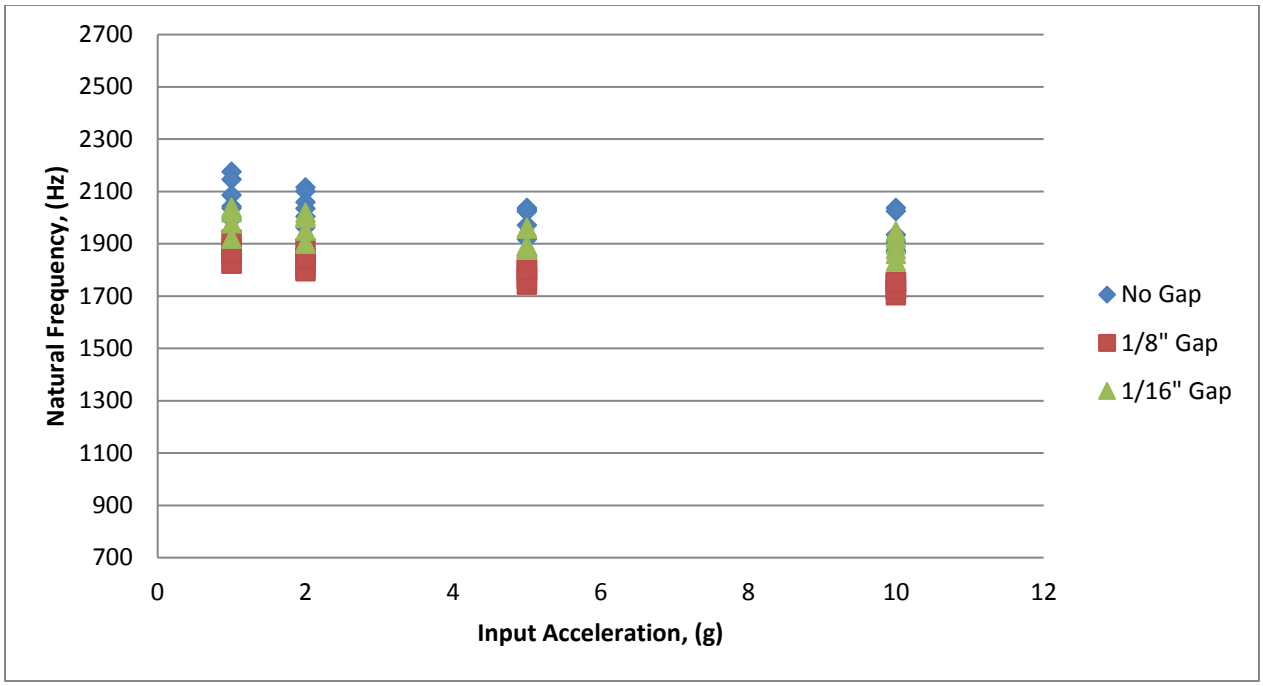

Figure 24: Distribution of Natural Frequency per Gap Size with a 700lb Preload through the Solid Mass Only.

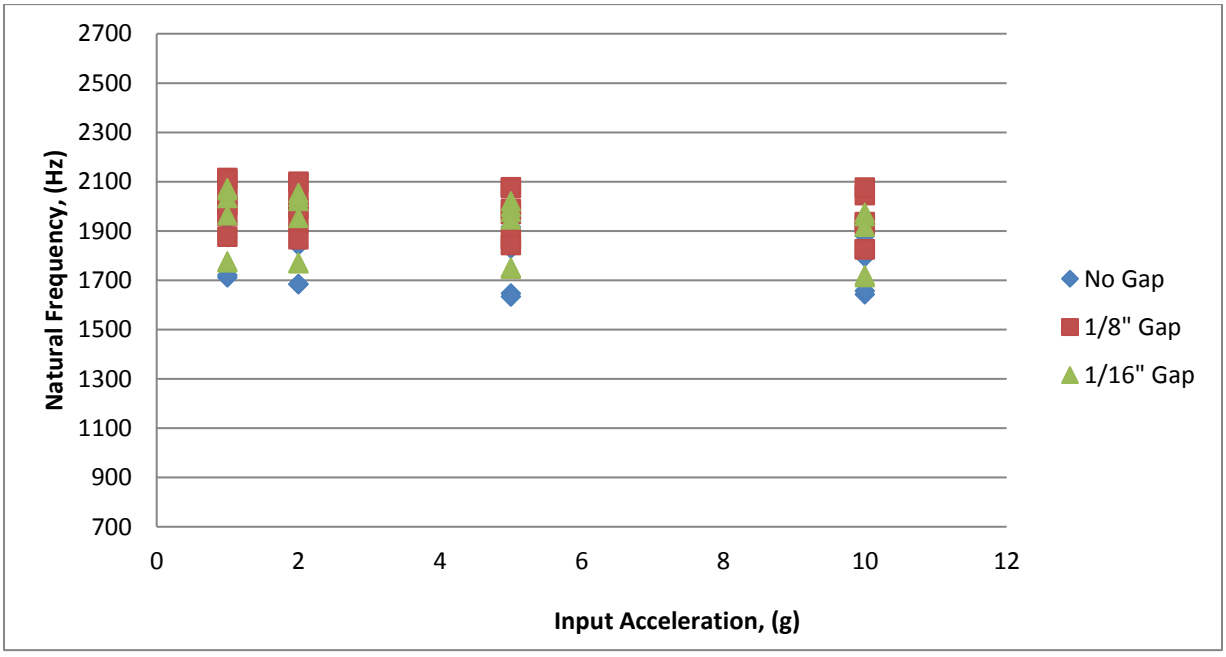

Figure 25: Distribution of Natural Frequency per Gap Size with a 1000lb Preload through the Solid Mass Only.

When the load path goes through the mass only, the snugness of fit has no appreciable effect on the variance of the natural frequency. Additionally, the natural frequency is higher in the case where there is no gap than in the cases where there are gaps. These results suggest that the snugness of fit has a larger

effect on the stiffness of the system when the load path goes through the mass and the foam than when the load path goes through the mass only. Additionally, the uncertainty of the natural frequency is larger in the case of the preload going through the mass and the foam. For modeling implications, if the item does not fit snugly in the foam, it is not critical to know how loose it is to determine the natural frequency of the foam/item system when the load path is through the part alone.

3.1.5.2. Effect of Snugness of Fit on Energy Dissipation

The second parameter studied is the energy dissipation. Figure 26 through Figure 28 show the distribution of the energy dissipation of the specimen as a function of input acceleration and preload for specimens with a load path through the foam and solid mass. A power line is fit to the data to determine the coefficient of the energy dissipation equation. The amount of energy dissipation when the specimens that are preloaded through the foam and solid mass is greater for the specimens that include a radial gap than the specimens that contained no radial gap. In all cases the energy dissipation coefficient is close to 2.

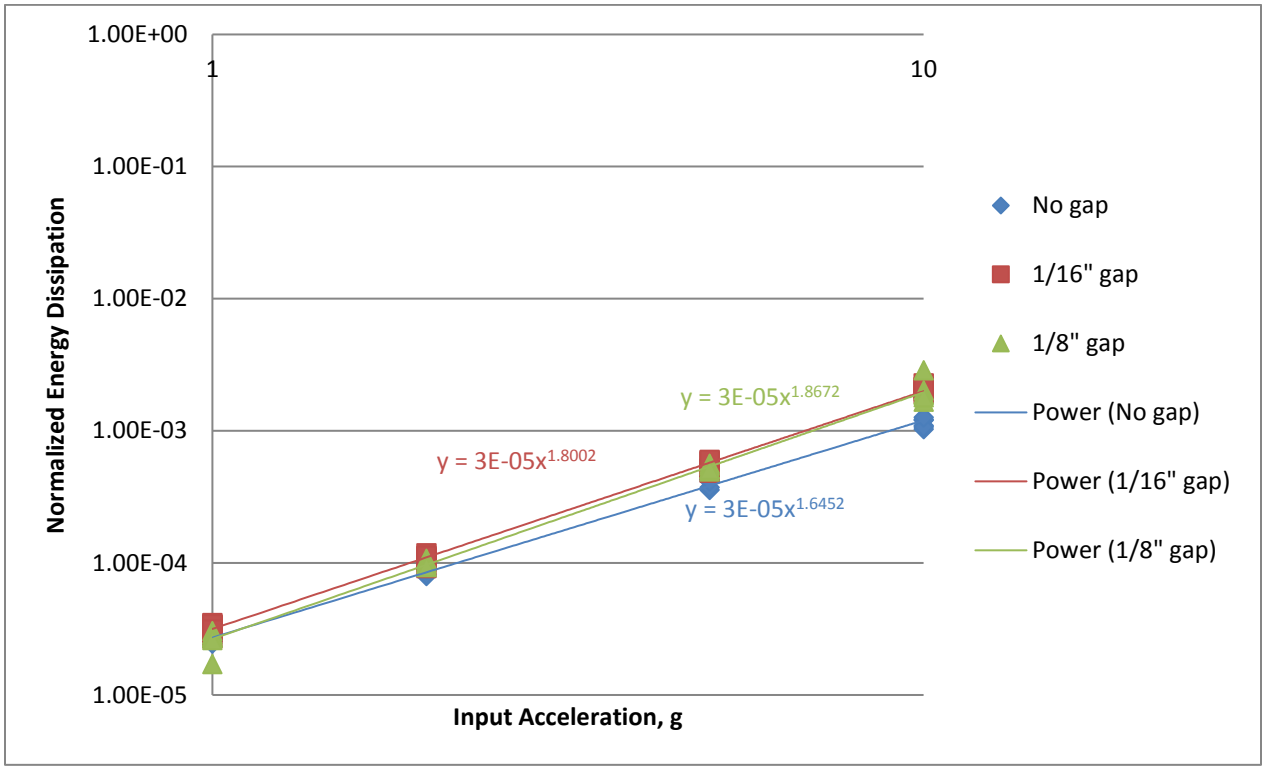

Figure 26: Distribution of Normalized Energy Dissipation per Gap Size with a 400lb Preload through the Foam and Solid Mass.

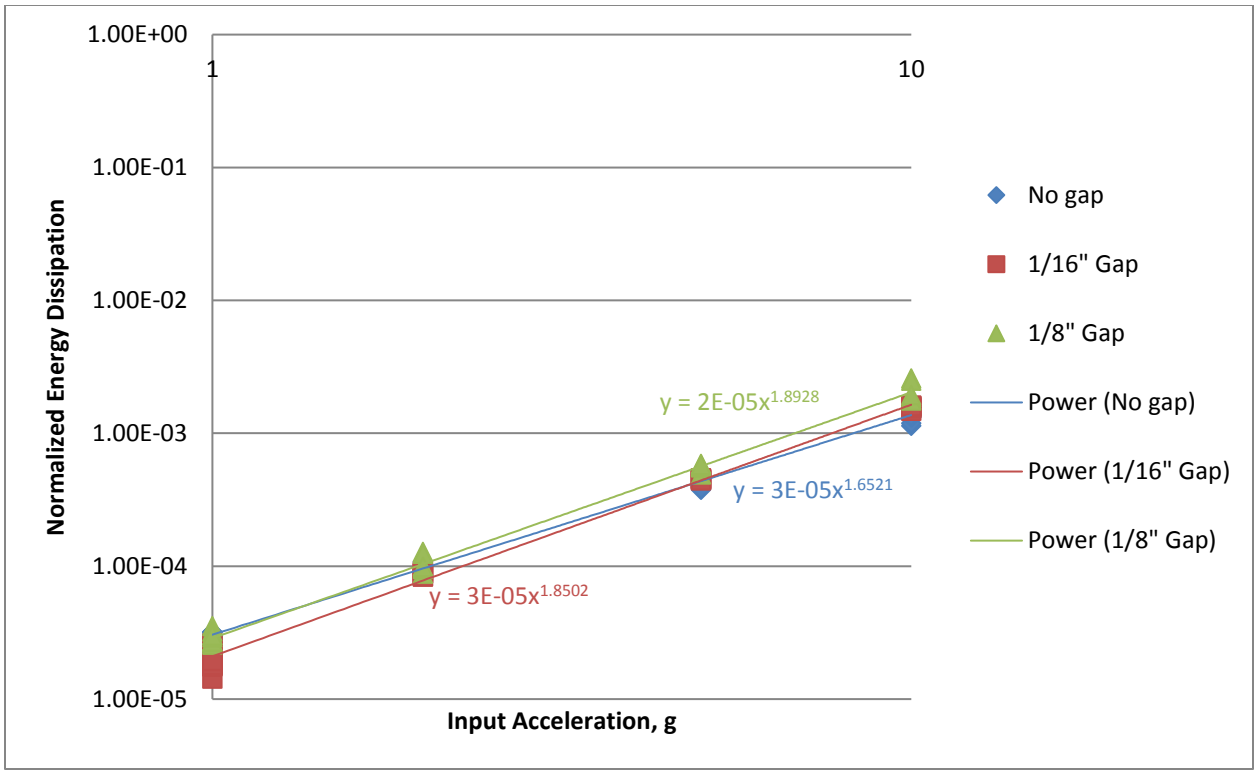

Figure 27: Distribution of Normalized Energy Dissipation per Gap Size with a 700lb Preload through the Foam and Solid Mass.

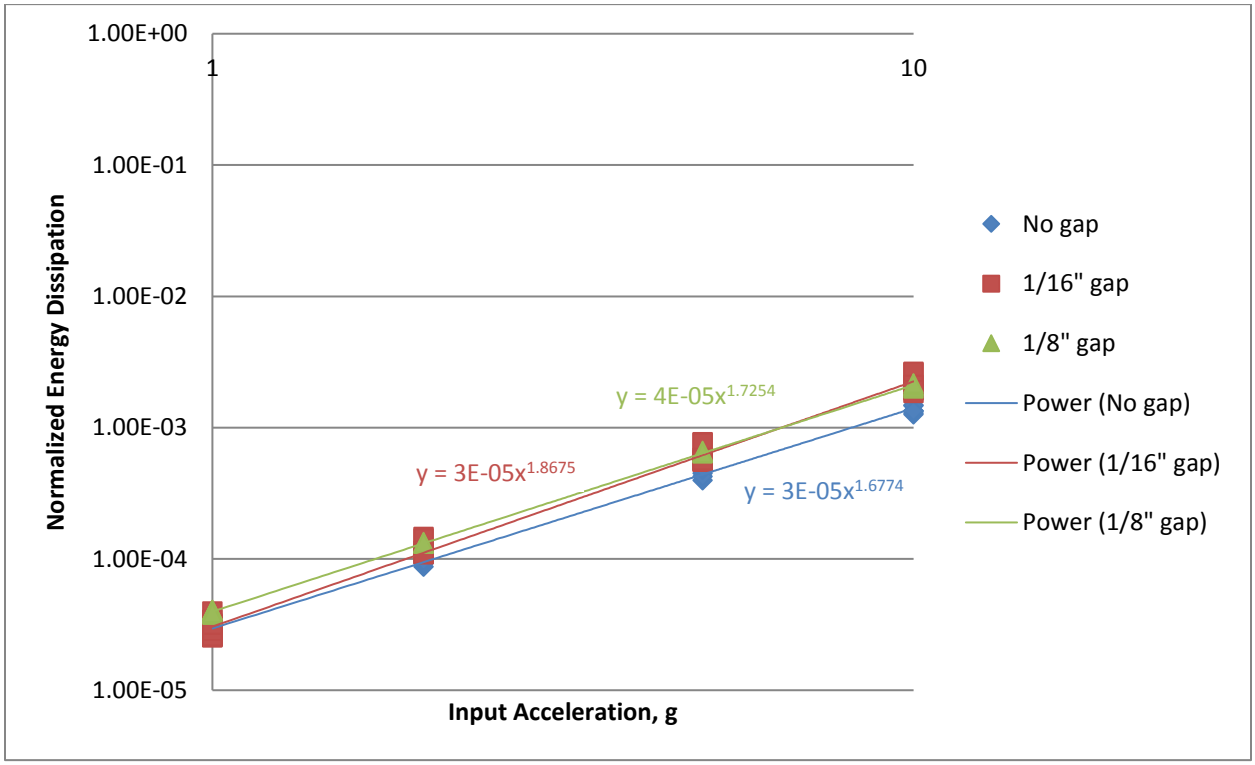

Figure 28: Distribution of Normalized Energy Dissipation per Gap Size with a 1000lb Preload through the Foam and Solid Mass.

These results show that the presence of a gap (but not necessarily the magnitude of the gap) has an effect on the energy dissipation. The amount of energy dissipated when the specimens are preloaded through the foam and solid mass is greatest when there is a radial gap. One hypothesis for this could be that when there is no gap between the foam and solid mass, the large amount of sliding friction prevents the mass from moving within the container. However, when this large frictional interface is removed with a radial gap, the mass has less resistance to motion and is more likely to impact with the top and bottom surfaces of the foam; these impacts likely dissipate energy differently than sliding friction alone. There will still be some friction along the length of the mass, due to contact along the sides. Additionally, the mass is able to slide laterally with the cross-axis motion of the shaker, introducing a different frictional interface. Finally, the mass and foam are no longer confined as they are when the mass snugly fits in the foam, allowing for additional motion and deformation of the foam and mass due to the lack of confinement. In summary, there are additional mechanisms of energy dissipation that occur when there is a radial gap, so it is not surprising that there is more energy dissipation in those cases. For modeling implications, these results suggest that it is important to understand the amount of friction that occurs between the contacting surfaces but also the coefficient of restitution for impacts.

As done in previous studies [3-12], the normalized energy dissipation is plotted vs the input acceleration on a log-log plot. The data show the anticipated straight line, indicating a power law relationship between energy loss per cycle and the input acceleration. In the fitted results, the slope ranges from 1.65 to 1.89, where 2 is the theoretical value of for a linear system with contact friction [3].

Figure 29 through Figure 31 show the distribution of the energy dissipation of the specimen as a function of input acceleration and preload for specimens with a load path through the solid mass only. A power line is fit to the data to determine the coefficient of the energy dissipation equation. The amount of energy dissipation when the specimens that are preloaded through the solid mass only are preloaded to 700lbs or 1000lbs is larger for the case of the specimen with the 1/8” radial gap. The amount of energy dissipation of the 400lb preloaded specimens is greater in the case of the 1/16” radial gap. In all cases the energy dissipation coefficient is close to 2.

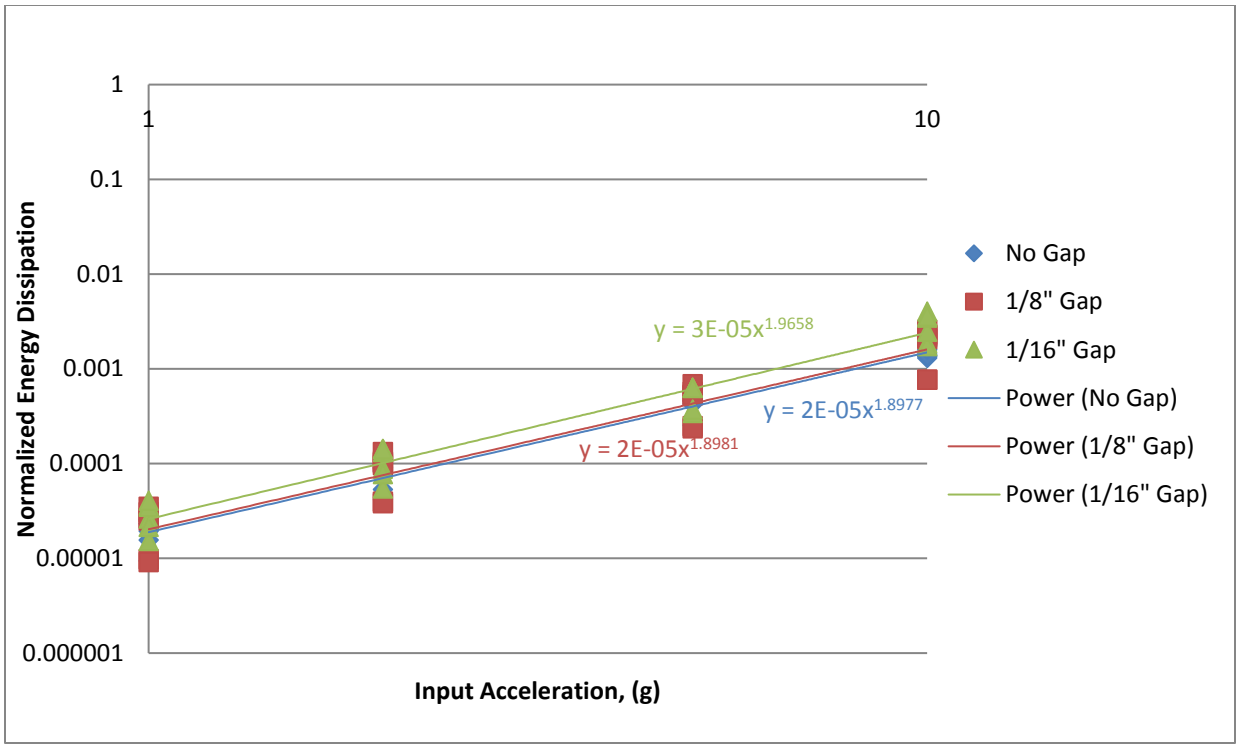

Figure 29: Distribution of Normalized Energy Dissipation per Gap Size with a 400lb Preload through the Solid Mass Only.

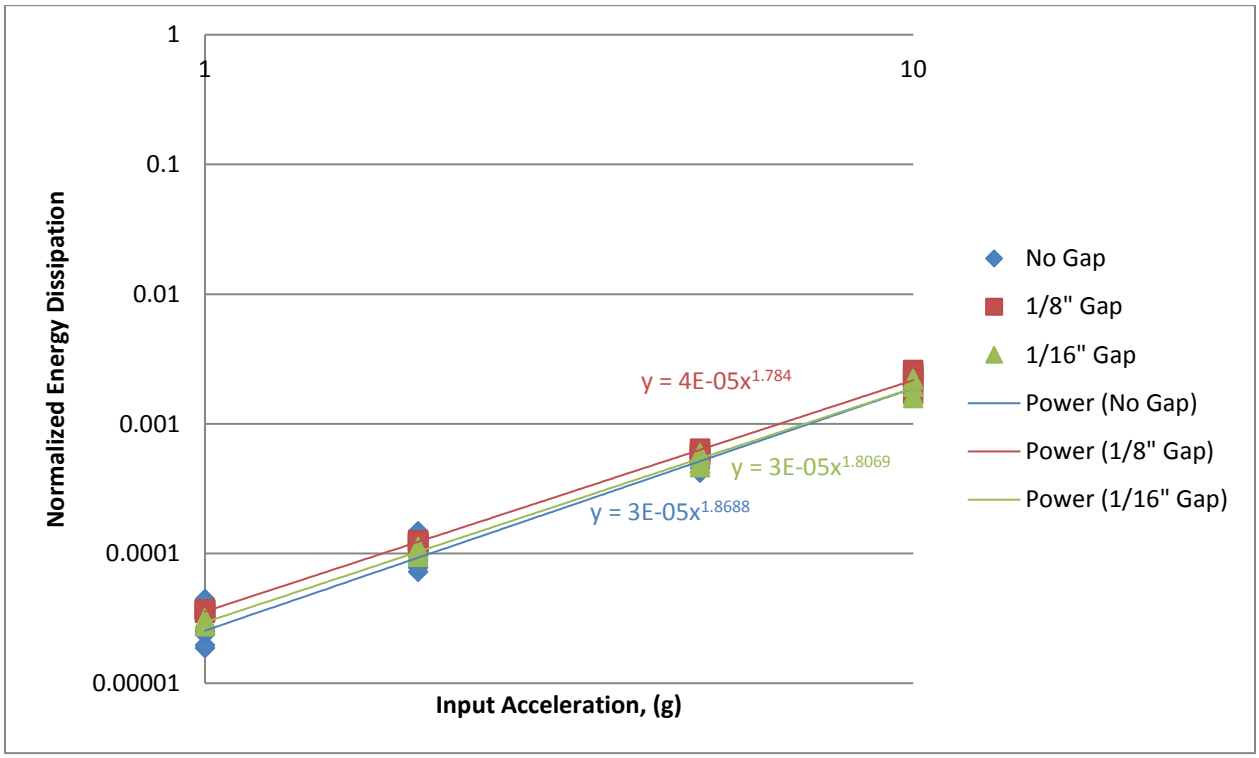

Figure 30: Distribution of Normalized Energy Dissipation per Gap Size with a 700lb Preload through the Solid Mass Only.

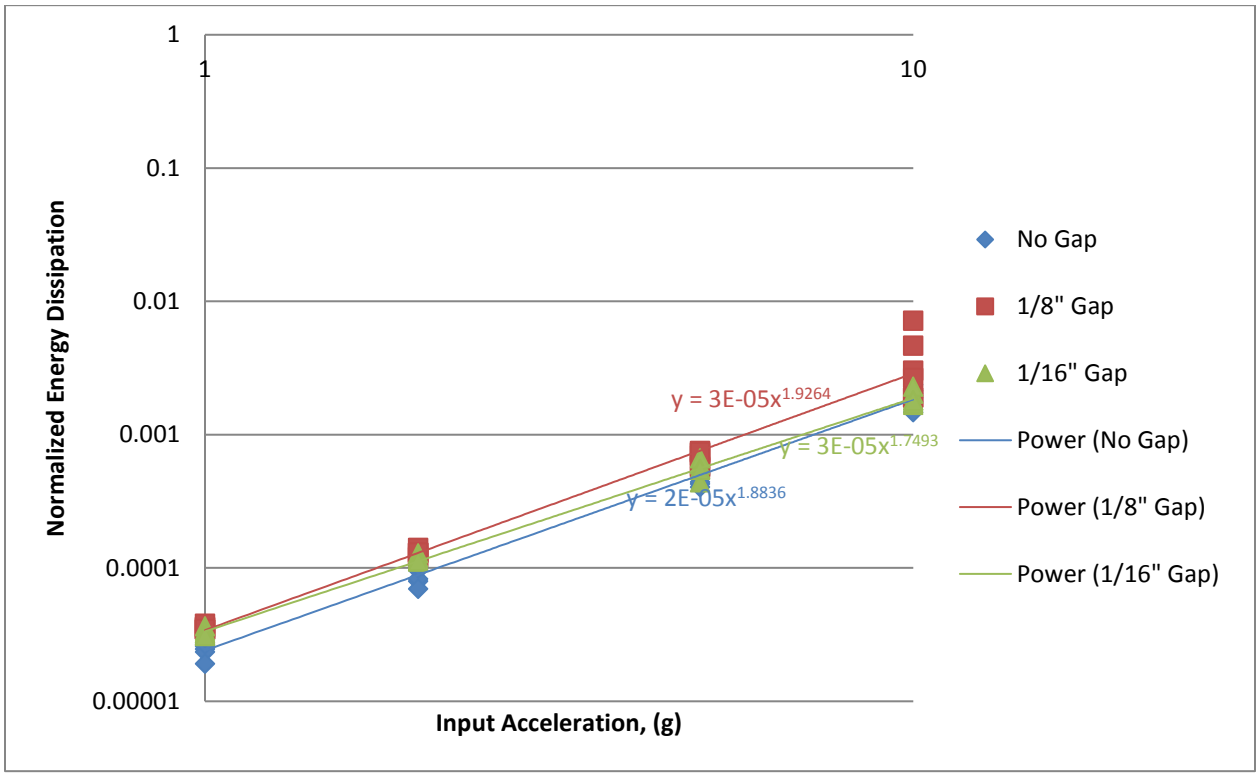

Figure 31: Distribution of Normalized Energy Dissipation per Gap Size with a 1000lb Preload through the Solid Mass Only.

3.1.6. Effects of Load Path

The effects of the load path on the experiments are considered for the natural frequency, the energy dissipation and the amplitude and sweep order. The following paragraphs will discuss the data and their implications.

The load path has no effect on the natural frequency (data shown in Section 3.1.4 and 3.1.5). The spread of natural frequencies and the values of the natural frequencies are consistent regardless of load path. The consistency of the natural frequencies indicates that the stiffness of the oscillator is primarily governed by the stiffness of the solid mass. The consistency of the variation of the natural frequency when the load path goes through the foam and when it goes through the solid mass only indicates that the variation of natural frequency has to do with the variations in assembly. The implication to modeling is that the uncertainty from the assembly process dominates the uncertainty in the natural frequency, and the material uncertainty in the foam plays a smaller role.

The load path has an effect on the energy dissipation (data shown in Sections 3.1.4 and 3.1.5). The exponent of the curves fitted to the normalized energy dissipation is larger, and closer to two, when the load path is through the solid mass only rather than through the foam and solid mass. There is more energy dissipation when the preload is through the solid mass only and not through the foam interfaces.

This result indicates that the energy dissipation mechanism is more efficient when the load path does not go through the foam interface. It is likely that there is some separation and reconnection of the foam interface during vibration causing the less efficient energy dissipation than if the foam interface did not exist.

The load path has an effect on the significance of the sweep order of the test (data shown in Section 3.1.4 and 3.1.5). When the load path is through the foam and the solid mass, there is a change in the natural frequency and the energy dissipation amount for the same amplitude the second time through the sweep series when starting at 1g and going to 10g. However, when the sweep series starts at 10g and goes to 1g, there is no change in the natural frequency and the energy dissipation. When the load path goes through the solid mass only, there is a change in the natural frequency and energy dissipation regardless of the order of the sweeps. This result suggests that at the higher amplitudes there is a loss of preload. The loss of preload is larger and consistent in the foam, so when the load path goes through the foam, there is no more change after the specimen is exposed to a 10g sine sweep. However, when the load path goes through the solid mass only, the system continues to change, indicating that the loss of preload continues to change as the system is vibrated at different levels.

3.2 Lateral Tests: Sinusoidal Excitation, Upward Sweep Only

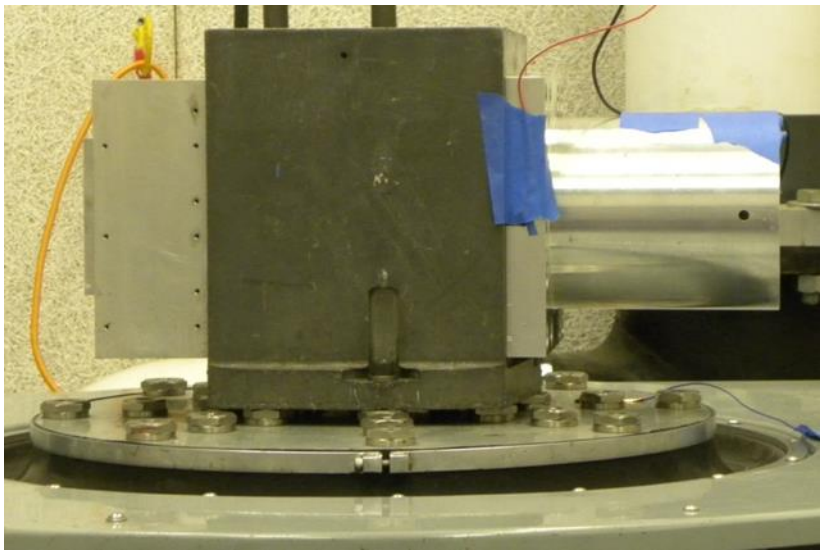

Figure 32: Test Article on Shaker in Bending Testing Orientation

3.2.1 Effects of Amplitude

This subsection shows the resulting transfer functions for the three test sequences in Table 1 on the configuration with the foam cup depth of 2 inches and the solid mass diameter of 3 inches (i.e. no gap). In this configuration, the load path goes through both the foam and the solid mass and the solid mass fits snugly into the foam cups. The results for the test sequences shown in Figure 33 through Figure 35 show that the natural frequency decreases and the amount of energy dissipation increases as the excitation amplitude increases. The frequency shifts suggest that the foam to metal interface loses stiffness at high excitation levels, likely due to micro- or possibly macro-slip. The impacts and the friction between the frictional interfaces introduce nonlinear energy dissipation observed at higher excitation levels.

When starting the test series at 1g and increasing the amplitude to 10g, the natural frequency from the second run is approximately the same as the first; and the amount of energy dissipation is lower. This phenomena can be seen in the data in both Figure 33 and Figure 34. Conversely, when starting the test series at 10g and decreasing the amplitude down to 1g, there is no appreciable difference in the natural frequency and energy dissipation as seen in Figure 35. One hypothesis for this behavior could be attributed to the higher amplitude sine sweeps causing wear or loss of preload in Ministack. Going from the 1g to 10 g sweeps and repeating, the settling position of the solid mass after the 10g run may be different than the initial 1g run. This could explain why the stiffness and the damping in the transfer functions during the second runs shifted a noticeable amount. It should also be noted that the magnitude of the response of the system changes a nearly imperceptible amount from assembly to assembly, which indicates a consistency in the assembly process.

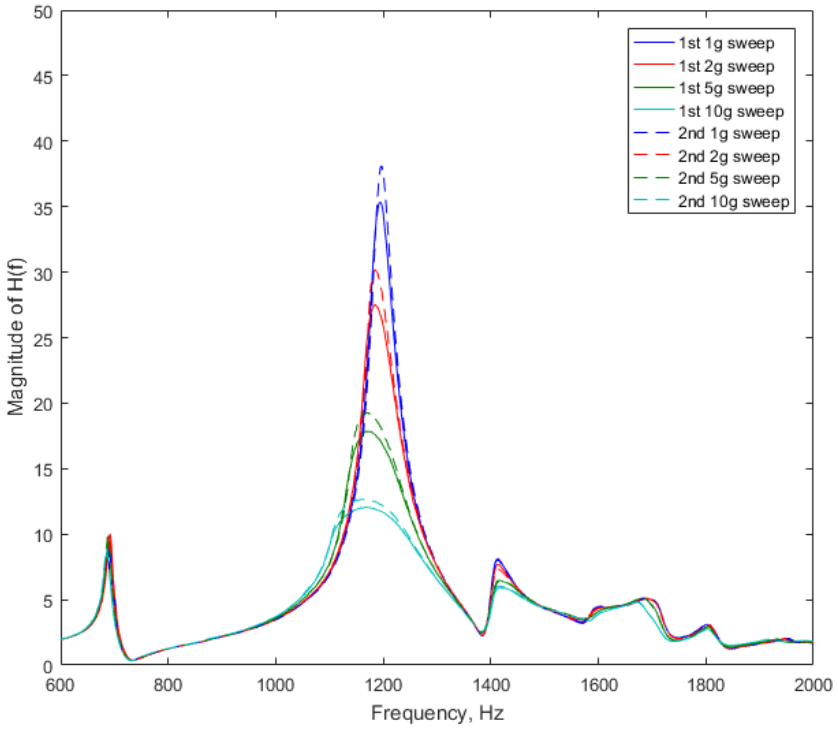

Figure 33: Transfer Functions for a Specimen Preloaded to 700lbs Through Foam and Solid Mass, Assembly 1.

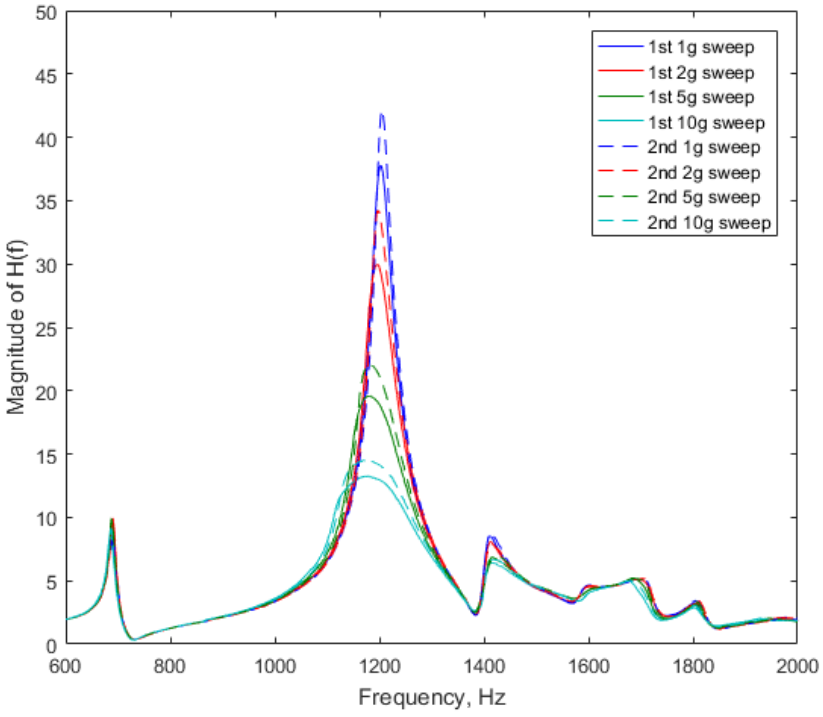

Figure 34: Transfer Functions for a Specimen Preloaded to 700lbs Through Foam and Solid Mass, Assembly 2.

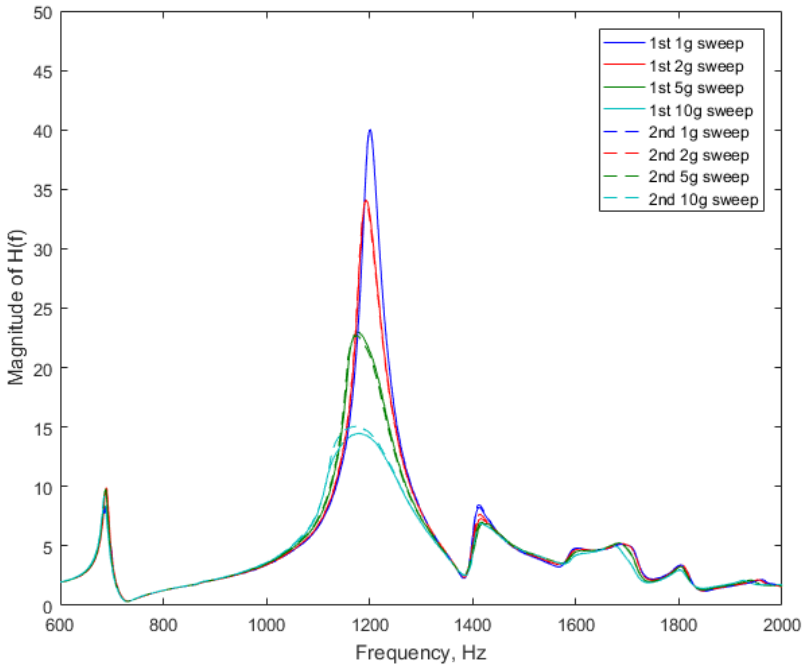

Figure 35: Transfer Functions for a Specimen Preloaded to 700lbs Through Solid Mass Only, Assembly 3.

3.2.2 Effects of Preload

As with the axial tests, in assessing the effects of preload on the dynamics of the system, two parameters are studied: the natural frequency and the normalized energy dissipation.

3.2.2.1 Effects of Preload on Natural Frequency

The first parameter studied is the natural frequency. Figure 36 through Figure 38 show the distribution of the natural frequency of the specimen as a function of input acceleration and preload for specimens with the preload path through the foam and the solid mass.

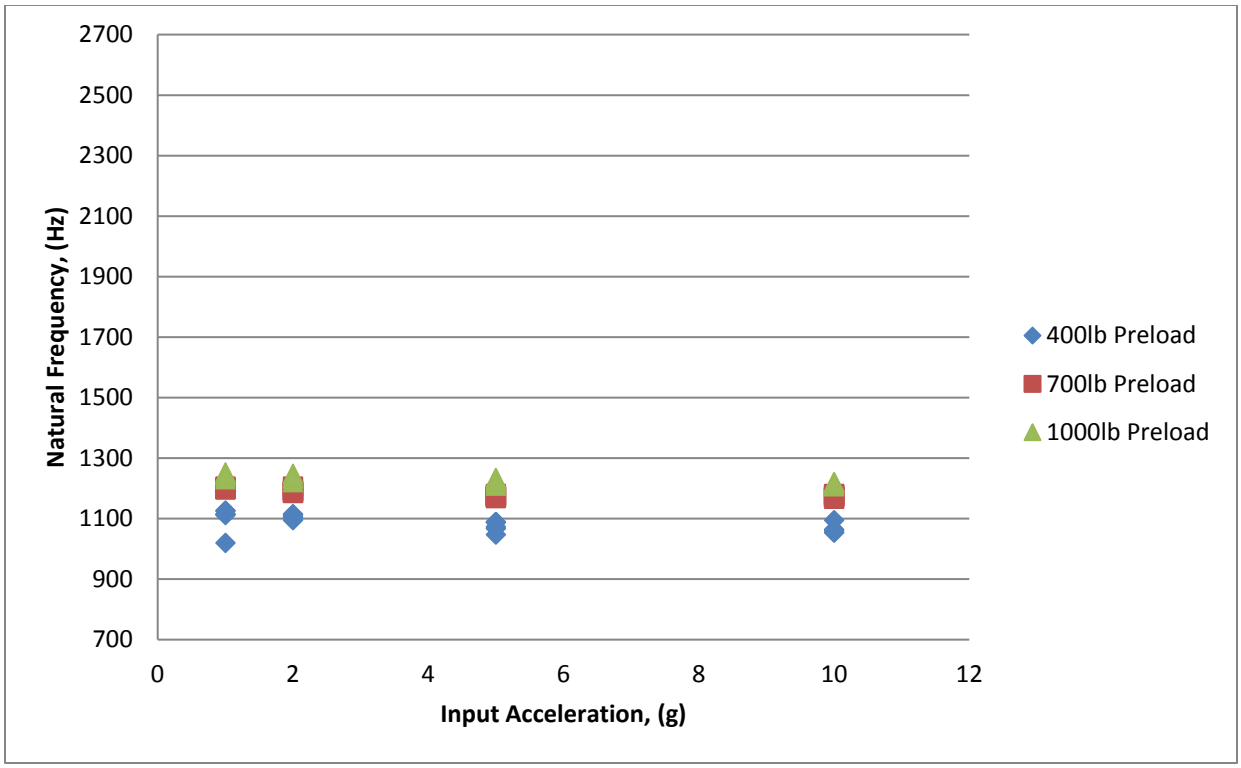

Figure 36: Distribution of Natural Frequency per Preload with No Radial Gap and Preload through the Foam and Solid Mass.

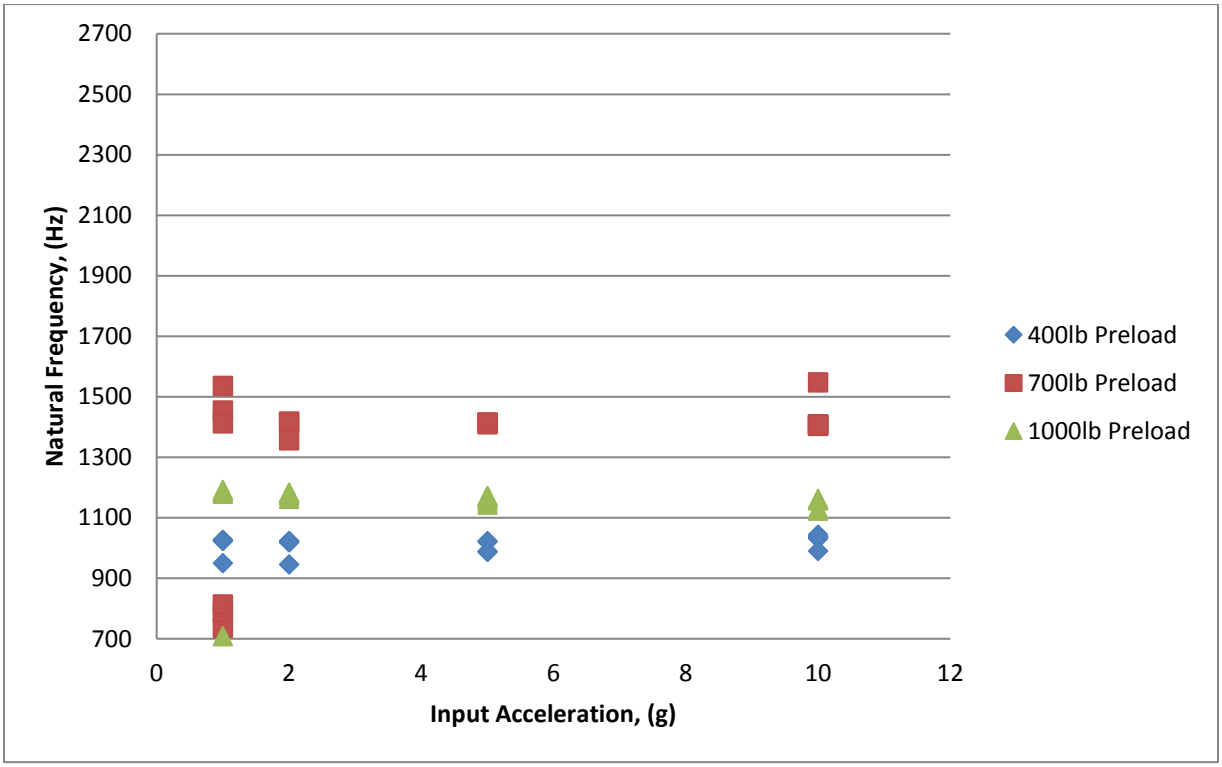

Figure 37: Distribution of Natural Frequency per Preload with a 1/16" Radial Gap and Preload through the Foam and Solid Mass.

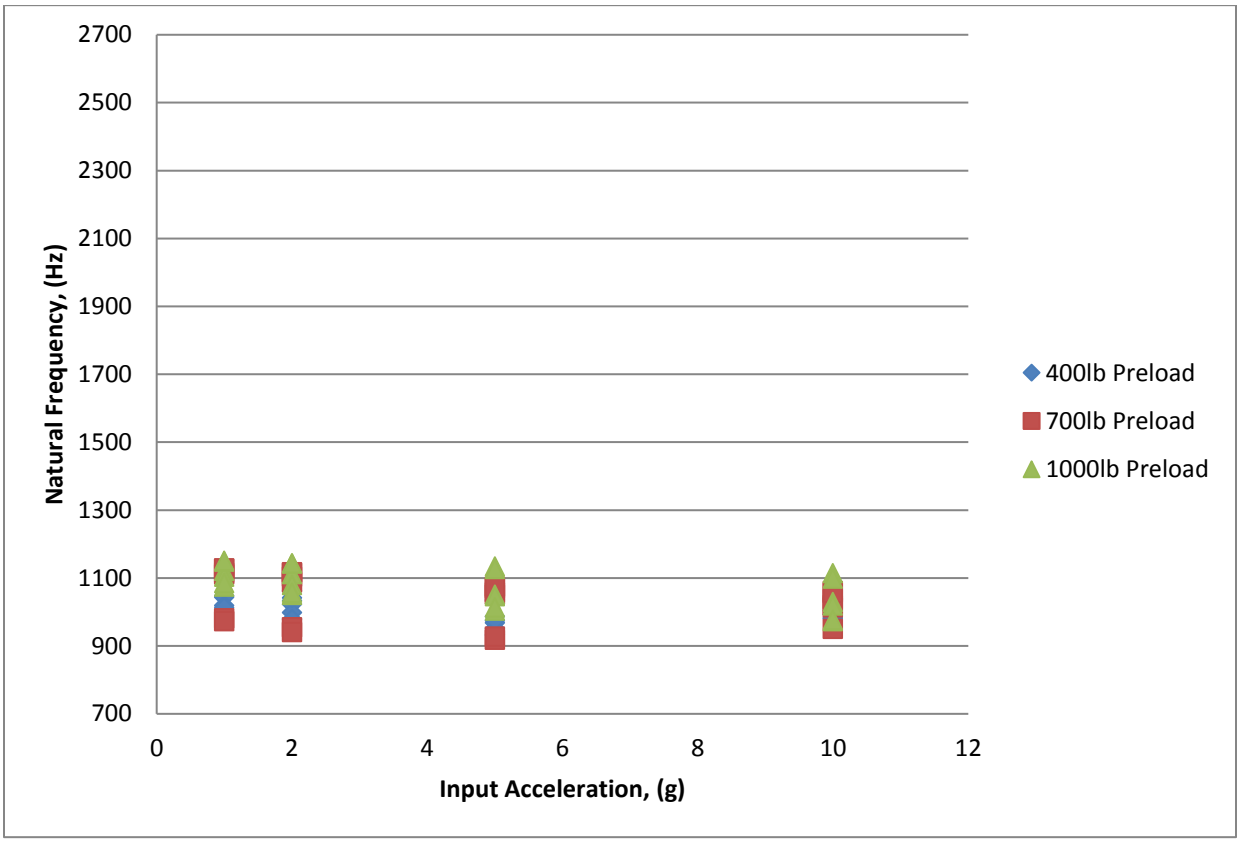

Figure 38: Distribution of Natural Frequency per Preload with a 1/8" Radial Gap and Preload through the Foam and Solid Mass.

When the preload goes through the foam and the solid mass, for the preload of 400lbs and 1000lbs the variation of the natural frequency is fairly consistent regardless of the gap size. For the 700lb preload, the variation of the natural frequency is consistent with the other preloads for the no gap case and the 1/8" gap case. For the 1/16" gap case, there is significantly more spread in the values of the natural frequency. It is not clear why this combination produced a response that is out of family with the rest. Since this is the only combination of preload, load path, and gap size where this occurred, this results suggests that there was something unique about the foam cups used for this assembly. Perhaps the slip-stick friction at the foam-foam interface of this particular set of specimens led to this out of family response.

There is overlap in the values for the natural frequency among all of the preloads, suggesting that the preload cannot be a reliable predictor of the system stiffness and therefore the natural frequency. Additionally, although there are shifts in the natural frequency as the amplitude of excitation is increased, it is within the variation of natural frequency seen at a given input acceleration. Therefore, the changes in natural frequency seen due to amplitude changes can be accounted for in models within the uncertainty for the value of the natural frequency itself.

Figure 39 through Figure 41 show the distribution of the natural frequency of the specimen as a function of input acceleration and preload for specimens with the preload path through the solid mass only.

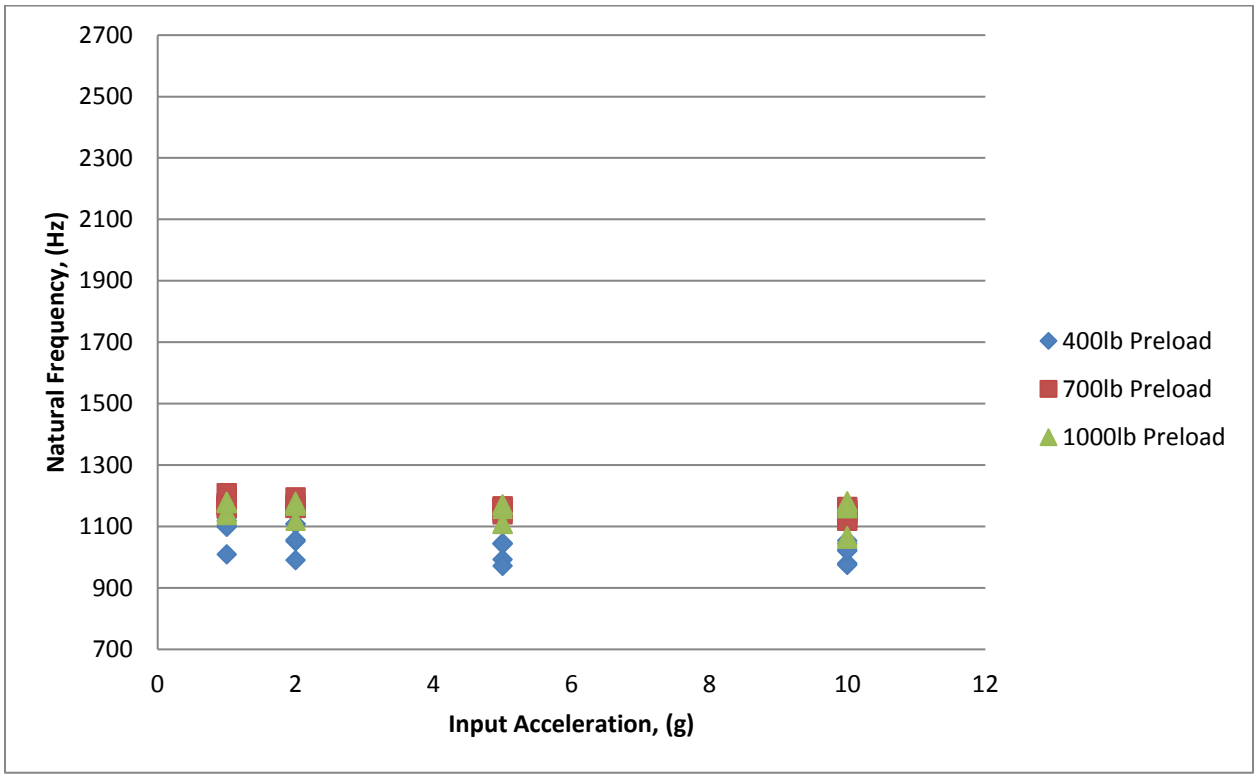

Figure 39: Distribution of Natural Frequency per Preload with No Radial Gap and Preload through the Solid Mass Only.

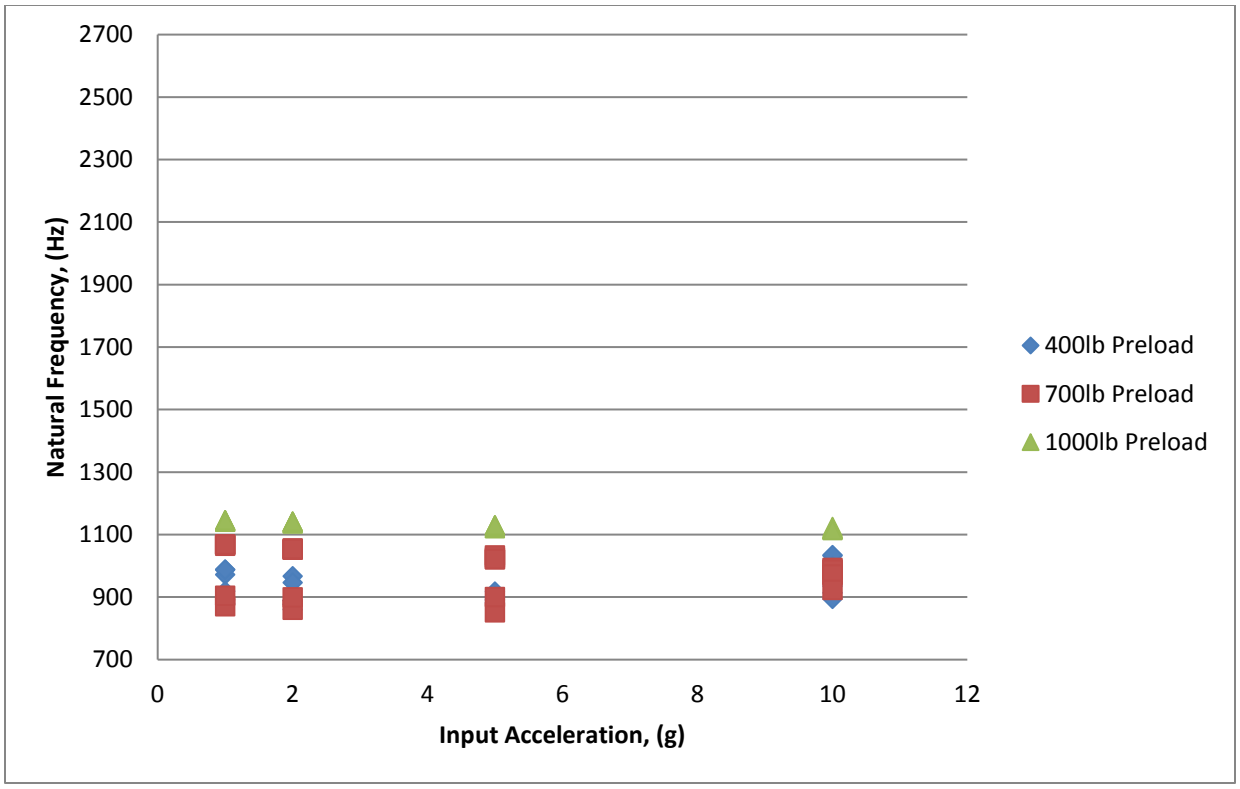

Figure 40: Distribution of Natural Frequency per Preload with a 1/16" Radial Gap and Preload through the Solid Mass Only.

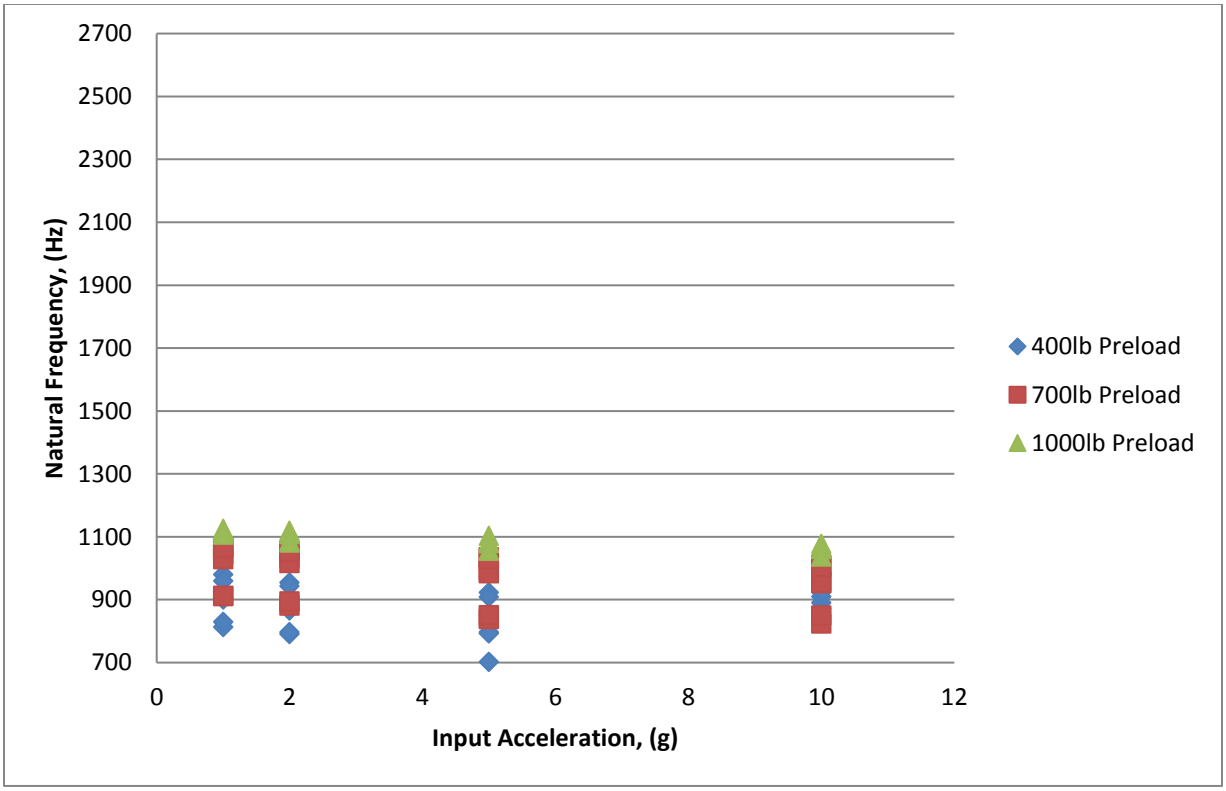

Figure 41: Distribution of Natural Frequency per Preload with a 1/8" Radial Gap and Preload through the Solid Mass Only.

When the preload goes through the solid mass only, the variation of the natural frequency is consistent regardless of the preload and gap size. There is overlap in the values of the natural frequency among all of the preloads, reinforcing what was seen in the other experiments in this study, suggesting that the preload is not a significant factor in the system stiffness and therefore the natural frequency. Additionally, the natural frequencies do shift some with amplitude of excitation, but the values are within the spread of the natural frequencies at a given input acceleration.

Regardless of load path, the preload cannot be used to predict either the value of the natural frequency or the uncertainty in the prediction of the natural frequency. Additionally, the lack of spread in the natural frequencies suggests that the natural frequency is relatively insensitive to assembly to assembly variation. For modeling purposes, it is important to characterize the modes of the system, but the slight shifts in natural frequency due to the nonlinearities of the system can be accounted for in the uncertainties of the values of the natural frequencies themselves.

3.2.2.2 Effects of Preload on Energy Dissipation

The second parameter studied is the energy dissipation. Figure 42 through Figure 44 show the distribution of the energy dissipation of the specimen as a function of input acceleration and preload for specimens with a load path through the foam and solid mass. A power line is fit to the data to determine the coefficient of the energy dissipation equation.

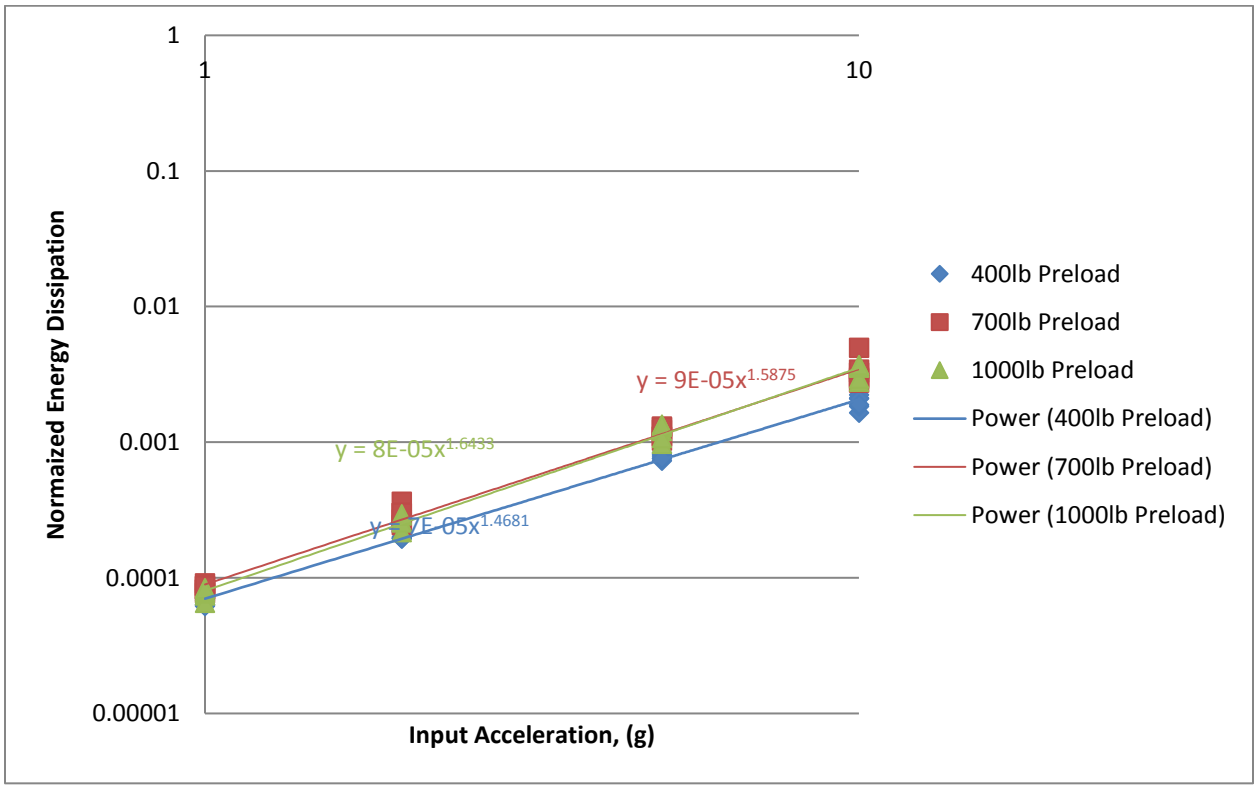

Figure 42: Distribution of Normalized Energy Dissipation per Preload with No Radial Gap and Preload through the Foam and Solid Mass.

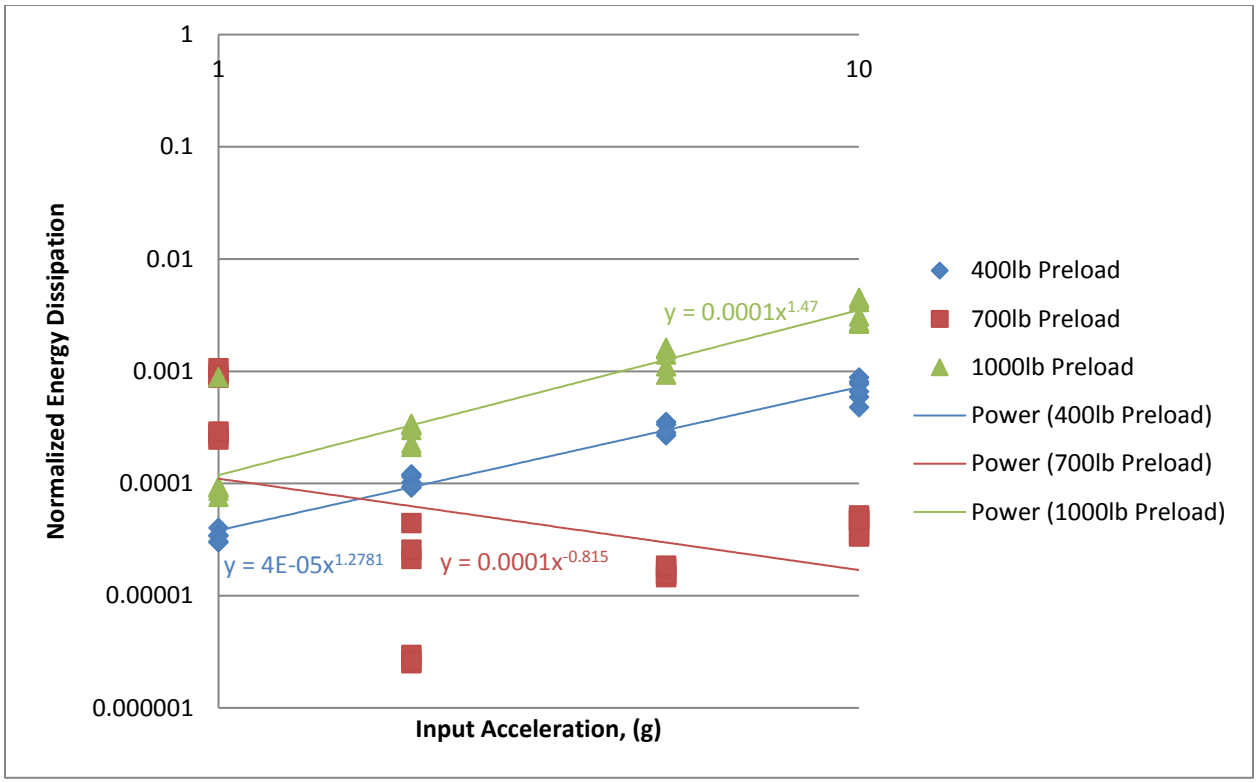

Figure 43: Distribution of Normalized Energy Dissipation per Preload with a 1/16" Radial Gap and Preload through the Foam and Solid Mass.

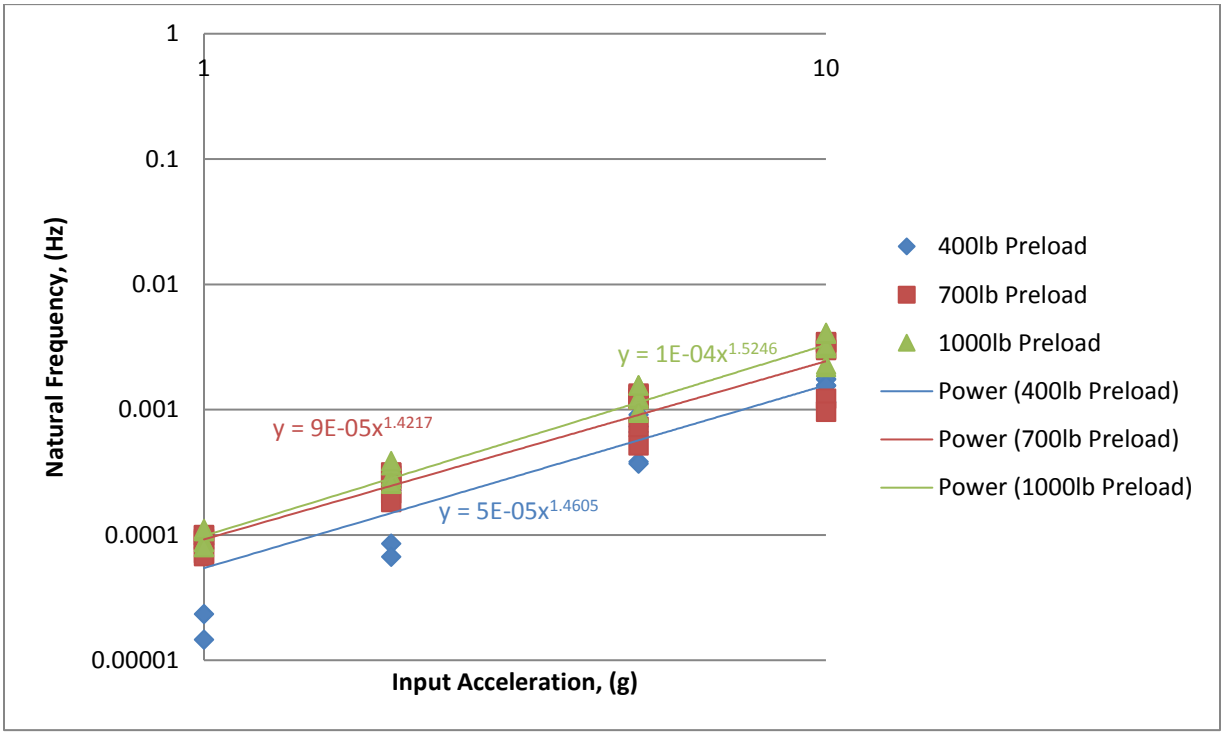

Figure 44: Distribution of Normalized Energy Dissipation per Preload with a 1/8" Radial Gap and Preload through the Foam and Solid Mass.

For the case of the load path going through the foam and solid mass, the amount of energy dissipation is greater for the 700lb and 1000lb preload than it is for the 400lb preload. This result suggests that the amount of preload influences how much the foam dissipates energy. For modeling implications, it is important to know the preload and the relationship between preload and energy dissipation.

With the exception of the specimen with the 1/16" gap and 700lb preload, the amount of energy dissipation increased with increasing amplitude. This is hardly surprising because some of the energy dissipation is likely due to micro- and macro-slip between the solid mass and the foam. There is going to be more slip, and therefore more energy dissipation, as the input acceleration increases. It is not clear why the 1/16" gap and 700lb preload combination produced a response that is out of family with the rest. Since this is the only combination of preload, load path, and gap size where this occurred, this results suggests that there was something unique about the foam cups used for this assembly.

As with the axially loaded experiments, the energy dissipation is plotted as a function of the input acceleration on a log-log plot. With the exception of the specimen with the 700lb preload and the 1/16" gap solid mass, there is a clear linear trend, indicating a power relationship between the amounts of energy dissipated and the input acceleration. This result agrees with theory [3] and previous studies [3-12]. The theoretical value for the exponent of the power relationship is 2. For the specimens with the load path going through the foam and solid mass, the exponents range from 1.28 to 1.64, which is lower than the theoretical value and the results from the same configurations tested axially. The lower value for the exponent suggests that the energy dissipation mechanism is not solely friction, which is what the value of 2 is based on.

Figure 45 through Figure 47 show the distribution of the energy dissipation of the specimen as a function of input acceleration and preload for specimens with a load path through the solid mass only. A power line is fit to the data to determine the coefficient of the energy dissipation equation.

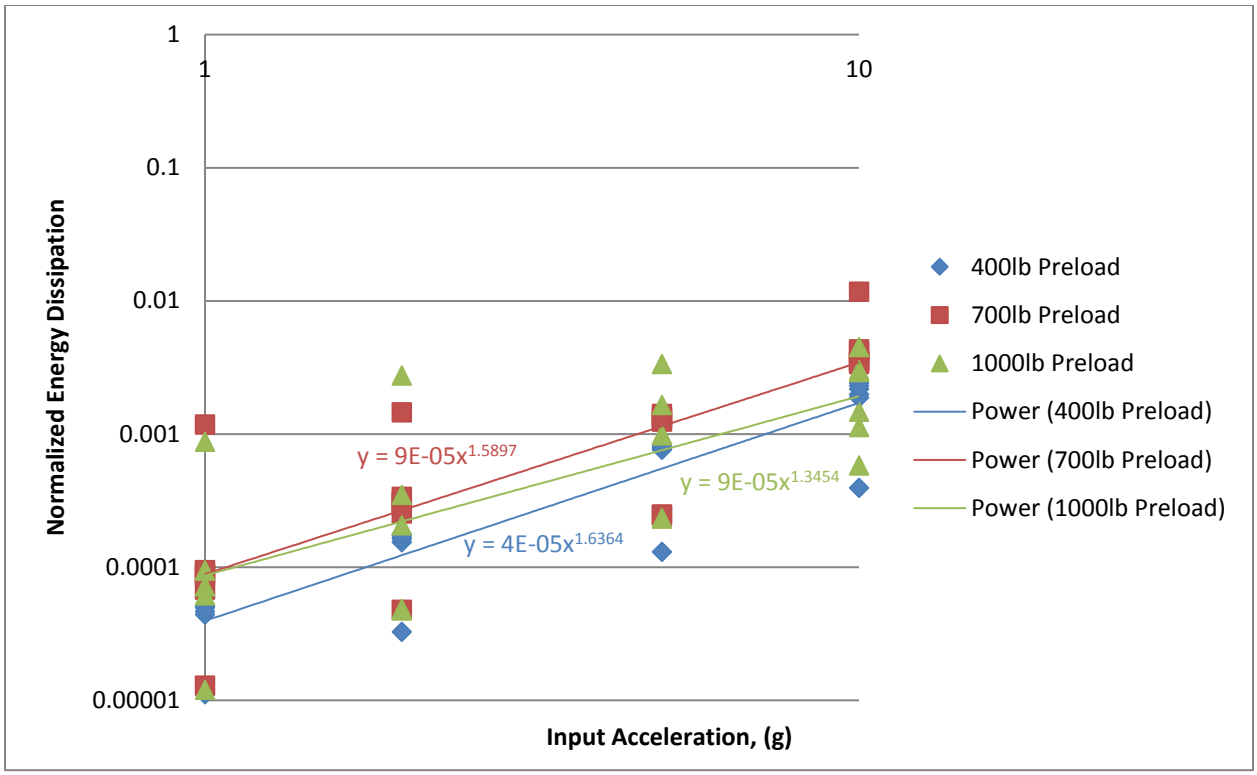

Figure 45: Distribution of Normalized Energy Dissipation per Preload with No Radial Gap and Preload through the Solid Mass Only.

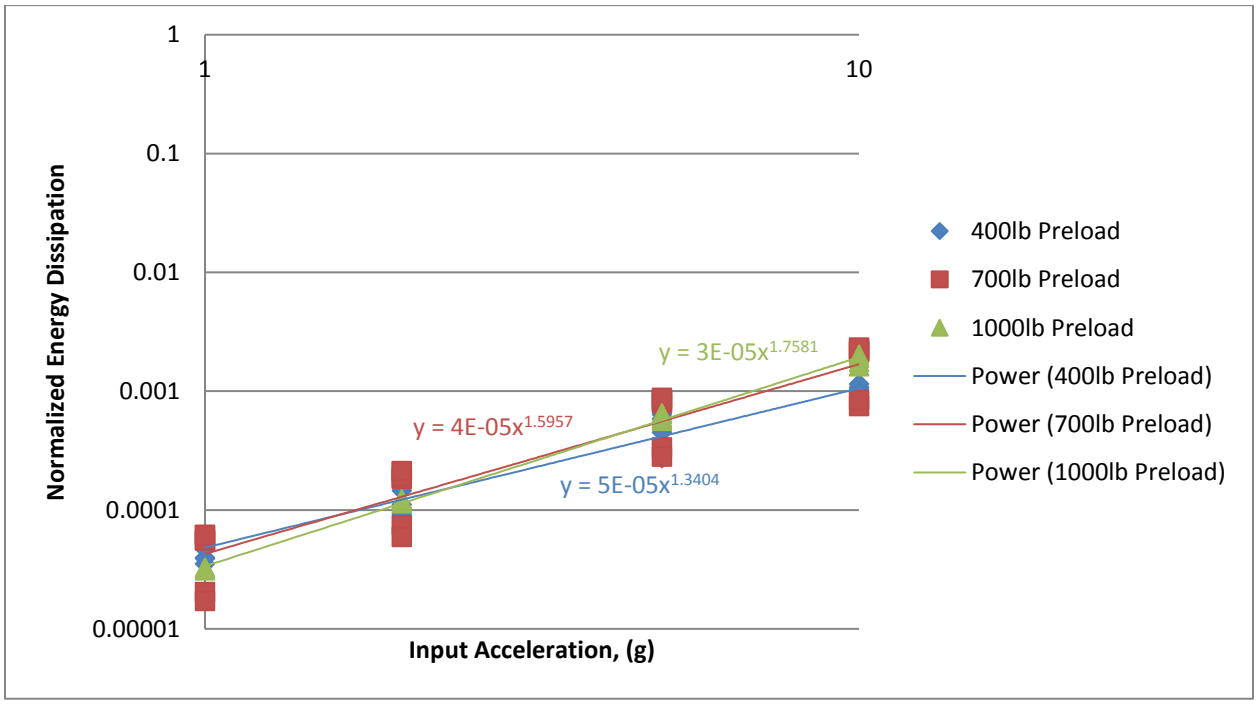

Figure 46: Distribution of Normalized Energy Dissipation per Preload with a 1/16" Radial Gap and Preload through the Solid Mass Only.

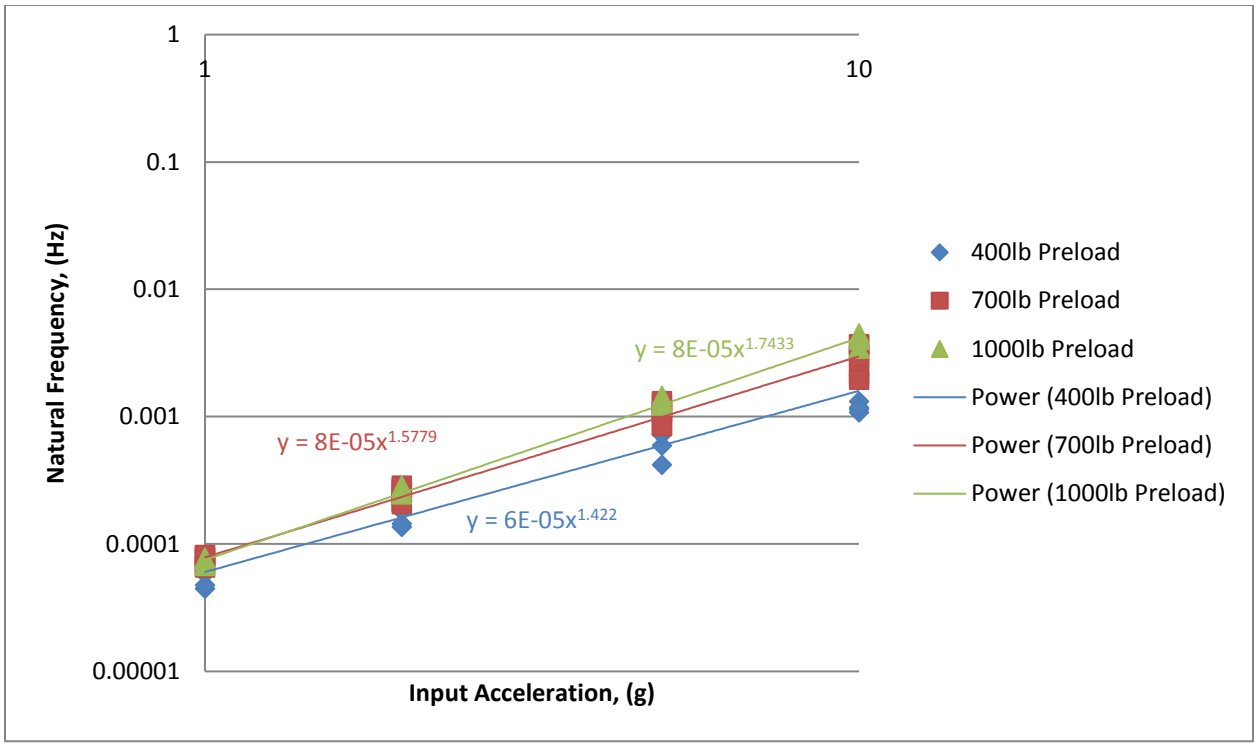

Figure 47: Distribution of Normalized Energy Dissipation per Preload with a 1/8" Radial Gap and Preload through the Solid Mass Only.

When the load path goes through the solid mass only, the energy dissipation is greater in the cases with the 700lb and 1000lb preload than the cases with the 400lb preload. This result reinforces what was seen in the previous experiments, suggesting that the preload is an important parameter in predicting energy dissipation. One of the possible mechanisms for energy dissipation is material damping of the foam, so the preload could have an influence on how much material damping is present.

When the load path goes through the solid mass only, the energy dissipation increases with increasing input amplitude. This result reinforces what we have seen in the previous experiments. The larger amplitude of input leads to greater micro- and macro-slip, and therefore the amount of energy that is dissipated.

As with all of the other experiments, the energy dissipation is plotted with respect to the input acceleration on a log-log plot. The data show a clear linear trend, indicating a power relationship between the amount of energy dissipated and the input acceleration. This result agrees with theory [3], previous studies [3-12], and the other experiments in this study. When a trendline is fit to the data, the resulting exponents have values ranging from 1.34 to 1.76, which is lower than the theoretical value of 2, but agrees with the values of the specimens preloaded through the foam and solid mass when excited laterally.

3.2.3 Effects of Snugness of Fit

As with assessing the effects of preload, when evaluating the effects of snugness of fit on the dynamics of the system, two parameters are studied: the natural frequency and the normalized energy dissipation.

3.2.3.1 Effect of Snugness of Fit on Natural Frequency

The first parameter studied is the natural frequency. Figure 48 through Figure 50 show the distribution of the natural frequency of the specimen as a function of input acceleration and gap size for specimens with the preload path through the foam and solid mass.

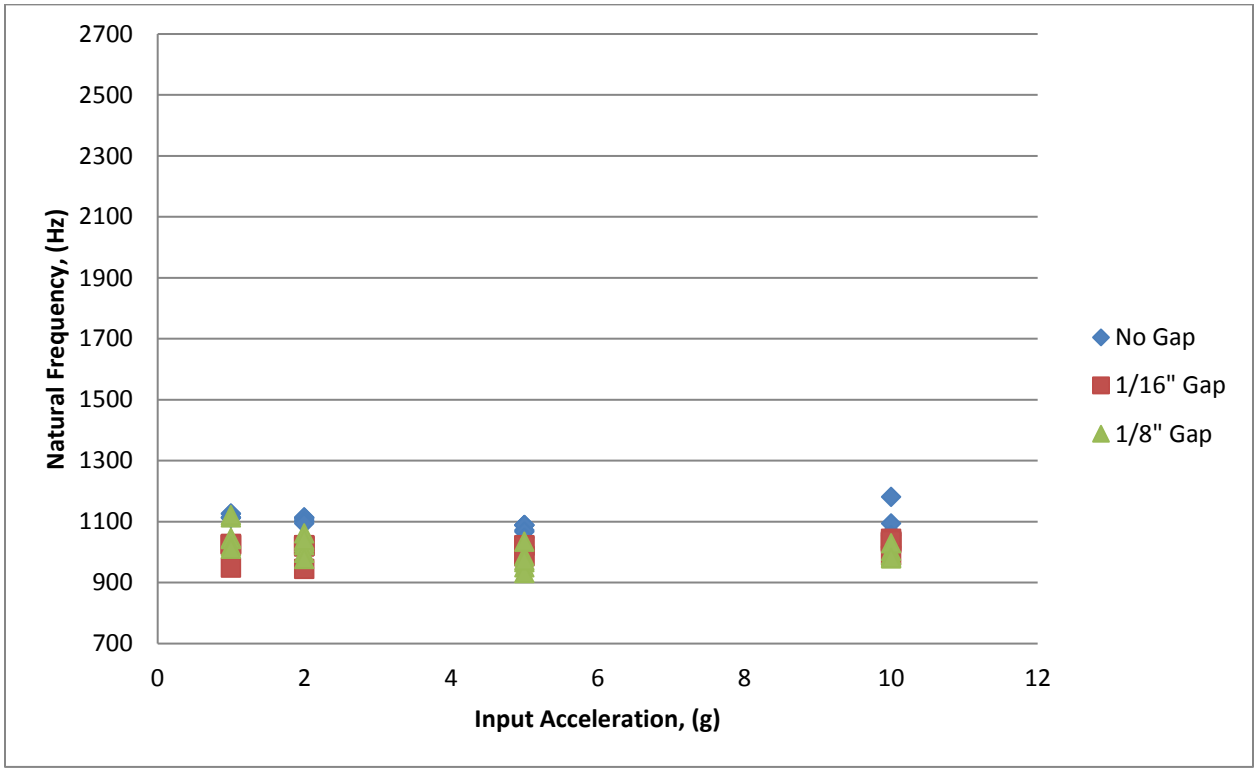

Figure 48: Distribution of Natural Frequency per Gap Size with a 400lb Preload through the Foam and Solid Mass.

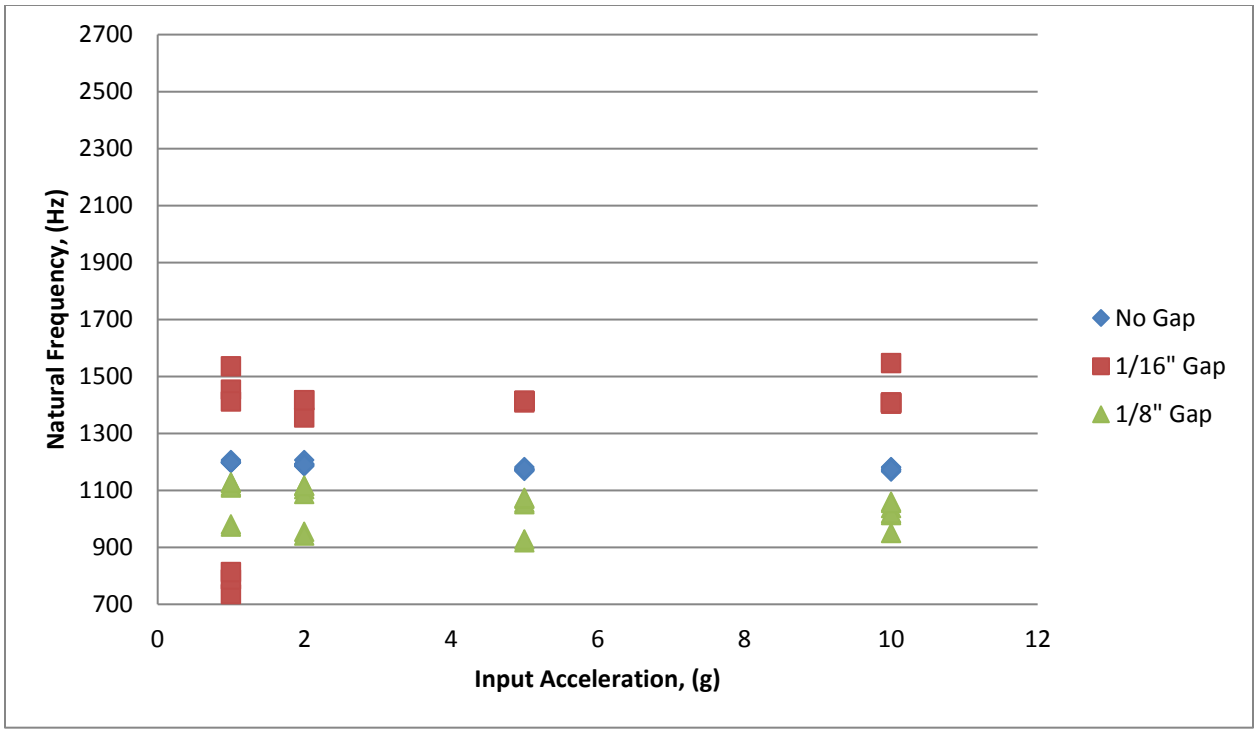

Figure 49: Distribution of Natural Frequency per Gap Size with a 700lb Preload through the Foam and Solid Mass.

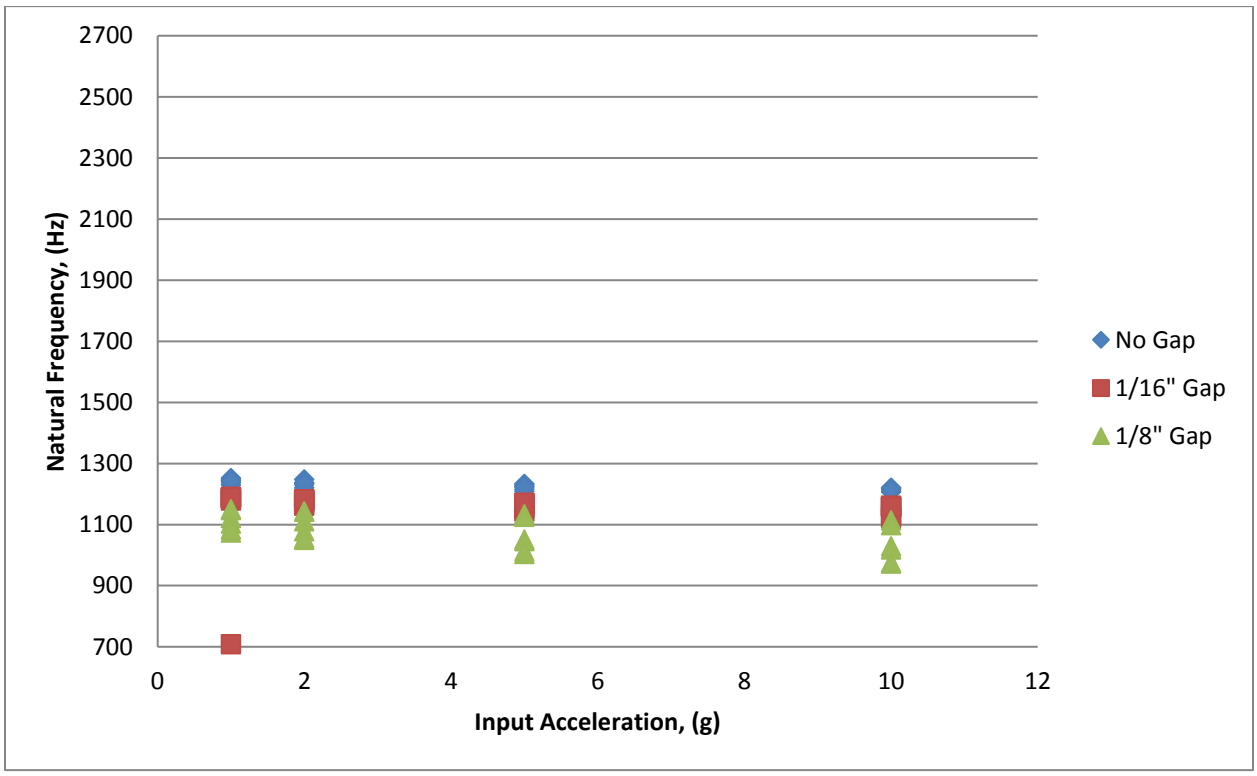

Figure 50: Distribution of Natural Frequency per Gap Size with a 1000lb Preload through the Foam and Solid Mass.

With the exception of the 700lb preload, the snugness of fit has no statistically significant effect on the variance of the natural frequency, indicating gap size does not affect the repeatability of the assembly process. The variance of the natural frequency for the 1/16" gap specimens is significantly larger than for the no gap and 1/8" gap specimens. For some reason there was significant variation in the stiffness and thus likely the assembly process. Since this is unique to the circumstances of preload, solid mass size and loading direction, it suggests that the variation is due to the foam cups and not the solid mass. There is overlap of the natural frequencies among the different gap sizes, suggesting that the preload is not a valid predictor of the natural frequency of the system.

Figure 51 through Figure 53 show the distribution of the natural frequency of the specimen as a function of input acceleration and gap size for specimens with the preload path through the solid mass only. When the preload goes through the solid mass only, the specimens show no appreciable difference in the distribution of natural frequencies and the values of the natural frequencies.

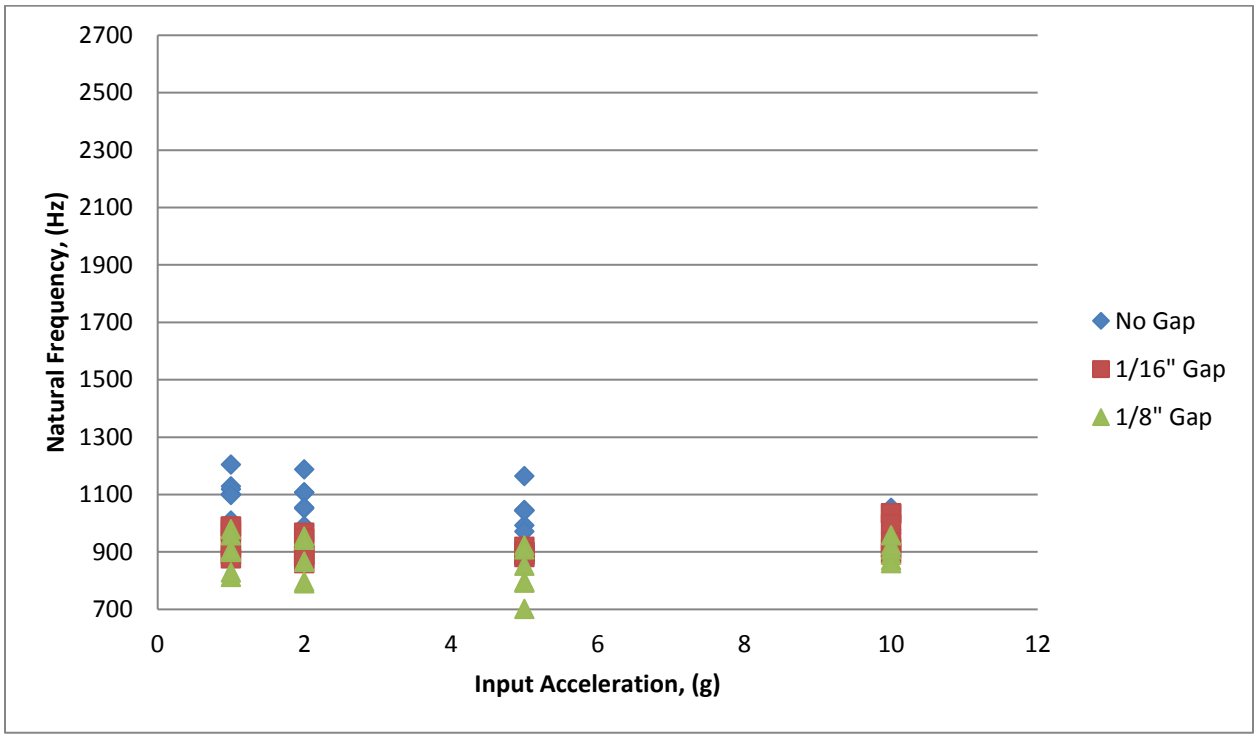

Figure 51: Distribution of Natural Frequency per Gap Size with a 400lb Preload through the Solid Mass Only.

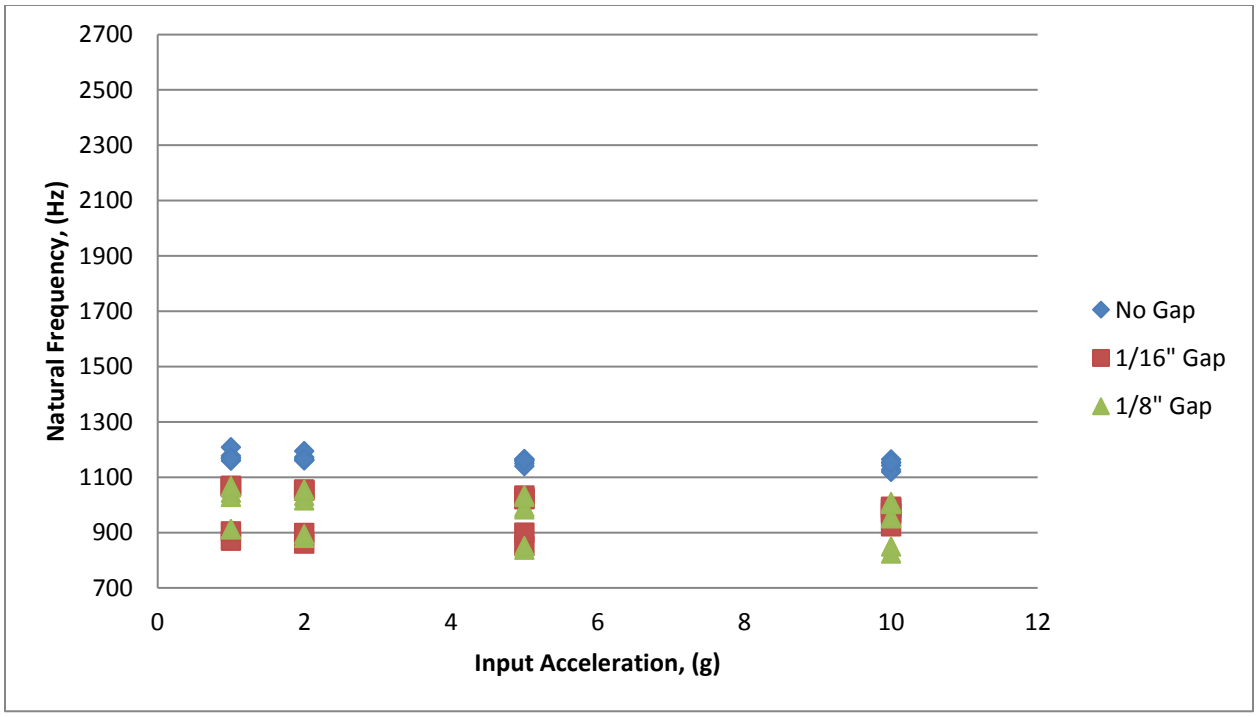

Figure 52: Distribution of Natural Frequency per Gap Size with a 700lb Preload through the Solid Mass Only.

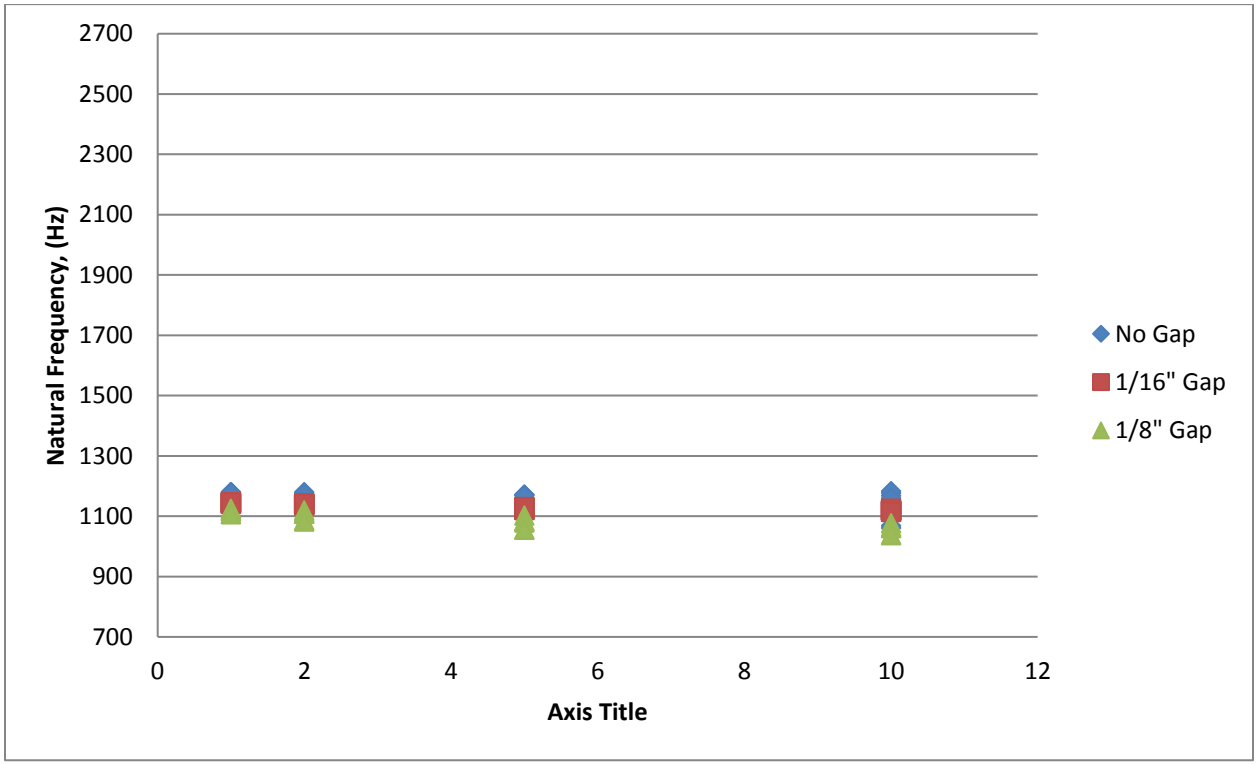

Figure 53: Distribution of Natural Frequency per Gap Size with a 1000lb Preload through the Solid Mass Only.

When the load path goes through the solid mass only, the snugness of fit has no appreciable effect on the variance of the natural frequency. For modeling implications, if the item does not fit snugly in the foam, it is not critical to know how loose it is to determine the natural frequency of the foam/item system when the load path is through the part alone.

3.2.3.1 Effect of Snugness of Fit on Energy Dissipation

The second parameter studied is the energy dissipation. Figure 54 through Figure 56 show the distribution of the energy dissipation of the specimen as a function of input acceleration and preload for specimens with a load path through the foam and solid mass. A power line is fit to the data to determine the coefficient of the energy dissipation equation. The amount of energy dissipation when the specimens that are preloaded through the foam and solid mass is greater for the specimens that do not include a radial gap than the specimens that contained a radial gap.

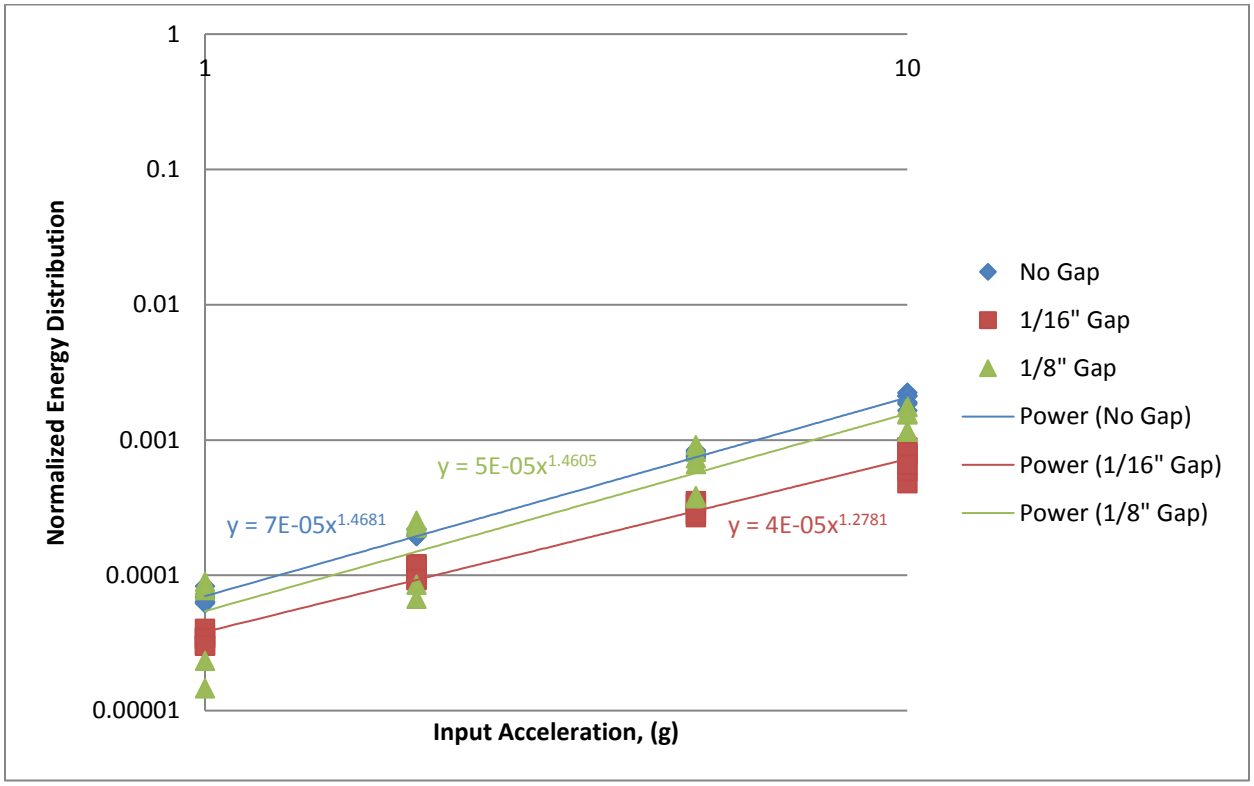

Figure 54: Distribution of Normalized Energy Dissipation per Gap Size with a 400lb Preload through the Foam and Solid Mass.

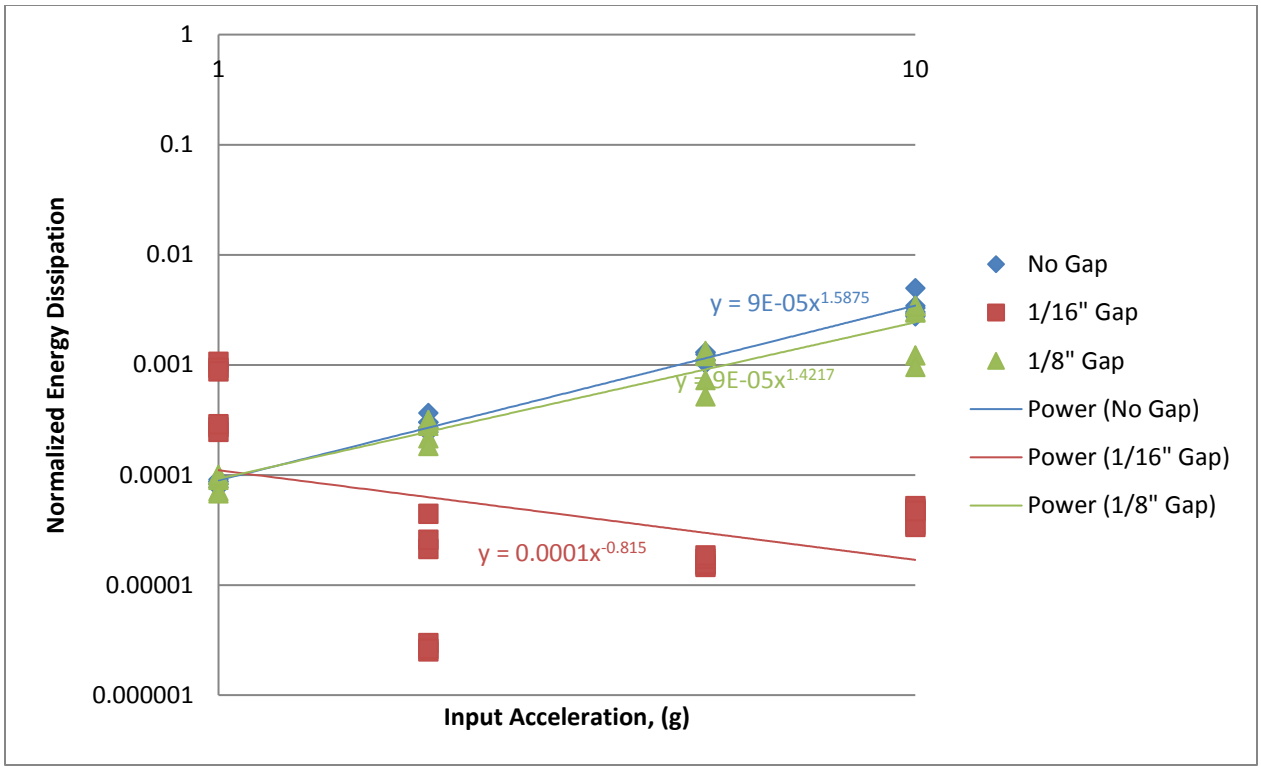

Figure 55: Distribution of Normalized Energy Dissipation per Gap Size with a 700lb Preload through the Foam and Solid Mass.

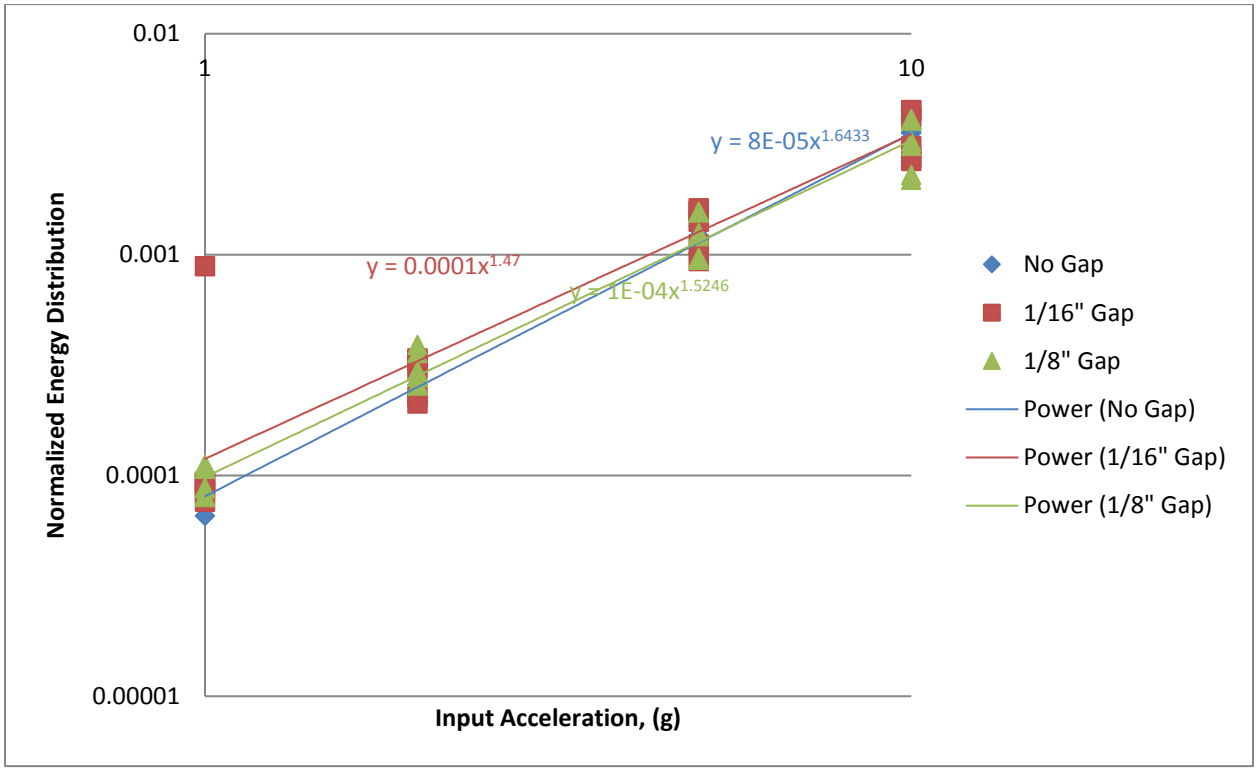

Figure 56: Distribution of Normalized Energy Dissipation per Gap Size with a 1000lb Preload through the Foam and Solid Mass.

These results show that the snugness of fit has an effect on the energy dissipation. The amount of energy dissipated when the specimens are preloaded through the foam and solid mass is greatest when there is no gap between the solid mass and the foam. The amount of energy dissipation was lowest in the cases when the radial gap was 1/16" and somewhere in between when the gap was 1/8". This differs from when the energy was applied axially. One hypothesis for the difference is that when the specimens are excited laterally, there is less opportunity for impacting, which is an effective energy dissipation mechanism. Therefore, there are fewer energy dissipation mechanisms when the excitation energy is applied laterally. Thus, the foam being in contact all the way around the solid mass leads to better energy dissipation than when there is a gap.

As done in previous studies [3-12], and previously in this study, the normalized energy dissipation is plotted with respect to the input acceleration on a log-log plot. With the exception of the 1/16" gap, 700lb specimen, the data show the anticipated straight line, indicating a power law relationship between energy loss per cycle and the input acceleration. In the fitted results, the slope ranges from 1.28 to 1.64, where 2 is the theoretical value for a linear system with contact friction [3]. These values are well below the theoretical value of 2. This result suggests that there is not perfect contact friction around the solid mass and that the mechanism for energy dissipation is more complex than that.

Figure 57 through Figure 59 show the distribution of the energy dissipation of the specimen as a function of input acceleration and preload for specimens with a load path through the solid mass only. A power line is fit to the data to determine the coefficient of the energy dissipation equation.

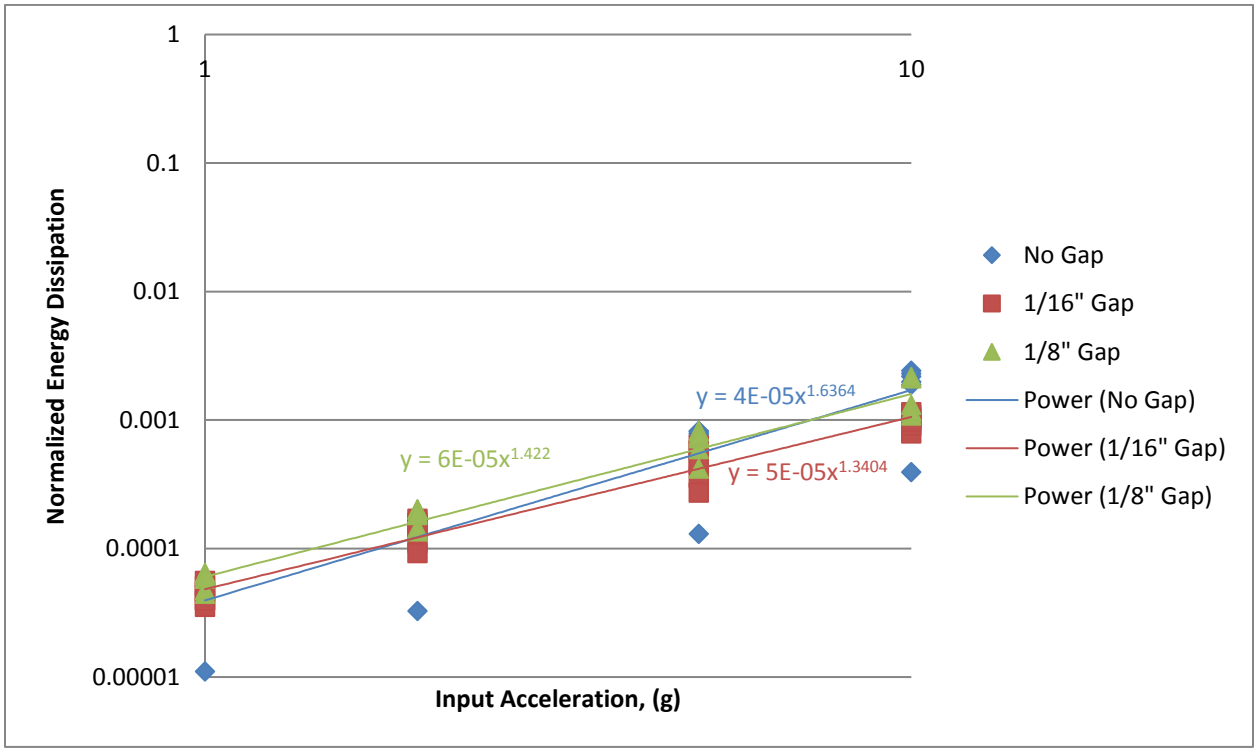

Figure 57: Distribution of Normalized Energy Dissipation per Gap Size with a 400lb Preload through the Solid mass Only.

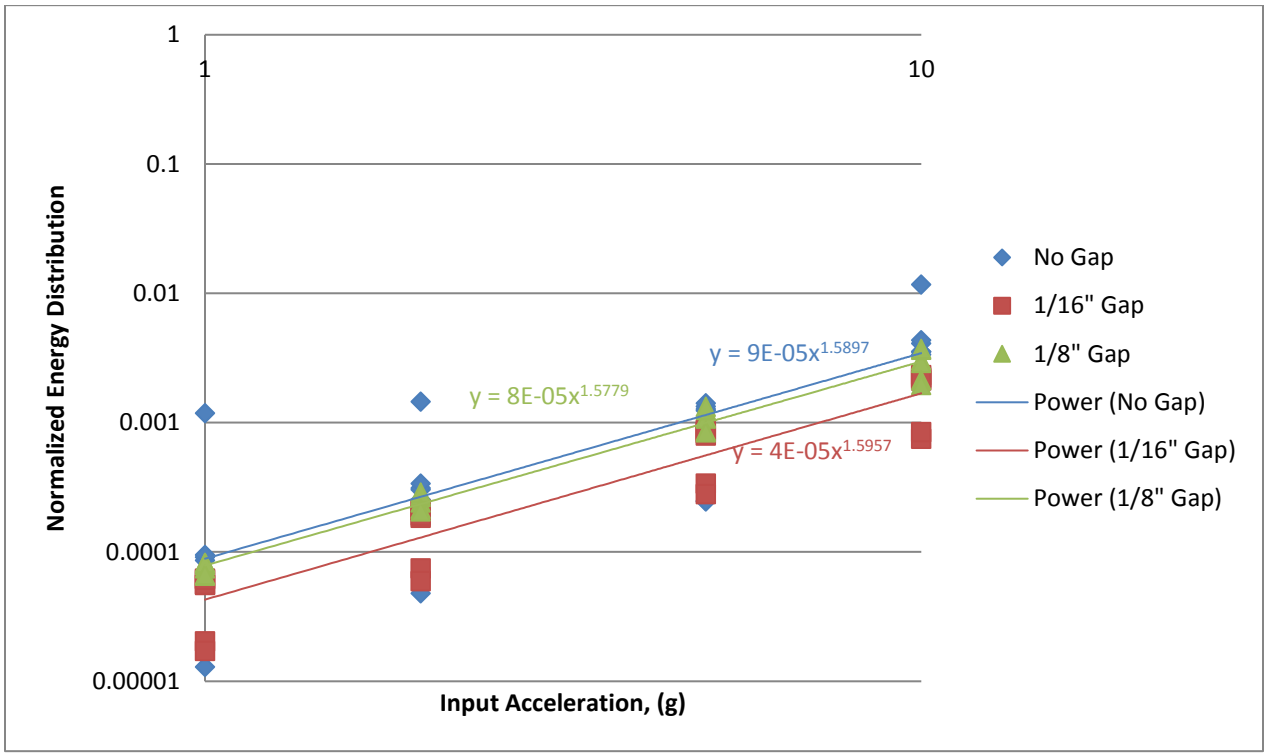

Figure 58: Distribution of Normalized Energy Dissipation per Gap Size with a 700lb Preload through the Solid mass Only.

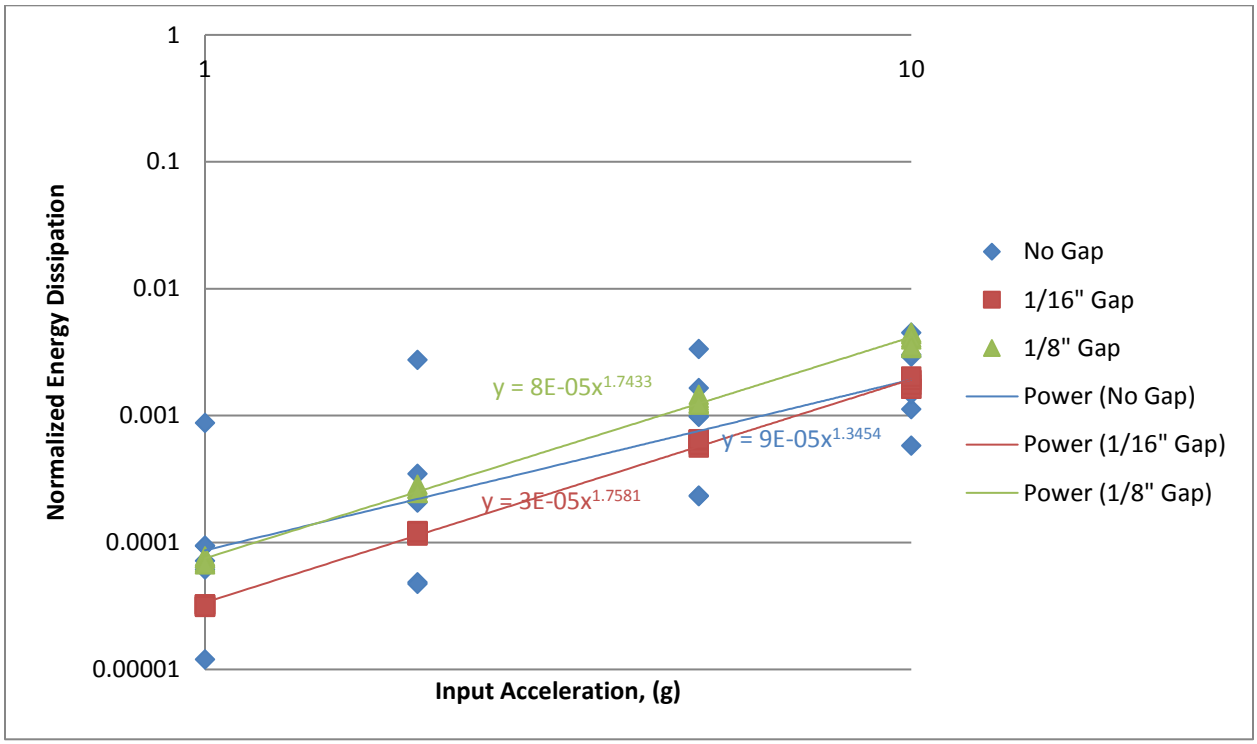

Figure 59: Distribution of Normalized Energy Dissipation per Gap Size with a 1000lb Preload through the Solid Mass Only.

The results of the experiments where the load path is through the solid mass alone are similar to those when the load path goes through the solid mass and the foam. This supports the hypothesis that due to the lateral excitation, there is less opportunity for impacting when the excitation is applied axially which can contribute to energy dissipation.

As done in previous studies [3-12], and previously in this study, the normalized energy dissipation is plotted with respect to the input acceleration on a log-log plot. The data show the anticipated straight line, indicating a power law relationship between energy loss per cycle and the input acceleration. In the fitted results, the slope ranges from 1.34 to 1.76, where 2 is the theoretical value of the for a linear system with contact friction [3]. As seen in the previous case, these values are well below the theoretical value of 2. This result suggests that there is not perfect contact friction around the solid mass and that the mechanism for energy dissipation is more complex than that.

3.2.4 Effects of Load Path

The effects of the load path on the experimental results are considered for the natural frequency, energy dissipation, and amplitude and sweep order. The following paragraphs contain a discussion of the data and their implications.

There is very little difference between the natural frequencies when the load path goes through the solid mass and the foam. This suggests that the preload on the foam does not significantly change the stiffness of the foam. Also, the system's stiffness is dominated by the stiffness of the solid mass, so small changes in the stiffness of the foam will not significantly change the overall stiffness, and thus the natural frequency.

Under lateral loading, there is little difference in the energy dissipation of the system when the load path goes through the solid mass and the foam or the solid mass alone. The friction that causes the energy dissipation is consistent regardless of the load path when the system is loaded laterally. Some of the impacts that occur during axial loading do not occur under lateral loads, so the energy dissipation is almost exclusively due to friction, micro- and macro-slip. This leads to more consistent energy dissipation than when impacts are present.

The load path has an effect on the significance of the sweep order of the test. When the load path is through the foam and the solid mass, there is little change in the natural frequency but significant change in the energy dissipation amount for the same amplitude the second time through the sweep series when starting at 1g and going to 10g. However, when the sweep series starts at 10g and goes to 1g, there is no change in the natural frequency and the energy dissipation. When the load path goes through the solid mass only, there is a change in the natural frequency and energy dissipation regardless of the order of the sweeps. This result suggests that at the higher amplitudes there is a loss of preload. The loss of preload is larger and consistent in the foam, so when the load path goes through the foam, there is no more change after the specimen is exposed to a 10g sine sweep. However, when the load path goes through

the solid mass only, the system continues to change, indicating that the loss of preload continues to change as the system is excited with vibration at different levels.

3.3 Loss of Preload During Testing

During the vibration process a certain amount of preload is lost. This loss of preload is due to the specimen experiencing forces that are great enough to overcome that preload during excitation. To determine the amount of preload lost, the exact value of the preload is recorded during assembly, and then the amount of load required for disassembly is then recorded. The difference between the pre- and post-test load values is the amount of preload lost. Table 3 summarizes the load data collected during testing. The variability in the load is consistent regardless of the preload value. This small amount of variation means that the uncertainty in the preload is fairly small. The variability in the amount of load for disassembly was significantly larger than the amount of variability in the preload values. This observation means that the amount of preload lost in each test is highly variable and a significant factor in the uncertainty. The variation in the amount of preload lost is the same for the 400 and 1000 pound preloads, but it is higher for the 700 pound preload. The loss of preload is probably a key factor in the change in the natural frequency and energy dissipation seen from one sweep to the next.

Table 3: Preload and Disassembly Load Data

	400lb preload	400lb unload	400lb loss of preload	700lb preload	700lb unload	700lb loss of preload	1000lb preload	1000lb unload	1000lb loss of preload
mean	413.	251	162	719	469	251	1026	674	352
st. dev.	10	86	87	16	158	158	23	187	190
CV	0.024	0.342	0.540	0.022	0.336	0.630	0.022	0.278	0.539

3.4 Axial Tests: Shock Excitation

The configuration for this series of tests is a set of foam cups that are 2 inches in depth, the solid mass that is 3 inches in diameter (i.e. the “no gap” specimen), and a preload of 700lbs. It should be noted that the foam specimens used in this set of tests was a different set than the foam cups used in the sine sweep testing. The specimens are then subjected to a series of shock pulses that were designed to excite the natural frequency of Ministack. After the application of the shock pulse, the ring down is captured and analyzed. From the ring down data, it is possible to determine the instantaneous effective stiffness and effective damping, which allows for the determination of the type of nonlinearity present.

The shock pulses were applied in the following order: 8.5g, 12g, 17g, 24.5g, 35g. That sequence was then repeated. The sequence was also repeated in the reverse order twice.

Once the data was collected, the effective stiffness and damping could be calculated. The procedure to calculate the effective stiffness and damping is outlined in [19] as well as in Section 1.2.1.4. The first step was to establish an envelope for the ring down response, Figure 60 (Top). From that response it is possible to calculate the instantaneous frequency, Figure 60 (Middle), and effective damping, Figure 60 (Bottom). The instantaneous frequency stays constant over the time of the ring down. This result suggests that when the excitation is transient in nature, the system stiffness does not change with amplitude as it does with the harmonic excitation. The effective damping changes with time, increasing as the ring down ends.

After the envelope of the response, instantaneous frequency, and effective damping are calculated, it is possible to plot the frequency versus amplitude, yielding the backbone curve, Figure 61 (Left), and damping skeleton, Figure 61 (Right). Looking at the backbone curve, the stiffness does not change with amplitude, which is different than what was observed in the response due to sine excitation. Investigating the damping skeleton shows that the damping increases with amplitude, as would be expected in a system with dry friction [19]. Again, this contradicts what was seen in the sine sweeps, where the nonlinear damping showed an increase with increasing amplitude. A possible explanation for these phenomena is that the dominant nonlinearity of this system is sensitive to the type of excitation.

Once the backbone and damping skeleton are calculated, it is possible to use the mass from the system to calculate the effective stiffness and damping, which can be used as parameters for models. The effective stiffness and damping curves can be seen in Figure 62.

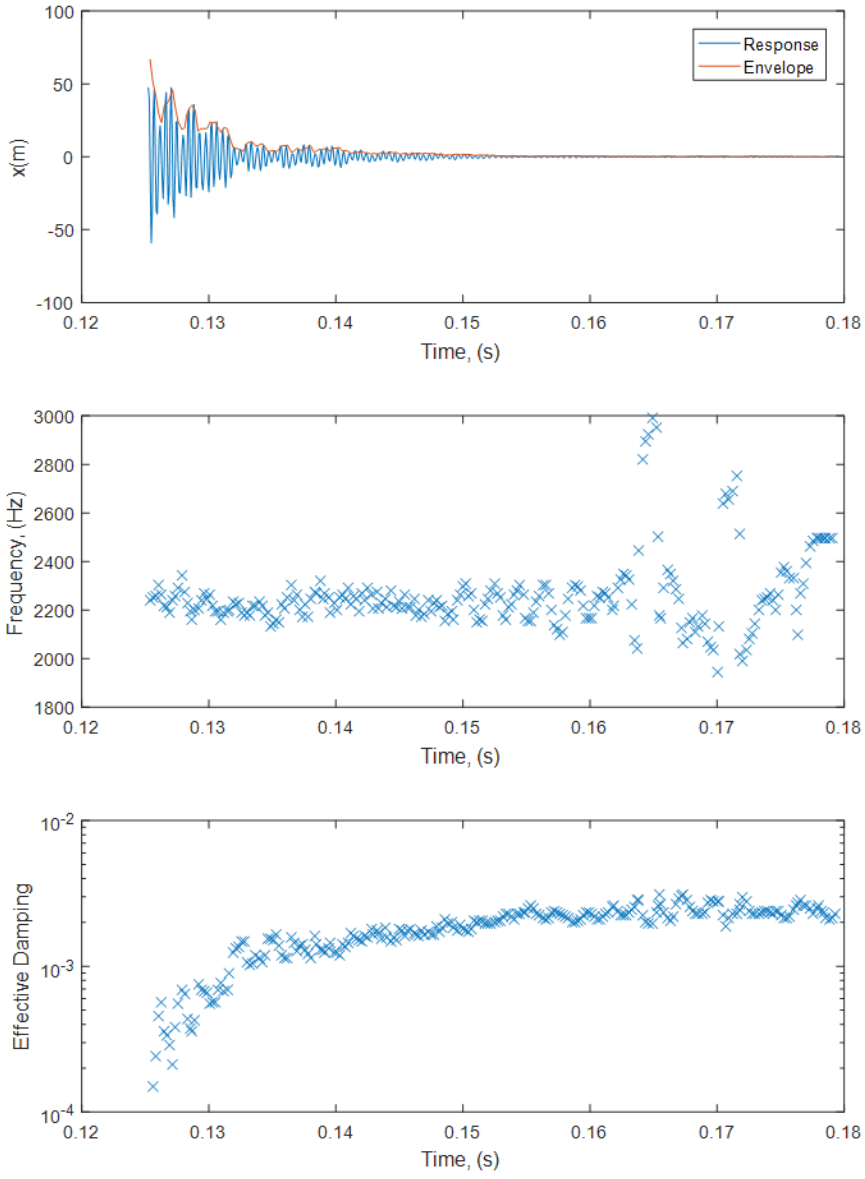

Figure 60: Response at 35g excitation level. (Top) Estimation of envelope. (Middle) Instantaneous frequency. (Bottom) Instantaneous Damping

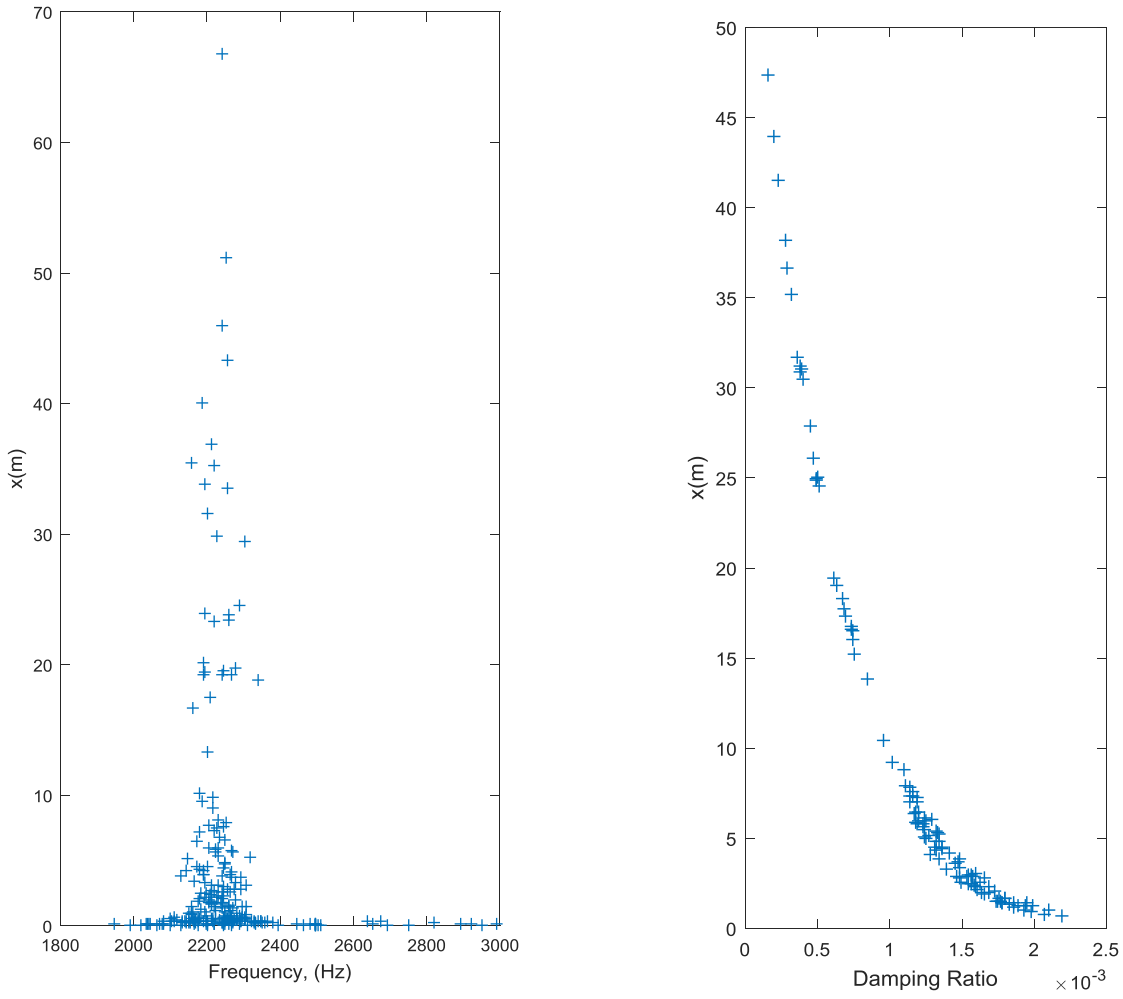

Figure 61: Response at 35g Excitation. (Left) Backbone Curve. (Right) Damping Skeleton.

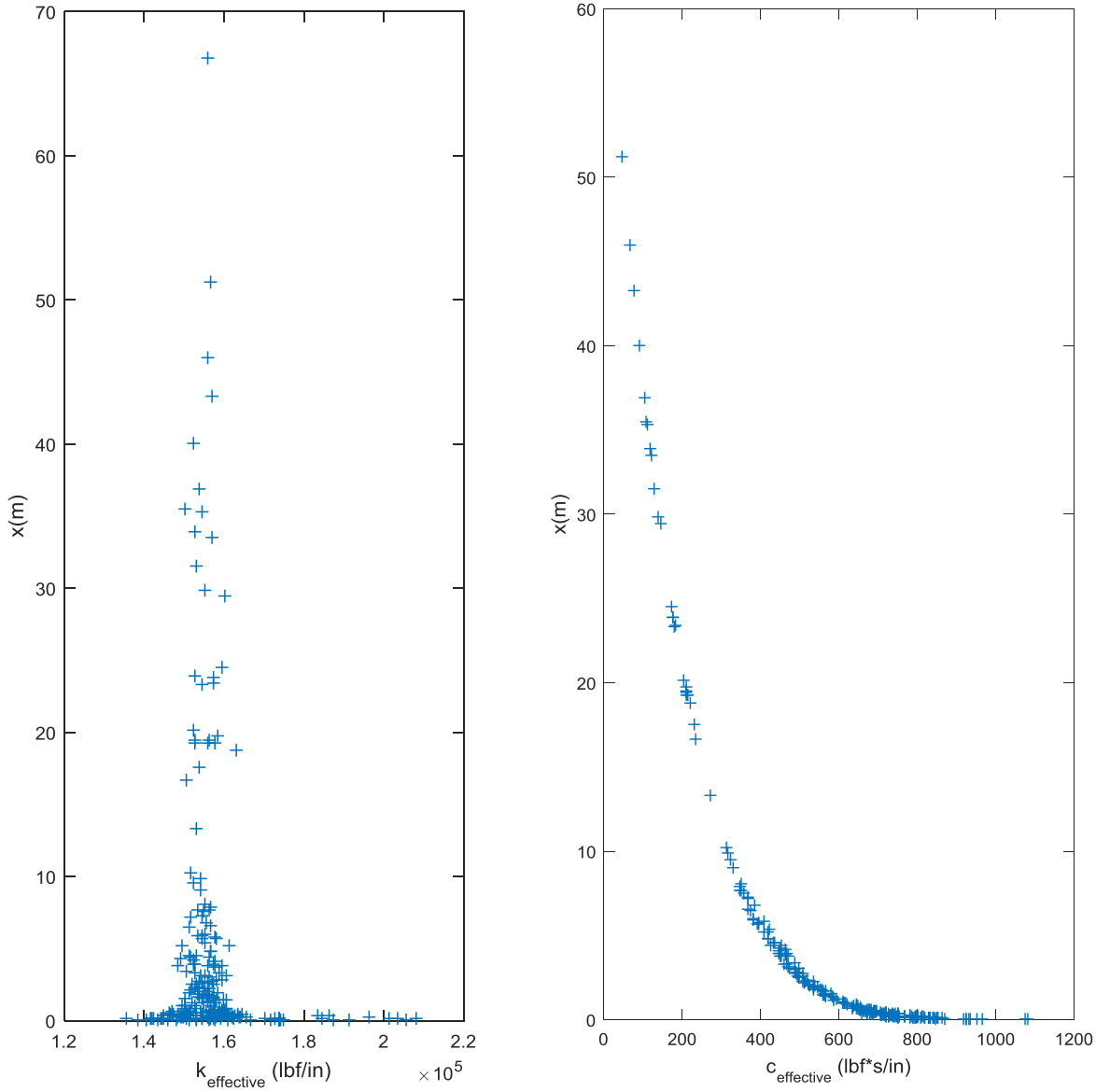

Figure 62: Effective Stiffness and Damping Estimated from the Backbone Curve.

Comparing the effective stiffness and damping from the ring down effects at the 5 different excitation amplitudes yields some interesting observations. First, the effective stiffness does not change with the different excitation amplitudes, Figure 63 (Left). This is notable because the stiffness changed based on excitation levels when the excitation method was harmonic. Second, the effective damping curves, while showing a similar trend, differ depending on the excitation amplitude of the transient function, Figure 63 (Right). This result suggests that the response of the system is dependent on starting point of the system. The loading history is important to the response, which is indicative of a nonlinear system. It should also

be noted that damping calculated from a lower level excitation cannot be used to extrapolate to a higher level of excitation.

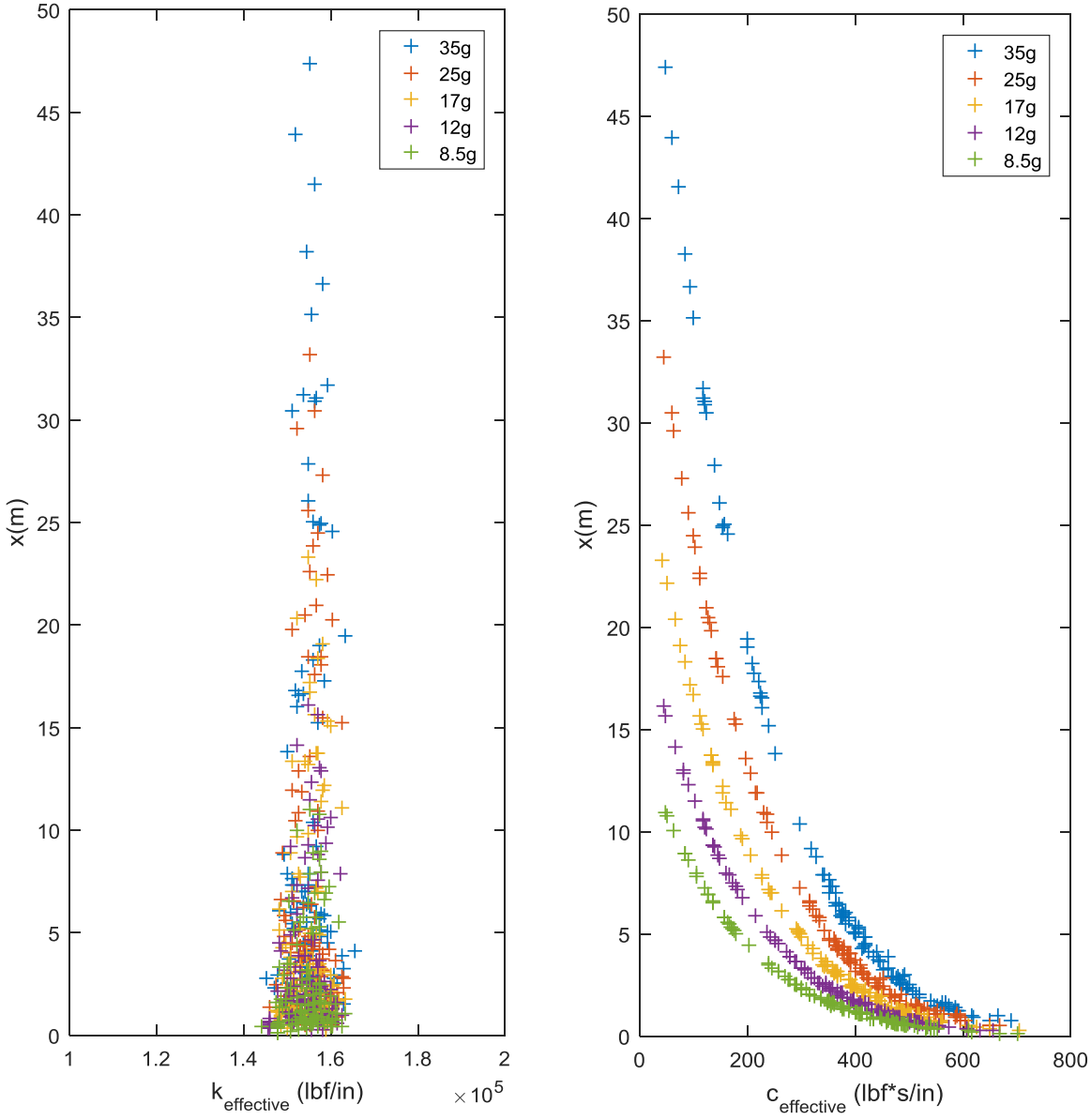

Figure 63: Effective Stiffness and Damping Estimated from the Backbone Curve for Multiple Excitation Amplitudes.

4. CONCLUSIONS

A series of upward sine sweeps, upward and downward sine sweeps and a transient excitation were run on Ministack, which is a simple system representing a metal component packaged in foam. The measured results give insight into the influence of input amplitude, snugness of fit, load path and sequence of testing on the energy dissipation and natural frequency in the system. Additionally, the data can give estimates of effective frequency and stiffness as a function of amplitude. For the harmonic excitation, as the amplitude of excitation increases, the natural frequency decreases and the amount of energy dissipated each cycle increases. The foam to metal interface seems to be responsible for this behavior due to friction, impact, loss of preload, and material damping. The nonlinear nature of these physics presents itself in the measured transfer functions and estimated parameters.

The first set of results show the effect of the order of the amplitudes of the sine sweeps. When the sine sweeps start at a low amplitude and increase, the natural frequency from the second run shifts to a lower frequency in comparison to the first run. Similarly, the amount of energy dissipation is lower on the second run. When starting the test series at a high amplitude and decreasing the amplitude there was no appreciable difference in the parameters. Starting the run with a 10g load case may cause the mass to initially settle and lose some of its preload, which could explain why the order of sweep amplitude influence the behavior.

Three different size sold masses were tested along with sets of foam cups with two different depths, which change the load path of the preload. Regardless of the load path, the snugness of fit has no statistically significant effect on the variance of the natural frequency, indicating gap size does not affect the repeatability of the assembly process. When the load path goes through both the mass and the foam, the snugness of fit has an impact on the natural frequency. The smaller gap case has higher natural frequencies than the no gap case and the larger gap case has lower natural frequencies than the no gap case. When the load path goes through the mass alone, the natural frequency is higher in the case where there is no gap than in the cases where there are gaps. These results suggest that the snugness of fit has a larger effect on the stiffness of the system when the load path goes through the mass and the foam than when the load path goes through the mass only. Additionally, the uncertainty of the natural frequency is larger in the case of the preload going through the mass and the foam, likely due to the variation in the foam.

The results of this study show that the snugness of fit has an effect on the energy dissipation. Regardless of load path, the amount of energy dissipated is greatest when there is a radial gap. It is likely that the increased energy dissipation in the presence of a radial gap is due to mechanisms of energy dissipation that occur when there is a radial gap in addition to the contact friction that is present when there is no radial gap. For modeling implications, these results suggest that it is important to understand the amount of friction that occurs between the contacting surfaces but also the coefficient of restitution for impacts.

The results of the study show that there are several methods of extracting nonlinear features from the data. In addition to demonstrating the insight gained from multiple analysis techniques, these experiments demonstrate the significance of different experimental excitations and their effect on the resulting analysis. Comparing the FRFs at different amplitudes for the harmonic excitation clearly demonstrated that there were nonlinearities in stiffness and damping. The Hilbert transform on the sine sweep data showed that not only were there nonlinearities present, but that they were due to stiffness and damping. Additionally, looking at the effective stiffness and damping from the ring down from a transient excitation, it was possible to determine that some of the nonlinearity is due to dry friction. The results for the sine sweep and the transient data indicated different nonlinearities. This suggests that the method of excitation can expose different aspects of the nonlinearities in the system.

5. REFERENCES

1. U.S. Department of Defense Standard Practice for Military Packaging, MIL-STD-2073-1E w/Change 1, January, 2011.
2. U.S. Department of Defense Environmental Engineering Considerations and Laboratory Tests, MIL-STD-810G, Oct. 2008.
3. Goodman, L.E. "A review of progress in analysis of interfacial slip damping", Structural Dumping, papers presented at a colloquium on structural damping held at the ASME annual meeting in Atlantic City, NJ, December, 1959, edited by Jerome E Ruzincka, pp 35-48.
4. Goodman, L. E. and Brown, C. B., "Energy Dissipation in Contact Friction: Constant Normal and Cyclic Tangential Loading", Journal of Applied Mechanics, 1962, pp. 17-22.
5. Ungar, E. E., "The Status of Engineering Knowledge Concerning the Damping of Built-Up Structures", Journal of Sound and Vibration, 26, August, 1977, pp. 141-154.
6. Metherell, A. F. and Diller, S. V., "Instantaneous Energy Dissipation Rate in a Lap Joint - Uniform Clamping Pressure", Journal of Applied Mechanics, 35, March 1968, pp. 333-340.
7. Groper, M., "Micoslip and Macroslip in Bolted Joints", Experimental Mechanics, June, 1985, pp. 171-174.
8. Menq, C.H., Bielak, J., and Griffin, J. H, "The Influence of Microslip on Vibratory Response, Part 1, A New Microslip Model", Journal of Sound and Vibration, 107, 1986, pp 279-293.
9. Gaul, L. and Lenz, J., "Nonlinear Dynamics of Structures Assembled by Bolted Joints" ACTA Mechunica, 125, April, 1997, pp. 169-181.
10. Sanliturk, K. Y., Stanbridge, A. B., and Ewins, D. J., "Friction Dampers: Measurment, Modelling and Application to Blade Vibration Control", ASME Design Engineering Technical Conferences, Volume 3, Part B, 1995.
11. Rogers, P. F. and Boothroyd, G. "Damping at Metallic Interfaces Subjected to Oscillating Tangential Loads", Transactions of the ASME, Journal of Engineering for Industry, August, 1975, pp. 1087-1093
12. Padmanabhan, K. K. and Murty A. S. R, "Damping in Structural Joints Subjected to Tangential Loads", Proceedings of Institution of Mechanical Engineers, Vol. 205, 1991, pp. 121-1 29.
13. Craig, R. R. J., and Kurdila, A. J., "Fundamentals of Structural Dynamics", 2nd ed., Wiley, New York, 2006, pp. 531-570.
14. Segalman D.J., "A Four-Parameter Iwan Model for Lap-Type Joints." ASME. *J. Appl. Mech.* 2005; 72(5): pp. 752-760. doi:10.1115/1.1989354.
15. Chopra, A.K., "Dynamics of Structures", 2nd ed. Prentice Hall, New Jersey, 2001, pp. 65-118.
16. Worden, K., "Nonlinearities in Structural Dynamics: Detection, Identification, and Modeling", IOP Publishing, Philadelphia, PA, 2001.
17. Lalanne, C. "ISTE: Mechanical Vibration and Shock Analysis, Sinusoidal Vibration (3):. Somerset, US. Wiley-ISTE, 2014, pp 319 – 352.
18. Simon, M., and Tomlinson, G.R., "Use of the Hilbert Transform in Modal Analysis of Linear and Non-Linear Structures", Journal of Sound and Vibration, 96(4), pp 421-436, 1984.
19. Londono, J.M., Neild, S.A., and Cooper, J.E., "Identification of backbone curves of nonlinear systems from resonance decay response." Journal of Sound and Vibration, 348(2015), 2015, pp. 224-238.

DISTRIBUTION

1	MS0346	Jill Blecke	1556
1	MS0346	Robert Kuether	1556
1	MS0346	Mikhail Mesh	1553
1	MS0386	Michael J. Starr	1557
1	MS0555	Theresa E. Cordova	1521
1	MS0557	John Hofer	1521
1	MS0613	Laura Jacobs	1521
1	MS0828	Michael Ross	1553
1	MS0840	Adam Brink	1553
1	MS0840	Antonio R. Garcia	1555
1	MS0899	Technical Library	9536 (electronic copy)


Sandia National Laboratories